Università degli Studi di Ferrara

ISTITUTO ITALIANO DI TECNOLOGIA

DOTTORATO DI RICERCA IN

"Neuroscienze Traslazionali e Neurotecnologie"

CICLO XXXII

COORDINATORE Prof. Fadiga Luciano

Olfaction and whisker tactile sense in skilled reaching: behaviour and kinematics

Settore Scientifico Disciplinare BIO/09

Dottorando

Dott. Parmiani Pierantonio

(firma)

Tutore

Dott. Franchi Gianfranco

(firma)

Anni 2016/2019

1 Abstract

1.1-Bulbectomy experiments

We focused on how the rat uses olfactory cues in a single-pellet reaching task, which is composed of three sequential learned responses: Orient, Transport and Withdrawal. High-speed video-recording enabled us to describe the features of responses in controls vs. 3–5 and 12–14 days after bilateral bulbectomy in trials with (P trial) vs. without (no-P trial) pellet. In controls: a- the sequence of responses was complete in P trials, while it was interrupted after Orient in no P-trials; b- there is no difference in duration between the first two events of orient in P vs. no-P trials. After bulbectomy: a- the frequency of approach to the front wall decreased; b- the sequence of responses was complete in both P and no-P trials; c- there is an increase in Orient duration due solely to the increased time in slot localisation; d- the first nose contact with the front wall took place below the shelf/pellet level; e- the number of nose touches preceding poking was significantly higher. Otherwise, after Bulbectomy the pattern of reach and the ability to grasp the pellet do not change, suggesting that the preserved whisker/nose tactile input triggers the transport movement. In conclusion, bulbectomy, but not necessarily olfaction, affects Orienting whereas olfaction is used to navigate the box and determines the choice to reach/grasp the target.

1.2 - Bilateral Macrovibrissae trimming and Infraorbital nerve severing experiments

Skilled reaching is a complex movement, in which a forelimb is extended to grasp food that is placed in the mouth for eating. In rat, olfaction is used to guide reaching, but the relevance of whisker sense suggests that this could also have a role. To test this hypothesis, we studied skilled reaching behaviour in rats trained in a single-pellet reaching task before and after infraorbital nerve (ION) severing. Bilaterally ION severed rats display an impressive change in the architecture of skilled behaviour already detectable in the first post-surgical recording session. Specifically, the behavioural sequence was interrupted either before approaching the front wall of the box or before poking with the nose into the slot to locate the food pellet. In the following days, rats began to

display a new phase of exploration of the front wall with repetitive forelimb movements, a prelude to the reappearance of reaching, which took place between 6 and 12 days after ION severing, depending on the rat. From this time onward the skilled behaviour architecture completely recovered. These findings strongly indicate that whisker sense play a role in guiding skilled reaching behaviour in the rat.

1.3- Skilled Reaching Kinematics experiments

In rats, skilled reaching includes orienting (OR), reaching (RC), grasping (GR) and retracting (RT) movements. Here we present the first quantitative description of this behaviour by means of a 3D recording system. OR movement featured three steps: head approaching the front wall (HA), slot localization with head movements (SL), and nose poke through it (PK). SL was the longest-lasting step ($p=0.0000$), while HA was the fastest ($p=0.0000$). RC showed two bimodal start point distributions: i) along the X axis, beyond or within the first quartile from the target, long and short RC trajectories were distinguished, each presenting different shapes and velocity peaks; ii) along the Z axis, there were two modalities of reach start, in the stance or swing phase of the last step. 3D plots evidenced that at the end of RC, the wrist/paw occupied the same spatial position as the nose at the end of OR. In GR, averaging the trajectories confirmed the lowering and approach of the marker towards the target. Averaging the velocity profile showed equal amplitude velocity peaks, at around 20–30% of the normalized GR duration, on the X and Z axes. Finally, logistic regression analysis suggested which kinematic variables were decisive for successful prehension.

Acknowledgements

I would really like to thank my parents for their love and all my friends for their affection during these years.

None of this would have happened without you.

I would also also like to thank Professor Franchi for his invaluable advice during these years.

Table of Contents

Table of Figures

Abbreviations

AM AnteroMedial group of thalamic nuclei

CL CentroLateral group of thalamic nuclei

GR Grasping movement

HA Head Approaching step of OR movement

IAM InterAnteroMedial group of thalamic nuclei

ION Infraorbital Nerve

IQR Interquartile Range

M1 Primary Motor Cortex

MAD Median Absolute Deviation

MD MedioDorsal thalamic nuclei

MOB Main Olfactory Bulb

No-P trial trial without Pellet on the shelf

OR Orienting movement

P trial trial with Pellet on the shelf

Phase A Approach Phase

Phase N Nose into the slot Phase

Phase R/G Reach-Grasp Phase

Phase Rt Retracting the grasped food Phase

PK Nose Poke step of OR movement

POm POsteromedial thalamic nuclei

RC reaching movement

RT Retracting movement

S1 Primary Somatosensory Cortex

SL Slot Localization step of OR movement

VPM VentroPosteroMedial thalamic nuclei

1- Introduction

1.1 – Overview of the rat olfactory system

The ability of animals to evaluate the surrounding environment is fundamental to their survival and they use the inputs coming from all of their sensory systems to achieve that goal. These sensory systems are not equally developed in all taxa but while the chemical perception is present in all vertebrate animals the visual and acoustic ones have been lost by some of them during evolution thus highlighting its general usefulness compared to the latter two. Each sensory system has its own peculiarities making each of them maximally effective under diverse and narrow sets of environmental conditions. For example light perception needs a sufficient quantity of reflected light going from the signaller to the perceiver without obstruction between them while sound does not need light for propagation but can too be easily distorted and deflected by structures along the path between them. The olfactory perception has the advantage over these two sensory systems that only needs the perceiver to be close enough from the odour source while the for signaller is sufficient to have left some odour molecules earlier in time (Stoddart, 1980).

The olfactory system is triggered when molecules make contact with the sensory epithelium located inside the nasal cavities (Figure 1). In there are present first-order neurons that transduce molecules and then project via the olfactory nerve, the first cranial nerve, to the main olfactory bulb (MOB). Then MOB output neurons, mitral and tufted cells, convey olfactory information to the other higher brain areas such as the anterior olfactory nucleus, piriform cortex, olfactory tubercle, entorhinal cortex and some amygdaloid nuclei (Paxinos, 2004).

In rats the olfactory system is implicated in many important ecological functions such as the reproductive one, the recognition of conspecifics, predators and preys, emotional responses, aggression and neuroendocrine regulation. It also has a role in food selection together with the gustatory one (Paxinos, 2004). Their ability to increase the inspiration rate, polypnoea, is present just after birth while other behaviour such as protraction and retraction of mystacial vibrissae, protraction and retraction of the snout and orientation of the head towards an odour source appear and are fully functional before the end of the eleventh day (Stoddart, 1980).

1.2 Overview of the rat whisker system

Rats, such as many mammals are provided with vibrissae, that are specialized tactile hair characterized by their increased length and thickness compared to ordinary hair and by the presence at their base of well innervated hair follicles with identifiable representations in the somatosensory cortex. They are located in various parts of the body but the most studied are the facial vibrissae also called whiskers (Prescott et al., 2016). These are usually divided in two categories: macrovibrissae and microvibrissae. There is no clear boundary between them but while microvibrissae are smaller, mostly pointing downward and immobile, macrovibrissae are bigger, projecting outward and forward from the snout of the animal and can be actively moved back and forth with a movement pattern called whisking. Macrovibrissae are arranged on each side of the snout in a bidimensional grid with five rows (Figure 2) and a variable number of whiskers per row ranging between five and nine thus forming a movable tactile sensory array surrounding the head that the animal uses to actively scan the environment (Carvell and Simons, 1990). This makes the whisker system a "closed loop" system in which the sensory input and the motor output influence each other bidirectionally. This is also reflected in the connection happening both cortically and subcortically inbetween sensory and motor structures so that brain regions cannot be divided perfectly into motor and sensory ones (Figure 3). For example S1 can significantly control whisker motion (Matyas et al., 2010) and M1 can process sensory signal (Hatsopoulos et al.,2007; Naito et al.,2011; Nii et al.,1996; Hatsopoulos et al.,2011; Huber et al.,2012). But a starting point of this closed loop I will start with the description of the ascending pathways bringing the sensory information coming from the whiskers.

The mechanical movements of the vibrissae are reliably transduced by the different receptors that innervate them (Jones et al., 2004). These first order neurons form the trigeminal ganglion and in there the information about the stimulus is very similar to the stimulus itself (Szwed 2003 and 2006).These neurons then form the trigeminal tract that project to the brainstem where the second order neurons bodies reside. In the brainstem the trigeminal complex is divided in two nuclei: the rostral principal nucleus and the caudal spinal nucleus. The latter is in turn subdivided in three regions (oralis, interpolaris and caudalis). Both these nuclei then send projections to the contralateral thalamus and specifically to the ventroposteromedial (VPM) and posteromedial (POm) nuclei. Finally thalamic nuclei send projections to the primary somatosensory cortex (S1) (Deschenes and Urbain, 2009). At the cortical level the most important projection of S1 is with the ipsilateral primary motor cortex (M1) and this projection is the most likely source for tactile input to M1 as tactile responses in M1 are dependent on S1 (Farkas et al., 1999; Chakrabarti et al.,2008;

Aronoff et al.,2010). Starting the description of the motor part of the loop M1 connects in turn with S1 and S2 and with M1 of the contralateral hemisphere.

M1 has also bidirectional connections with various ipsilateral thalamic nuclei such as the mediodorsal (MD), the centrolateral (CL) group of nuclei and the medial aspect of the posterior nucleus (POm) while the interanteromedial (IAM), the anteromedial (AM) and the ventrolateral (VL) groups of thalamic nuclei receive projections from whisker M1 of both hemispheres (Cicirata et al., 1986, Rouiller et al., 1991, Myiashita et al., 1994, Alloway et al., 2008a, 2009, Hooks et al., 2013). Going further down subcortically the whisker M1 also projects to the ponteocerebellum (Schwartz and Möck, 2001), dorsaolateral neostriatum (Alloway et al., 2006, 2009), intermediate and deep layers of the superior colliculus (Miyashita et al., 1994; Alloway et al., 2010), bilaterally to the claustrum (Smith and Alloway, 2010; Smith et al., 2012). Also direct projections from whisker M1 to vibrissal motoneurons in the facial neurons have been recently demonstrated (Sreenivasan et al., 2014) creating a parallel with the primate hand system in which direct M1-motoneuronal connections have been demonstrated too (Rathelot and Strick, 2006).

The contribution of the Whisker system to rat behaviour has been evaluated by means of various experimental manipulations such as whisker clipping, cauterization of the whisker follicles and lesions of central and peripheral nervous system structures comprising the whisker pathway (Prescott et al., 2016). These manipulations have demonstrated significant deficits in various behaviours such as explorative, thigmotactic and locomotive ones and also in maze learning, swimming, food pellets locating, equilibrium maintenance and fighting (Ahl 1982; Gustafson and Felbain-Keramidas 1977 for reviews). Also alterations of posture have been reported after whisker removal in adult rats resulting in the snout contacting the surfaces (Meyer and Meyer, 1992; Vincent, 1912) while animals in which whiskers are continuously removed starting from shortly after birth exhibit as adults behavioural compensations (Gustafson and Felbain-Keramidas, 1977; Volgyi, 1993) and show alterations also when whiskers are allowed to regrow (Carvell and Simons, 1996). A very important use of the whisker system in rats is for predation and it has been demonstrated that they can detect, track and immobilise their preys without vision (Gregoire and Smith, 1975).

1.3 Olfaction as a cue for spatial navigation and skilled reaching coordination

A great deal of interest has been directed to the manner in which animals employ specific cues for spatial navigation and identification of food (Welker, 1964; Nadel, 1991; Jacobs, 2012; Hok et al. 2016; Wiltschko & Wiltschko, 2017). In odour-guided tasks, olfactory cues, together with additional sensory cues, shape animal behaviour (Larson & Stein, 1984; Berthoz & Viaud-Delmon, 1999; Arleo & Rondi-Reig, 2007; Ravassard et al., 2013). A model suitable for studying how olfactory and tactile cues together influence rat's motor behaviour is the so-called "skilled reaching" (Whishaw & Tomie, 1989; Hermer-Vazquez et al., 2007; Parmiani et al., 2018).

Skilled reaching is a complex behaviour in which an animal optimises movement towards a goal location to grasp food for eating (Iwaniuk & Whishaw, 2000). Skilled reaching is considered to be composed of three successive learned responses, 1) Orient, 2) Transport, and 3) Withdrawal (Gharbawie & Whishaw, 2006; Alaverdashvili et al., 2008; Alaverdashvili & Whishaw, 2013. Orient comprises the rat's approach to the front wall to locate the slot, and poking the nose through it to identify the pellet. Transport involves the rat lifting its paw from the box floor and directing it through the slot to grasp the pellet, and Withdrawal consists of retracting the paw through the slot to eat the pellet. While Orient engages flexible and sophisticated multisensory feedback control (Whishaw & Tomie, 1989; Parmiani et al., 2018), Transport to target is a ballistic or semi-ballistic movement (Whishaw & Karl, 2014). Although in this task, rats use a combination of olfactory, whisker/nose tactile and proprioceptive cues to coordinate sequential movements of the head and forelimb, the specific use of each sensory cue during Orient and Transport has not yet been fully described. Whishaw and Tomie (1989) performed an experiment using slots differentially located throughout the wall so that rats were not aware of the pellet position during each trial. In that study, bulbectomised rats were unable to detect the location of the pellet, but did preserve the capacity to guide the reaching toward the pellet with a high success rate. They concluded that it is olfaction rather than vision that is used to locate food for reaching (Whishaw & Tomie, 1989). On the other hand, the specific role of whisker/nose tactile cues in the different components of skilled reaching has been demonstrated in a single-pellet reaching task with a single slot in fixed position (Parmiani et al., 2018). Following whisker/nose de-afferentation, rats displayed severe task impairment with transient interruption of the normal behavioural sequence. Since both olfactory and tactile cues are involved in the skilled-reaching task, we thought to define the specific role of olfactory cues in the same behavioural task used to study the role of the whisker/nose tactile sense. To value how olfaction is employed in this task, we set out to describe the temporal relationship between Orient

and Transport movements in different experimental conditions: with or without the presence of the olfactory cue and before and after olfactory bulb removal.

1.4 Whisker sense as a cue for spatial navigation and skilled reaching coordination

Sensory–motor integration involves coupling the sensory system and motor system. It is not a static process, since for a given behaviour there is no one single sensory input and no one single motor command. Neural responses at almost every stage of a sensorimotor pathway can be modified at short and long timescales by biophysical and synaptic processes, recurrent and feedback connections, and learning, as well as many other internal and external variables (Huston et Jayaraman 2011; Sereno and Huang, 2014; Luo et al., 2017). Besides this, multisensory integration allows information from the different sensory modalities, such as sight, sound, touch, taste, smell and self-motion, to guide motor behaviour (Kleinfeld et al., 2014; Miller et al., 2017).

A suitable model for studying multisensory integration in motor behavior is the so called "skilled reaching", a complex movement common to many animal species, in which a forelimb is extended to grasp food that is placed in the mouth for eating. Multiple parallel parietofrontal circuits, devoted to specific sensorimotor transformations during skilled reaching, have been described in monkeys (Matelli and Luppino, 2001; Omrani et al., 2016 and 2017), and evidence from functional brain imaging studies suggests that the organization of this complex behaviour is based on the same principles in humans (Filimon, 2010). Skilled reaching, the act of reaching to grasp an object as occurs in a reach-to-eat task, shares many similarities among both primates (Jeannerod, 1988; Jolly, 1964; Roy et al., 2000) and rodents (Whishaw and Pellis, 1990; Whishaw, 1996; Sacrey et al., 2009). In rodents, skilled reaching to eat is a learned and composite movement in which the rat, inside a reaching box, uses olfactory cues, proprioception, whiskers, and tactile nose sense to locate food, and to define a reaching path for the paw to target the pellet (Whishaw and Tomie, 1989; Whishaw et al., 2017; Parmiani et al., 2018). Skilled reaching task starts with orienting (OR), which consists of the rat's approach to the front wall of the reaching box, and nose positioning over the pellet. OR is followed by reaching (RC), i.e. transporting the paw towards the pellet; grasping (GR), which involves prehension of the pellet; and paw retraction (RT), to bring the pellet to the mouth (Alaverdashvili and Whishaw, 2013).For many years, rodents have been trained in skilled reaching in order to study diverse aspects of this behaviour, such as neural control of the forelimb (Alaverdashvili and Whishaw, 2008; Kawai et al., 2015), functional recovery from neural injury (Moon et al., 2009), and assessment for brain damage (Klein et al., 2012). Indeed, the skilled

reaching task is a composite behaviour involving a sequence of movements, namely: orienting of the rat within the reaching box, food localisation, reaching-grasping food, and bringing food to the mouth (Alaverdashvili et al., 2008). The observation that skilled reaching-grasping is relatively inflexible supports the notion that it is produced by complex fixed neural circuitry (Metz and Whishaw, 2000). It is probable that the intrinsic recurrent synaptic connections between sensory and motor cortices and within the motor cortex are the cortical circuits that allow coupling between the spatial location of the pellet and the spatial location to which the limb is commanded to move. The projection from the vibrissa-S1 (vS1) is most likely the main source of sensory input to the vibrissa-M1 (vM1) (Farkas et al., 1999; Chakrabarti et al., 2008; Aronoff et al., 2010; Hooks, 2016), and the horizontal reciprocal cortico-cortical connections between vM1 and forelimb-M1 (fM1) (Huntley, 1997) could be the network directly involved in whisker, head and forelimb movement coordination during skilled reaching.

In humans, the kinematic parameters utilized for characterizing prehension movement components are essentially the trajectory shape and duration, the movement peak velocity, and the occurrence of the latter in normalized movement duration (Jeannerod, 1984; Roy et al., 2000).

Skilled reaching has been previously described in rats by means of notation techniques (Whishaw et al., 1992; Gharbawie and Whishaw, 2006), video (Whishaw et al., 2008), as well as cineradiographic recordings (Alaverdashvili et al., 2008). More recently, high-speed single (Wong et al., 2015; Ellens et al., 2016; Nica et al., 2018; Parmiani et al., 2018) and multiple cameras have respectively been used in kinematic studies to reconstruct reaching trajectories (Azim et al., 2014; Mathis et al., 2018; Bova et al., 2019). The most recent innovation for describing/analysing rat reaching, however, includes a machine-learning algorithm to enable digitization of joint segments from markerless videorecordings (Mathis et al., 2018; Bova et al., 2019).

We, on the other hand, used an infrared three-dimensional motion-tracking system, which, unlike the machine-learning approach, did not require significant time and effort to manually mark videos, coupled with behavioural video-recordings. Our primary goal was to characterize head and forelimb movement coordination in a single-pellet reaching task inside a reaching box, where the animal can freely reposition its body. In detail, we set up 3 digital cameras that precisely captured the 3D motion of all markers attached to the rat body, in a capture volume containing the entire expected range of markers movements. The expectation was that the combined behavioural and kinematic study would reveal insight into the spatio-temporal features of movements used to perform orienting and reaching movements.

Interestingly, it has been shown that in the rat it is olfaction rather than vision that is used to locate food and guide reaching (Whishaw and Tomie, 1989; Hermer-Vasquez et al., 2007; Parmiani et al., 2019 under revision). Nevertheless, the relevance of whisker sense in the rat (Diamond and Arabzadeh, 2013; Kleinfeld et al., 2014), suggests that such information could also have a role in driving skilled reaching behaviour. However, the effect of trigeminal input removal, i.e. sensory whisker pad denervation, on skilled reaching performance has never before been evaluated, and it would be useful to determine which movement of the skilled reaching sequence is affected by whisker sense suppression. To this end, we investigated orienting-reaching behaviour in rats trained in a single-pellet reaching task, before and after whiskers trimming and infraorbital nerve (ION) severing.

1.5 The Rat skilled reaching kinematics

Skilled reaching, the act of reaching to grasp an object as occurs in a reach-to-eat task, shares many similarities among both primates (Jeannerod, 1988; Roy et al., 2000) and rodents (Whishaw and Pellis, 1990; Whishaw, 1996; Sacrey et al., 2009). In rodents, skilled reaching to eat is a learned and composite movement in which the rat, inside a reaching box, uses olfactory cues, proprioception, whiskers, and tactile nose sense to locate food, and to define a reaching path for the paw to target the pellet (Whishaw and Tomie, 1989; Whishaw et al., 2017; Parmiani et al., 2018). Skilled reaching task starts with orienting (OR), which consists of the rat's approach to the front wall of the reaching box, and nose positioning over the pellet. OR is followed by reaching (RC), i.e. transporting the paw towards the pellet; grasping (GR), which involves prehension of the pellet; and paw retraction (RT), to bring the pellet to the mouth (Alaverdashvili and Whishaw, 2013).

The rat's skilled reaching behaviour emerges as an important model for investigating many topics in neurosciences research, from motor behaviour (Whishaw and Tomie, 1989, Alaverdashvili et al., 2008) to sensorimotor integration (Whishaw and Pellis, 1990; Hermer-Vasquez et al., 2007, Parmiani et al., 2018), and also serves as a model for studying many motor system injuries that affect motor behaviour (Klein et al., 2012; Viaro et al, 2016).

Skilled reaching has been described in rats by means of notation techniques (Whishaw, 2005), video (Whishaw et al., 2008) and high-speed video analysis (Ellens et al., 2016, Parmiani et al., 2018), as well as cineradiographic recordings (Alaverdashvili et al., 2008). All these studies relied on different scoring systems to describe the reaching for food movement and its impairments following brain injuries. However, one drawback of such descriptive methods is that they do not provide

quantitative information on how the nervous system coordinates the movement of different body parts involved in such complex behaviour. Hence, there are important relationships between OR and RC-GR in the reach-to-eat movement that have not yet been determined; specifically, the spatio-temporal kinematic features of skilled-reaching components have never been evaluated.

In humans, the kinematic parameters utilized for characterizing prehension movement components are essentially the trajectory shape and duration, the movement peak velocity, and the occurrence of the latter in normalized movement duration (Jeannerod, 1984; Roy et al., 2000). In the rat, kinematic recording has recently been used to characterize the reaching movement and kinematic synergy of the forelimb in a staircase skilled-reaching task (Balbinot et al., 2018). However, in that study the task forced a relatively fixed body position, and kinematics were calculated using 2D marker trajectories in 3 planes of movement, rather than a true 3D tracking of the markers.

We, on the other hand, set out to use novel 3D kinematic recording and analysis tools, coupled with behavioural video-recordings, in order to characterize head and forelimb movement coordination in a single-pellet reaching task inside a reaching box, where the animal can freely reposition its body. To this end, we set up 3 digital cameras that precisely capture the 3D motion of markers attached to the rat body, which is described in relation to frame-by-frame movements, as revealed by 200 Hz-video recording. The expectation was that the study would reveal insight into the spatio-temporal metrics of the kinematics of movements used to perform OR and RC-GR movements. Moreover, applying logistic regression analysis to our data was expected to indicate which of the kinematic variables plays a role in determining the trial outcome.

2- Aims of research

The data presented in this thesis are part of a wider project which main focus is to study the integration of different sensory modalities in guiding a complex behaviour such as spatial navigation and food identification. In particular here we study the specific role of whisker and olfactory sense in skilled reaching behaviour using combined behavioural and kinematic approaches. Hence, we compare qualitatively and quantitatively the skilled reaching behaviour in three condition: before and after olfactory bulb ablation, macrovibrissae trimming, and whisker pad denervation. As for behavioural approach we follow procedures of a previous experiment whereas for kinematic study we set out to use novel 3D kinematic recording and analysis tools, in order to characterize head and forelimb movement coordination. The expectation is that this study would reveal insight into the spatio-temporal metrics of the kinematics of movements used to perform OR and RC movements. Moreover kinematic results can support the hypothesis that in the skilled

reaching task the nose works as a pointing system for wrist positioning. Finally, applying logistic regression analysis to our data is expected to indicate which of the kinematic variables plays a role in determining the trial outcome.

3- Methods and Procedures

3.1- Subjects and Ethical Approval

Adult male albino Wistar rats, each weighing between 280 g and 330 g, raised in the University of Ferrara animal house, were used for this study. Five rats underwent bilateral bulbectomy, and in three rats a sham surgery (craniotomy without bulbectomy) was performed bilaterally. In five rats, the Infraorbital nerve (ION) of both sides was cut (bilaterally ION-severed rats); in three rats the macrovibrissae were bilaterally trimmed (bilaterally trimmed rats); and in three rats a sham surgery without ION severing was performed bilaterally. The experimental plan was designed in compliance with Italian law regarding the care and use of experimental animals (DL26/14), and approved by both the University of Ferrara Ethics Board (OBA) and the Italian Ministry of Health; and all procedures complied with the ethical standards of the European Council Directive of 4 March 2014 regarding the treatment of animals in research.

3.2- Feeding and Food Restriction

Rats were housed in polycarbonate cages (53 cm long, 37 cm wide, and 21 cm deep) with sawdust bedding, in groups of three or four in a colony, under a 12 h:12 h light/dark cycle with light starting at 07:30 h. All testing and training was performed during the light phase of the cycle at the same time of day. The animals received water *ad libitum*, but were food-deprived before the start of training. The week before training began, each rat received 20 banana-flavored round food pellets (Rodent Tab 45 mg, AIN-76A, TestDiet, Richmond, VA, USA) 1 h prior to the daily fodder ration. These pellets would later serve as reaching targets in a single-pellet reaching box. Each animal maintained about 90% of their initial body weight throughout the experiment; to maintain body weight, the rats were given an additional amount of food in their home cages at least 1 h after finishing the training or testing session.

3.3- Reaching Box and Single-Pellet Training

The reaching box was made of clear Plexiglass (340 × 390 × 134 mm wide), and was similar to that described by Metz and Whishaw (2000) and Alaverdashvili et al. (2008). Briefly, the middle of the front wall featured a 10-mm-wide, vertical opening to allow the animal to reach for the pellets. These were placed on a shelf, 15 mm wide and 20 mm long, which was attached outside the front wall of the box, 25 mm above the base. The upper side of the shelf, aligned to the midline of the box, featured a round indentation (diameter 7 mm, depth 2.5 mm, distance from the front wall 10 mm) for food pellet positioning. During pre-training (about 1 week) the rat was placed in the box for 20-min daily sessions during which it was allowed to explore the reaching box and encounter the food pellets placed on the shelf to promote reaching-grasping through the slot. Pre-training ended when the rat started to reach with its forepaw for the food pellet. Training sessions also consisted of 20-min daily sessions during which the rat learned to grasp the pellet with the preferred paw. Paw preference was established when at least 60% of a minimum of 10 reach attempts were made using the left or the right forepaw. To verify the use of olfaction in the recognition of the presence of pellet, in each session, trials with a pellet (P trials) were intermingled with trials without a pellet (no-P trials). P trials and no-P trials were randomly presented with a P trial percentage of ≥70%. During training the rat was taught to advance from the posterior part of the box to the front wall, to sniff for the pellet on the shelf, and to perform the prehension sequence only if the pellet was present. If the pellet was absent, the rat was trained to go back to the posterior part of the box to start another trial. In order to facilitate learning of this movement sequence, a food pellet was dropped in the posterior part of the box in the first training sessions. Furthermore, at the end of each session several pellets were dropped into the box as a final reward, which gave us the chance to observe the rat's spontaneous grasping from the floor under the different experimental conditions. It should be mentioned, however, that the experimental set up did not allow us to quantify this spontaneous behavior. The success level of prehension was scored in the last week of training and during recording sessions. The percentage success rate of each rat was calculated as the ratio between the prehension movements in which the rat brought a food pellet to its mouth and the total number of trials multiplied by 100. For each rat, training ended when the percentage success rate achieved almost 50% in the last consecutive sessions.

3.4- Surgical olfactory bulb ablation and histology

For olfactory bulb removal, all surgical procedures were performed under ketamine anaesthesia (80 mg kg−1 i.p., and then supplemental doses i.m. as needed). Using standard stereotaxic techniques, the skull was exposed, the bone above the olfactory bulbs was removed, and the olfactory bulbs were ablated by aspiration. The skin was closed with 6–0 sutures, and then cleansed with an antibiotic solution. In the post-operative period, none of the rats displayed complications such as infection or overt signs of discomfort. At the end of the experimental procedure, the animals were perfused transcardially. In each animal, the brain was removed and post-perfusion examination under dissecting microscope was used to evidence the extent of the lesion.

3.5- Macrovibrissae Trimming

Each day of training began with a 5–10 min handling session in which the three rats were conditioned to tolerate being held firmly while its vibrissae were touched with a set of blunt-tipped scissors. This conditioning enabled us to cut off the vibrissae without anesthesia. After the rats achieve a pellet retrieval success rate above 50% in three consecutive daily sessions, all macrovibrissae—both mystacial and mental (whisker trident)—were bilaterally trimmed to <2 mm in length.

3.6- Surgical Procedures: Infraorbital Nerve Severing

All surgical procedures were performed under ketamine anesthesia (80 mg kg^{-1} i.p., and then supplemental doses i.m. as needed). Under the operating microscope, the ION of both sides was exposed, separated from its adjacent tissues and ligated; it was then cut distally to eliminate all remaining fine branches. The proximal stump was dried and covered with acrylic tissue adhesive (Histoacryl) to prevent the proximal axons from sprouting. The skin was closed with 6–0 sutures, and then cleansed with an antibiotic solution. In the post-operative period, none of the five operated rats displayed complications such as self-mutilation, infection, or overt signs of discomfort. Clinical observation during natural whisking clearly showed that the deafferented whiskers displayed bilateral rhythmic movements, but did not suddenly retract when hit against targets, as would normally be the case. After deafferentation the whisker pad proved unreactive to mild pain-inducing sensory stimuli (i.e., light touching, squeezing or piercing). The loss of whisker pad sensitivity following deafferentation was clearly evident in all animals for the entire survival period. In the sham rats the ION was isolated from the surrounding tissues but left intact (for more details see Franchi, 2001).

3.7- Histology

At the end of the experimental procedure, the animals were perfused transcardially. In each animal, gross post-perfusion examination of the injured nerves showed no nerve continuity at the acrylic stopper level. Under the operating microscope, care was taken to ensure that all ION fascicles had been tied and axotomized. In all animals studied, the exposed ION was cut proximal to the site of nerve injury and prepared for histological examination. After post-fixation in osmium tetroxide, toluidine blue was used to stain 1-μm thick sections. Morphological examination of sections (Axioskop Zeiss and DMC Polaroid camera for image acquisition) showed extensive degenerative processes involving all axons proximal to the lesion.

3.8- Video-Recording of Rat Behavior

Throughout each experimental session, rats were video-recorded at 200 frames/s using a JVC GC-PX100 camera with a resolution of 640 × 360 pixels. The recording video camera was positioned so as to obtain a right or left lateral view of the animal inside the box, according to the handedness of the animal. Recorded videoclips were visualized off-line, and when necessary frame-by-frame analysis was performed using Avidemux 2.6 software. Some rats used in these experiments were also used to carry out preliminary measures of skilled movement kinematics. This is the reason why, in some figures reported, rat show markers on their head and forelimb, which, however, in no way interfered with the execution of movements.

In all rats, video-recordings were performed on three consecutive days before surgery to allow any depressive effect of the anesthetic to subside. Then, whisker-trimmed rats were video-recorded daily from the day of trimming until the 17th day, ION severed rats were video-recorded daily from the 3rd to the 17th day, whereas bulbectomised rats were video-recorded from the third to the fifth day after surgery and then 12–14 days after surgery, to evaluate the post-lesion recovery.

3.9- Analysis of Rat Behavior

In the single-pellet reaching task, each rat is trained to approach the front wall of the reaching box from the rear, and to sniff through the slot to locate the pellet on the shelf. Then, if the pellet is present, the rat advances the preferred forelimb through the slot, grasps the pellet and then withdraws the paw to bring the pellet to the mouth for eating (Whishaw and Tomie, 1989). As the

aim of our research was to define the role of olfactory sensing and whisker/nose tactile sensing in a single-pellet reaching task, we considered each trial as composed of three successive learned responses, which were analyzed separately: (1) Orient; (2) Transport; and (3) Withdrawal (Gharbawie and Whishaw, 2006; Alaverdashvili et al., 2008; Alaverdashvili and Whishaw, 2013). The Orient comprised the rat's approach to the front wall, its locating the slot, and the nose poking through to sniff the pellet. The Transport involved the rat lifting its paw from the box floor and directing it through the slot to grasp the pellet. Withdrawal consisted of retracting the paw through the slot and placing the food pellet into the mouth for eating. These three components were chosen as they are present in all successfully completed trials, as missing one results in an error trial.

Qualitative and quantitative analysis, performed on video-recordings taken before and after bilateral whisker trimming and bilateral ION severing, provided insights into the structure of these learned responses. To study the temporal course of the effects of ION severing on behavior, the data were grouped into five successive 3-day intervals from the 3rd day after the lesion, and compared to data obtained in the same animal before the lesion. Data from each experimental group were pooled, and were presented as mean values with standard error.

To analyze the Orient component of skilled reaching under the different experimental conditions, we first measured the frequency of each rat's approaches toward the front wall. Then, to measure each rat's ability to locate the slot, we calculated the percentage of nose poking with respect to the number of approaches.

To measure the time spent in locating the slot, in control rats we identified the video frame in which the longer mystacial macrovibrissae first contacted the front wall of the box (Figure 14) and the first frame showing the nose inside the slot (nose poke), and calculated the interval between. In trimmed and ION-severed rats, which explored the front wall by repetitive nose touches (Figure 15), we calculated the number of nose touches before nose poking and the time between the first nose touch and nose poke (see Table 1 and 2).To study the temporal course of the effects of bulbectomy on skilled reaching behaviour, the data were grouped into two intervals: from the third to fifth day and from the twelfth to fourteenth day after the lesion, and compared to data obtained in the same animal before the lesion. For each rat, in control and after lesion, 25 P trials and 15 no-P trials were analysed frame-by-frame, and data were presented as mean values with standard error (see Table 1, 2 and 3). Behavioural variables under the different experimental conditions are presented in the Figures separately when there was a significant difference between P and no-P trials; otherwise a single value included the results of all the trials. The behavioural variables evaluated in bulbectomized were the same as in whisker trimmed and ION severed rats but in addition when the

rat was approaching the front wall, we determined the position of the first nose touch relative to the pellet position by means of frontal recordings. Video-frame analysis provided a clear detection of salient frames, which made it possible to characterise the skilled movement. In sequence, the frame in which the rat macrovibrissae made contact with the front wall, defined as 'Whisker touch', corresponded to the start of trial; this was followed by the frame in which the microvibrissae contacted the front wall (inferred when the nose contacted the front wall), defined as 'First nose touch'; then the frame in which the nose passed through the slot, defined as 'Poke'. In the light of this, Orient was split into three intervals of time: Whisker touch–First nose touch, First nose touch–Poke, and Poke–Reach start. This subdivision was motivated by the observation that each of these movements is specifically guided by sensory feedback (Parmiani et al., 2018). The Reach start defined the end of Orient, and Whisker touch–Poke plus Poke–Reach start was used to calculate the duration of Orient. In controls, no-P trials, where Poke was not followed by Reach start, the re-crossing of the nose defined the end of poke, which defined both the end of Orient and the end of trial. The Transport duration was defined as the time between the frame showing the paw lifting off the floor and the frame in which the paw crossed the slot, and Withdrawal duration was defined as the time between the frame in which the paw passed through the slot and the frame in which the paw re-crossed the slot. Finally, in P trials the time interval between the Whisker touch and the paw re-crossing the slot defined the trial duration. Tables 1–3 summarise the parameters estimated respectively in P and no-P trials under the three different experimental conditions.

Under the different experimental conditions, reaching behavior was assessed by measures of total success. Specifically, a successful reach was defined as one in which an animal grasped a food pellet and placed it into the mouth. Total success was defined as: Success % = (number of pellets obtained/total number of reaching)*100.

3.10- Kinematic recording of movements

Rat movements were recorded and measured using an infrared three-dimensional motion-tracking system (Qualisys Motion Capture System; Qualisys North America Inc, Charlotte, USA) (Bonazzi et al., 2013). Qualisys uses an Automatic Identification of Markers (AIM) model which is basically a marker classifier which learns from each trial it tracks. What this means is that after labelling each marker, it updates the AIM model. When a new file is opened, AIM model is applied so the Qualisys automatically labels the markers over the all trial and automatically filling in gaps of certain sizes. Four adhesive infrared-reflective spheres (diameter 4 mm and weight 0.09 g) were affixed to the rat's body for use as markers (Fig. 24 A and 25 A). In all recording sessions, markers

were placed by the same operator so as to minimize both variability in their position and upsetting the animal. Rats initially attempted to remove the markers, but then got used to their presence.

The 3D system used for tracking the markers is equipped with three infrared cameras, placed around the reaching box (Fig. 25 B). Cameras were adjusted to create a volume that is viewed by all three cameras (the capture volume) and contains the entire expected range of marker movement. Indeed, each marker must be seen by all cameras throughout the movement to have a correct 3D recording (fill level: 100%). Cameras were positioned at a distance of about 90 cm from the platform (on which the reaching box rests) and 10 cm above it, resulting in a viewing angle of about 20°. Two cameras were positioned lateral to the preferred paw, and the third camera was positioned in front of the pellet to be reached for (Fig. 25 B). The cameras were calibrated according to the Qualisys Motion Capture Analysis System protocol, placing a stationary L-shaped reference structure with 4 markers to define the origin and orientation of the 3D-coordinates system. The directions of X-, Y- and Z-axis coordinates were horizontal, depth and vertical, respectively. The pellet reference position was defined before each recording session by placing a marker in the indentation of the reaching box shelf (Fig. 25C). Each kinematic recording was triggered by the experimenter when the rat began to approach the front wall, and lasted 5 seconds to include a single full trial (mean trial duration ~1 sec). Light from two LEDs, one visible and the other infrared, positioned within the visual field of the cameras, was switched on by the experimenter upon triggering the kinematic recording, thereby allowing synchronization of the two recording systems. Movements were recorded with a 100-Hz sampling rate, and kinematic features were analysed off-line by Qualisys Track Manager software and custom MATLAB scripts (The MathWorks Inc., MA, USA). The trials in which all markers were not clearly recorded throughout the whole duration (fill level >100%) were not considered in the off-line analysis; for this reason the number of analysed trials was fewer than those recorded, and was different for each rat.

In order to record movement kinematics, four markers were positioned on each rat's body using hot glue as follows: the first two markers near the medial auricular border, the third on the nose (3–4 mm from the tip) and the fourth either on the lateral border of the wrist or the last phalangeal joint of the two middle digits, Fig. 25 A). The auricular markers were used only as a reference to unequivocally identify the nose marker during head movements: in this way the nose marker enabled record of orienting kinematics. The fourth marker, depending on its position, detects either limb or paw movements, and enables recording of the reaching or grasping kinematics, respectively. It was not possible to place the markers simultaneously on both wrist and digit, since the Qualisys system is unable to distinguish between very close markers when the rat is moving, especially when

the forelimb goes through the slot during a reaching movement. Hence, wrist and digit markers were applied in different blocks of trials, meaning that reaching and grasping movements were recorded in different sessions, and are consequently reported in different Figures (Figs. 26 and 27). The markers applied to the rat's body did not interfere with the movements, except the marker applied to the digits, which reduced the successful pellet-grasping score to <50%. In the present thesis the data from digit marker have not been presented and discussed.

3.11- Movement pattern analysis

Taking into account the sequence of movements that compose the trial (Fig. 24), in our analysis we considered the movements orienting, reaching and grasping. Orienting and reaching analyses were carried out on five rats, while grasping analysis on three rats due to the intolerance of the other two for the markers. We were unable to study the retract movement itself, since, in its final part, the wrist marker was not visible to all cameras; however, we referred to the beginning of retract, in which the wrist or digit marker was visible, to define the end of grasping. We then analysed orienting kinematics using the nose marker, reaching kinematics using the wrist marker, and grasping kinematics using the digit marker, as each marker provides an optimal description of the velocity peak, thereby characterizing the individual movements (Fig. 26).

Figure 26A shows an example of the nose (red) and wrist (green) marker trajectories along the horizontal and vertical axes; individual trials were split off-line into a sequence of three movements, namely, from the left side of the figure to the right: orienting (interval 1–2), reaching (interval 2–3) and grasping (interval 3–4). The simultaneous temporal displacement of the nose and wrist markers along the vertical axis during movements are reproduced in Figure 26 B and the instantaneous movement velocity profiles, calculated by MATLAB custom program, are shown in Figure 26C. For both orienting and reaching, onset was defined as the time-point (in ms) at which the tangential velocity exceeded 5% of the maximum velocity (Fig. 26C). End of orienting corresponds to the reaching starting time-point, as defined by the wrist marker (point 2); the end of reaching cannot be defined from the grasping velocity peak, since the wrist marker does not show a clear velocity peak during grasping (see farthest right interval 3–4 in Fig. 26C). For this reason the reaching end was defined as the time-point of minimum distance between the wrist marker and target (point 3).

3.12- Data presentation

In order to analyse the movement kinematics, for each rat, trajectories were plotted in a 3D reference frame (Fig. 28), and start/end point distributions are presented as horizontal/depth and horizontal/depth coordinates (Fig. 29). Each movement is identified by four kinematic variables: 1, movement trajectory length (in mm); 2, movement duration (in msec); 3, mean velocity (in mm/s); and 4, peak velocity (in mm/s) (see Table 8). In Figures 32, 33, and 34, data are plotted as 3D and single or average 2D trajectories and normalized speed profile averages.

To evidence that wrist/paw position at the end of reaching tended to occupy the same spatial position as the nose at the end of orienting, first we present two frames corresponding to PK end and reaching end, respectively (Fig 34, A and B); we also plotted the cumulative normalized displacements of the nose marker during orienting and wrist marker during reaching on the three dimensions (Fig. 34 C–F).

3.13- Statistical analysis

All statistical analyses were performed using the R language and environment for statistical computing (www.R-project.org/). All behavioural data are represented in Table form as the mean ± standard error of *n* determinations, and using a bar chart to represent the mean values and the associated standard error. All kinematic data are represented in Table form as the median ± interquartile range (IQR) of *n* determinations. Pair-wise comparison of proportion was used to determine statistically significant differences in proportion between groups, using control values as the reference group. For behavioural and kinematic parameters, a Kruskal-Wallis test by ranks, followed by Dunn's post-hoc test, were used to determine statistically significant differences between experimental group values. The Pearson Chi-square goodness-of-fit test was applied to compare differences in movement frequency time-course after the whisker deafferentation. For all tests a significance level of $\alpha = 0.05$ was set. When performing multiple comparisons, the Holm p-value correction method for multiple hypotheses was used.

3.14- Logistic regression

To identify which of the described kinematic variables could be relevant in determining trial outcome, we used logistic regression analysis. Logistic regression is a form of regression analysis that uses a logistic function to model a binary dependent variable through the log-odds of a linear combination of one or more independent variables (Hosmer and Lemeshow, 2000). We treated the variables detected by the nose/wrist marker and those detected by the digit marker separately, since they were recorded in the same animal but in different trials (see experimental Methods). For each logistic regression we began with two models, one including all variables related to the start of the movement, and one including all variables related to the movement's end. We then iteratively refined each of these models by discarding all variables whose associated p-values were >0.05 (Fig. 36A and B, black and white bars). We next combined start and end variables into a single model.

All models were comparatively evaluated by means of the Akaike Information Criterion (AIC). AIC is a synthetic score that assesses the efficacy and economy of a model simultaneously by evaluating its ability to retain the information contained in the dataset (efficacy), and promoting the model that uses the lowest number of variables (economy). Lower AIC scores indicate better models. It is important to note, however, that AIC does not enable absolute evaluation of a model, but only a relative assessment between models. The model that simultaneously presented the lowest AIC score and coefficients with associated p-values lower than 0.05 was defined the Final Model (Fig. 36 A and B, grey bar). The Final Model presented five significant variables for OR/RC regression whose coefficients are shown in Figures 36C.

We obtained the values of all the coefficients, their associated p-values, and AIC scores for all models using the GLM function provided in the R language and environment for statistical computing. The Final Model best predictors were expressed in the following log-odds function for nose/wrist and digit models.

Nose/wrist logistic equation:

$$\ln\left(\frac{P}{1-P}\right) = \beta_0 + \beta_1 x_1 + \beta_2 x_2 + \beta_3 x_3 + \beta_4 x_4 + \beta_5 x_5$$

Where: $\ln\left(\frac{P}{1-P}\right)$ = Logit P; β_0= y intercept; $\beta_{1\text{-}7}$= coefficient of predictors; x= predictors: x_1 = wrist position on X axis at RC end; x_2 = wrist position on Y axis at RC end; x_3 = nose position on X axis at RC end; x_4 = nose position on Y axis at RC end; and x_5 = nose position on Z axis at RC end.

3.15- ROC curve

To assess the model's ability to correctly distinguish between successful and unsuccessful trials, we used ROC (Receiver Operating Characteristic) curve analysis (Fig. 36E). In order to create the ROC curve, for each trial we compared the binary classification performed by the experimenter during the frame-by-frame video analysis and the binary classification obtained as the output of the model. In this way the following variables were defined: True Positive trials, i.e. successful trials for both the experimenter and model; False Positive trials, unsuccessful trials for the experimenter and successful trials for the model; True Negative trials, unsuccessful trials for both the experimenter and model; and False Negative trials, successful trials for the experimenter and unsuccessful trials for the model. The ROC curve was obtained by plotting the True Positive Rate (TPR: sensitivity) against the True Negative Rate (TNR: specificity) at various threshold settings. The TPR was obtained by dividing the number of True Positive trials by the sum of True Positive and False Negative trials. The TNR was obtained by dividing the number of True Negative trials by the sum of True Negative and False Positive trials. An area under the ROC curve (AUC) of 1 indicates perfect overlap between the two classifications, and a value of 0.5 indicates the degree of overlap obtainable with a random classifier, while a value of 0 indicates no overlap between the two classifications. A classifier is considered moderately accurate with AUC values ranging between 0.7 and 0.9, and highly accurate with AUC values ranging between 0.9 and 1. We performed all ROC curve analyses using the ROC function provided in the R language and environment for statistical computing.

4- Results

4.1- Rat behaviour before bulbectomy

The Orientation component consisted of the rat walking from the back of the box, approaching the front wall, locating the slot, and poking the nose through to sniff the pellet, and ended when the forepaw transport started. Walking was characterised by cyclic motion of the limbs and a head-down posture (Alaverdashvili et al., 2008). When the macrovibrissae contacted the front wall, the head was raised, the nose poked through the slot, and the rat located the food by sniffing (Fig.4). Frame analysis showed that Orientation (duration mean group value: 412.98±95.53 ms) could be split into three intervals: Whisk T–First NT, i.e., the time spent detecting the front wall; First NT–Poke, i.e., the time spent locating the slot; and Poke–Reach start, i.e., the time spent detecting the presence of the pellet before the start of Transport (see Table 1). These intervals did not present

statistically different durations (p=1.00; n. trials 680; Kruskal-Wallis rank sum test). Once the rat located the pellet, the subsequent Transport response occurred, with the rat directing its forepaw through the slot towards the pellet (Fig 4). After grasping the food, the Withdrawal sequence was initiated, with the rat retracting its forepaw through the slot and bringing the pellet to its mouth (Fig 4). All values for variables in P trials (Table 1 and Figures 10–13) were consistent with the values (mean ± SE) obtained in control rats in previous experiments (Parmiani et al., 2018).

In no-P trials, the rat poked, sniffed to detect the pellet, then retracted the nose from the slot and went back to the posterior part of the box without executing reach (Fig. 5 vs. Fig. 4). Consequently, the trial duration was significantly reduced (Mean group value: 806.25±27.82 vs. 565.34±24.51 ms; p=0.000; n. trials 195; Kruskal-Wallis rank sum test, Table 1). However, there were no statistical differences in Whisker T–First NT and First NT–Poke between no-P and P trials (p=1 and p=1, respectively; n. trials= 149; Kruskal-Wallis rank sum test; Table 1). In no-P trials the Poke duration corresponded to the amount of time the rat nose was beyond the slot.

The surgery given to sham rats induced no effects on either the temporal sequence or the execution of the behavioural task (results not shown).

4.2- Rat behaviour after bulbectomy

After having bulbectomized control rats, we first analysed the mean frequency of approaches to the front wall (Fig. 10A). Kruskal-Wallis test comparison of control and bulbectomised rats revealed a major significant effect of bilateral bulbectomy (Kruskal-Wallis chi-squared=16.68; P=0.000). As regards the approach frequency, Holm post-hoc testing showed that this was significantly reduced at days 3–5 (P=0.001; n=28 sessions with 1447 trials), and at days 12–14 the frequency was still reduced but did not appear significantly different from controls (P=0.13; n=28 sessions with 1430 trials; Fig. 10A). However, the lesion induced no effect on the full execution of the Orient–Transport–Withdrawal sequence in P trials at days 3–5 and 12–14 (Fig. 4vs. Figs. 6, 8 and Fig. 13A), and the full sequence also appeared in all no-P trials at days 3–5 and 12–14 (Fig. 5 vs. Figs. 7, 9 and Fig. 13B).

In bulbectomised rats, no statistical differences were found when comparing behavioural parameters in P vs. no-P trials at either 3–5 or 12–14 days (Whisker T–First NT: P=1; First NT–Poke: P=1; Poke–Reach start: P=1; n= 380 trials; Kruskal-Wallis rank sum test, Tables 2–3). In light of this, only P trials were used to compare behavioural parameters at 3–5 and 12–14 days vs. controls. The

bulbectomised rat preserved the ability to detect the front wall and to locate the slot, since almost all approaches to the front wall were followed by nose poking into the slot (Fig. 10B). More in detail, there was no statistical difference in the time interval between whisker contact with the wall and the first nose touch (Whisker T–First NT, control vs. 3–5 days: *P*=0.93; n=205 trials; controls vs. 12–14 days: *P*=1; n=199 trials; Kruskal-Wallis rank sum test; Tables 1–3). That being said, there was a change in the way the bulbectomised rats located the slot. In control rats, when the microvibrissae/nose came into contact with the wall, the animal found the slot after a single contact or poked the nose directly into the slot with the nose positioned at the level of the shelf/pellet (Fig. 11A). After bulbectomy, however, the first nose touch with the wall took place in a head-down posture below the shelf/pellet level (Fig. 11A vs. 11B and C) and the animal located the slot through repetitive nose touches ('nosing': Welker, 1964). A clear increase in the number of nose touches was evident at 3–5 days (P=0.000; n trials= 235; Kruskal-Wallis rank sum test; Fig. 12), and at 12–14 days the values decreased but were still significantly higher in comparison to controls (P=0.000; n trials= 244; Kruskal-Wallis rank sum test; Fig. 12). Likewise, a clear increase in the First NT–Poke interval in comparison to controls was evident at 3–5 and at 12–14 days (controls vs. 3–5 days: P=0000; n trials=205; controls vs.12–14 days: P=0000; n trials=199; Kruskal-Wallis rank sum test; Tables 1–3). By contrast, the Poke–Reach start interval did not change after bulbectomy (controls vs. 3–5 days: P=1; n trials=241; controls vs. 12–14 days: P=1; n trials=243; Kruskal-Wallis rank sum test; Tables 1–3). That being said, there was an increase in the Orient time at 3–5 days (P=0.000; n trials=241, Kruskal-Wallis rank sum test; Tables 1–2) and at 12–14 days (P=0.0003; n trials=243; Kruskal-Wallis rank sum test; Tables 1–3) in comparison to controls, but this was solely due to the increased time of First NT–Poke interval.

Bulbectomy resulted in no changes in the Transport duration (controls vs. 3–5 days: P=0.034; n trials=242; controls vs.12–14 days: P=1; n trials=244; Kruskal-Wallis rank sum test; Tables 1–3) nor the duration the paw spent out of the slot when compared to controls (controls vs. 3–5 days: P=0.316; n trials=241; controls vs. 12–14 days: P=0.306; n trials=243; Kruskal-Wallis rank sum test; Tables 1–3). Finally, the bulbectomy did not reduce the ability to grasp the pellet successfully as compared to controls (controls vs. 3–5 days: P=0.492; n trials=1047; controls vs. 12–14 days: P=0.055; n trials= 986; Kruskal-Wallis rank sum test).

4.3- Skilled Reaching in rat behaviour

Analysis of the video-recordings of the skilled reaching task at reduced speed not only provided an overview of their behaviour in the box, but also enabled us to distinguish the three successive components of behaviour that may potentially be influenced by whisker/nose input (Alaverdashvili and Whishaw 2013), namely Orient, Transport and Withdrawal.

As mentioned above, the Orient component consisted of the rat walking from the back of the box, approaching the front wall, and ended with their locating the slot and poking their nose through to sniff the pellet. The walking was characterised by cyclical motion of the limbs and a head-down posture (Alaverdashvili et al., 2008) with exploratory whisking, during which only the longer mystacial macrovibrissae of row D and E contacted the wall (Berg and Kleinfeld, 2003). When the macrovibrissae contacted the front wall, the head was raised, the nose poked through the slot, and the rat located the food by sniffing (Whishaw and Tomie, 1988; Hermer-Vazquez et al., 2007) (Fig. 4, A and B). In control rats (n=8) the mean frequency of approaches to the front wall was 3.98±0.28/min (range: 2.2-6.8/min). The ratio between approaching vs. poking was 100% in all control rats (n=6), and the mean delay between whisker touch–nose poke, which measured the time the rat spent locating the slot, was 214.47±6.75 ms (range: 100-530; n=167) (Fig. 14 A-B, single rat values in Tables 5 and 6).

Once the rat located the food, the subsequent Transport response occurred, with the rat directing its forepaw through the slot towards the pellet. Analysis of the video-recordings at reduced speed confirmed that the reaching-grasping featured movement elements in the sequence described in the literature (Alaverdashvili et al., 2008; Alaverdashvili and Whishaw 2013) (Fig. 14). Generally, the reaching movement started almost 193.96±13.04ms (range:20-2015; n=163) after the nose poke; it lasted for 138.16±5.01ms (range:50-340; n=160) (Fig. 14 B–D, single rat values in Tables 5 and 6) and was only rarely preceded by attempts (0.13±0.03).

After grasping the food, the Withdrawal sequence was initiated, with the rat retracting its forepaw through the slot and directing the pellet to the mouth to eat. This behaviour involved both forelimb and mouth movements (Fig. 14E).

The surgery given to sham rats induced no effects on either the temporal sequence or the execution of the behavioural task (results not shown).

4.4- Skilled reaching after macrovibrissae bilaterally trimming

After macrovibrissae trimming, the mean frequency of approaches to the front wall was not significantly different with respect to controls (trimmed vs. control: 3.98±0.28/min vs. 3.28±0.23min, n=3 *p*=0.45; Kruskal-Wallis test by ranks), and, like control rats, the ratio between trimmed rats' poking vs. approaching was 100%. That being said, there was a change in the way the trimmed rats detected the front wall and located the slot. Indeed before trimming, the same rats detected the front wall by whisker touch, the snout not touching it before the nose poke (Fig. 14A and B vs. Fig 15 A), while after trimming they detected the presence of the wall by hitting it with the nose, only locating the slot after repeated nose touches. Unsurprisingly, therefore, the number of nose touches preceding poking was significantly higher in trimmed rats than in controls (mean number of touches in trimmed vs. control: 2.45±0.14 vs. 0.52±0.07, *p*=0.0000**;**Wilcoxon rank sum test, single rat values in Table 5). The mean delay between first nose touch and nose poke was 202.74±16.19ms (range:30-675; n=61**;** Fig. 15 A–C, single rat values in Table 5), and in each trial the mean delay between the first nose touch and nose poke was directly related to the number of touches (R=0.79; p=0.000; Pearson's product moment correlation coefficient). This delay measured the time spent locating the slot by nose touches, and was not comparable to the corresponding whisker touch–nose poke interval in the same rats before trimming (see Table 5). In contrast, macrovibrissae trimming resulted in no changes in the reaching-grasping-retracting components of skilled reaching: neither the number nor the temporal sequence of the task differed with respect to the same rat before trimming. In particular, there was no difference between either the nose poke–reach start delay or the reach duration after trimming when compared to controls (Table 5 trimmed vs. control: p=0. 47 and p=0. 32, respectively; Wilcoxon rank sum test).

4.5- Skilled reaching after bilaterally ION-severed

In rats with bilateral ION-severing (n= 3), whisker deafferentation induced a marked effect on the structure of the skilled behaviour. Video-recordings were executed daily until about three weeks, when the rat recovered the reaching-grasping movement, but changes were already detectable in the first post-surgical recording sessions. Specifically, in 67% of trials (n=318), the ION-severed rat, after arriving at the front wall of the box, stopped in front of the slot, but failed to locate it and insert its nose; after standing in front of the wall, the rat went back to the rear of the box. In other words, the behavioural sequence of the task was interrupted before the end of Orient (Fig. 16). In the remaining 33% of trials, the ION-severed rat, when arriving at the front wall of the box, inserted

its nose through the slot and sniffed but without starting the reaching movement; while sniffing, the preferred forelimb remained resting on the floor of the box (Fig. 17). In this case, the behavioural sequence was considered to interrupt before Transport. From the sixth day onward, in some trials the animal, approaching the front wall, explored it with repetitive forelimb movements for a few seconds, but without inserting its nose into the slot or executing a reaching movement to grasp the pellet (Fig. 18). The reaching-grasping movement reappeared on either the same day or the subsequent day, and was then followed by Withdrawal (Fig. 19). The full reaching-grasping-retracting sequence reappeared between 6 and 12 days after ION severing, depending on the animal. Frame-by-frame video analysis showed that, although the complete Transport and Withdrawal sequence of behaviour was restored, it initially had a longer duration than in controls (Fig. 19). After about three weeks, however, the rat executed the task in a time comparable to that of controls (data not presented). In ION-severed rats, we analysed the mean frequency of approaches to the front wall. Kruskal-Wallis test comparing control and ION-severed rat revealed a major significant effect for bilateral ION-severing (Kruskal-Wallis *chi-squared*=21.84; *P*=0.0000). As regards the approach frequency, Holm post-hoc testing showed that this was significantly reduced at days 3–5 and 6–8 after ION severing with respect to the same rats before ION severing (3–5D: *P*=0.001; n=12 sessions with 318 trials; 6–8D: *P*=0.038; n= 10 sessions with 650 trials; Fig. 21).

In control rats, all approaches to the front wall were followed by nose insertion into the slot. However, 3–5 days after surgery, pair-wise comparison of proportions revealed a highly significant effect of ION severing on the percentage of nose insertion into the slot (*P*=0.000; n= 12 sessions with 318 trials; Fig. 22A) and in subsequent days percentages are still significantly lower than in controls (p=0.000; n= 28 sessions with 1845 trials; pairwise comparison of proportion; Fig. 22A). Likewise, after ION severing the animal approaching the front wall, explored it with repetitive paw movements. Pair-wise comparison of proportions comparing control and ION-severed rats showed that bilateral ION severing had a major significant effect in this regard (*P*=0.0018; n= 12 sessions with 318 trials; Fig. 22B). Indeed, this behaviour was not present in controls, appeared at very low frequency 3–5 days post-injury, and showed a significant increase at 6-8 and 9–11 days (*P*=0.0000; n=27 sessions with 1842 trials, pair-wise comparison of proportions computed using a binomial model; Fig. 22B). We also calculate how many times the animal executed the reaching-grasping-retracting sequence with respect to the number of approaches. Once again, pair-wise comparison of proportions comparing control and ION-severed rats showed a major significant effect, as the movement was totally absent 3–5 days after lesion (*P*=0.0000; n= 12 sessions with 318 trials; Fig. 22C), but at 6–8 days its frequency was significantly different (*P*=0.0000; n= 10 sessions with 650 trials; pair-wise comparison of proportions computed using a binomial model; Fig. 22C). On

subsequent days, however, this movement frequency was not significantly different to controls (9-11: *P*=0.20; pair-wise comparison of proportions computed using a binomial model; Fig. 22C). Then, reaching-grasping reappeared 6–8 days after lesion and returning to baseline levels in 9–11 days where each approach to front wall was followed by reaching-grasping. We also considered the ratio between reaching-grasping and nose poke that gave an indication of the triggering power of nose insertion for the subsequent reaching-grasping movement. At 3–5 days after surgery, nose poke did not trigger reaching-grasping in any rats and nose poke began to trigger reaching-grasping once again after 6–8 days

To quantify each component of the skilled reaching task, both at the time of its reappearance and in the following days, we analysed trials obtained in control rats, and in the same rats after bilateral ION severing 1–3 and 3-5 days after the reappearance of reaching behaviour. Like trimmed rats, ION-severed rats detected the presence of the wall by hitting it with their nose, and then located the slot through repetitive nose touches. A clear increase in the mean number of nose touches was evident at 1-3 days (*P*=0.0000;n trials= 100; Kruskal-Wallis rank sum test; Tab.2) and at 3-5 days the values decreased but were still significantly higher in comparison to controls (*P*=0.0003; n trials= 100; Kruskal-Wallis rank sum test; Tab. 2).

Qualitative observation about the reaching-grasping-retract sequence duration, suggests us to quantify, for each trial, the time the paw is outside the slot during the reaching-grasping-retract movement. Figure 23A, is a cumulative histogram showing the mean values of these measures obtained in control rats, 1-3 and 8-10 days after reaching reappearance. A significant increase of the mean values is observed at 3-5 days (*P*= 0.0000), while at 8-10 days the values are increased but with a trend of significance in comparison to the controls (*P*=0.0523). Finally, we investigate whether a slowed execution of the reaching-grasping-retract sequence corresponds to a reduced ability to grasp pellets successfully. The cumulative histogram in the Fig. 23B, shows that success frequency is slightly reduced only in 1-3 days after reaching reappearance, with a trend to significance (*P*= 0.0952) in comparison to control.

5. Kinematic Results

5.1- Orienting kinematics in control rat

All kinematic values for OR were derived from the nose marker displacement, which is distinguishable throughout the entire movement (Fig. 24). Table 8 reports the median and IQR of trajectory length and duration, and peak and mean velocities for each animal and population data. All kinematic parameters show a relatively high inter- and intra-subject variability, as demonstrated by the IQR range. In each rat there were direct relationships between trajectory length and duration (r ranging from 0.62 to 0.79, P=0.000), and between trajectory length and peak velocity (r ranging from 0.31to 0.69, P<0.05). The 3D reconstruction of all trajectories for each rat shows smooth and continuous trajectories whose length and shape vary according to the position of the start point relative to the target (Fig. 28A). The 2D distribution of start/end points on the XY and XZ axes shows that for each rat the start points are dispersed, while the end points are focused toward the target (Fig. 29A and B, empty and filled red triangles, respectively). Quantitative analysis of the starting point distribution on the X, Y and Z axes in all rats reveals that on the X axis the median starting point value was 41.06 mm (ranging in a single rat from 39.65 to 42.07 mm), and the IQR was 8.07 mm (ranging in a single rat from 12.61 to 5.06 mm); on the Y axis, the median start point was -0.12 mm (ranging in a single rat from -1.01 to 5.08 mm), and the IQR was 21.95 mm (ranging in a single rat from 27.88 to 13.82 mm); on the Z axis, the median start point was 0.36 mm (ranging in a single rat from -8.76 to 10.28 mm), and the IQR was 13.54 mm (ranging in a single rat from 10.5 to 5.24 mm). It is clear that all X axis values are positive, and are less dispersed than values on the other axes; the median along the Y axis coincides with zero (target position), with values symmetrically displaced with respect to it; and, finally, the median along the Z axis close to zero is due to the fact that in two animals the median value was negative, while in the other two it was around zero and in the last animal it was positive.

The frame-by-frame video-analysis of the OR movement highlights three successive steps: head approaching toward the front wall (HA), localizing the slot by touching the nose to the front wall with small head adjustment movements (SL), and poking the nose through the slot to sniff the pellet (PK) (Fig. 1; Parmiani et al., 2018). However, in some trials, the animal arrived close to the front wall and directly inserted its nose into the slot without head adjustments. Taking into account all rats, 83.08% of OR trajectories presented all three steps, while in the remaining 16.92%, HA was followed directly by PK (Fig. 31: A vs. B). The OR trajectories with three steps showed significantly greater length and duration than the trajectories that did not present the SL step (long trajectories, median length: 62.05 mm, MAD: 12.95 mm, vs. short trajectories, median length: 49.96 mm, MAD: 9.34 mm, p=0.0000; long trajectories: median duration: 440 ms, MAD: 100 ms, vs. short trajectories, median duration: 260 ms, MAD: 85 ms, p=0.0000, Wilcoxon rank test). Figure 31 shows an example of long and short trajectories (A vs. B) and their respective velocity

profiles on the X, Y and Z axes (C vs. D). The long trajectory (Fig. 31A) presents HA (interval 1–2), with major displacements on the X and Z axes; followed by SL (interval 2–3), with smaller successive displacements along the X, Y and Z axes; and then PK (interval 3–4), with a displacement mainly along the X axis. The short trajectory does not present the SL step (Fig. 31B). As highlighted by velocity profiles on the X, Y, and Z axes (Fig. 31C and D), HA onset (point 1) corresponds to OR onset, and its end is the time-point of first minimum velocity on the X axis (point 2), i.e. the point where the nose marker has arrived close to the front wall. SL is characterized by small velocity oscillations along the X, Y and Z axes between HA and PK (point 2). PK onset is defined as the time-point (in ms) at which the tangential velocity exceeds 5% of the last velocity peak on the X axis (point 3), and its end corresponds to the OR end point (point 4). Figures 31E and F shows that these steps are characterized by different duration and velocity values: SL is the longest-lasting step in long trajectories (p=0.0000, Kruskal-Wallis test by ranks, followed by Dunn's post hoc test), while HA is the step presenting the highest velocity when compared to SL and PK (p=0.0000, Kruskal-Wallis test by ranks, followed by Dunn's post hoc test).

5.2- Reaching kinematics in control rat

All kinematic values for RC are derived from the wrist marker displacement, which is well distinguished throughout the entire movement (Fig. 24). An exemplificative case of the wrist marker trajectory during RC is illustrated in the Figure 26A (green trace: 2–3): in this example the movement starts about 60 mm along the X axis (2), and ends just beyond the slot, about 10 mm above the target (3). The wrist marker displacement on the Z axis versus time also shows the maximum elevation at the end of RC (Fig. 26B, 3 on green trace). The tangential velocity profile is bell-shaped, with one predominant peak, which is always higher than the predominant peak velocity in the OR movement (Fig.26C green trace 2–3 vs. red trace 1–2). Table 8 reports the median of trajectory length and duration, and peak and mean velocities for each animal and population data. All kinematic parameters show a relatively high inter- and intra-subject variability, as demonstrated by the interquartile range (IQR, Table 8, numbers in italics). In each rat there is a direct relationship between trajectory length and duration (r ranging from 0.64 to 0.81, P=0.000), trajectory length and mean velocity (r ranging from 0.22 to 0.49, $P< 0.05$) and peak velocity (r ranging from 0.34 to 0.53, $P< 0.05$).

The 3D trajectory reconstruction, performed in each rat, shows a characteristic pattern; all trajectories appeared smooth and continuous with variable length and shape in function of the

position of the starting point relative to the target (Fig. 28B). To evaluate spatial distribution of the start/end points of reaching trajectories, a 2D representation of all start/end points on the XY and XZ planes were plotted for each rat. As can be seen from the example in Figures 29A and C (XY and XZ axes distributions, respectively, green circles), the start points of reaching are dispersed (Fig. 29A and C, empty green circles); conversely, all end points are focused towards the target and are localized in front of it, mostly at the inner side of the front wall, owing to the position of the wrist marker (Fig. 29A and C, filled green circles).

A quantitative analysis of RC start point distribution on the X, Y and Z axes in all rats shows that the median start point on the X axis was 66.61 mm (ranging in a single rat from 68.99 to 60.52 mm), with an IQR of 22.69 mm (ranging in a single rat from 29.64 to 12.54 mm); the median start point on the Y axis was 15.22 mm (ranging in a single rat from 24.40 to 6.01mm), IQR 16.30 mm (ranging in a single rat from 16.28 to 8.38 mm); and the median start point on the Z axis was -19.80 mm (ranging in a single rat from -24.97 to -16.74 mm), IQR 7.47 mm (ranging in a single rat from 9.99 to 2.15 mm). In all rats, X axis values were positive and more dispersed than those on the other axes; the Y axis values were also positive, since all animals were right-handed, and those on the Z axis were negative, since the start points were below the target position.

In Figure 29C, we can discern two different bimodal RC start point distributions, one along the X axis and the other along the Z axis. Along the X axis, in relation to the distance from the target, we can distinguish between far and near start points i.e. beyond or within the first quartile from the target. Based on this, long and short RC trajectories may be analysed separately (Fig. 29A vs. C: long trajectories, median: 76.35 mm, MAD: 7.81 mm, vs. short trajectories, median: 49.36 mm, MAD: 5.86 mm, p=0.0000, Wilcoxon rank test), as they are also characterized by different durations (long trajectories, median: 200 ms, MAD: 30 ms, vs. short trajectories, median: 140 ms, MAD: 20 ms, p=0.0000, Wilcoxon rank test). Long trajectories are characterized by an intermediate phase of wrist/paw advancement (one velocity peak on the X axis: Fig. 32A2) between two phases of elevation (two velocity peaks on the Z axis: Fig. 32A3). Both velocity peaks on the Z axis are approximately three times lower than those on the X axis. Short trajectories, on the other hand, are characterized by a single phase of wrist elevation and advancement toward the target with a single peak on the X and Z axes, occurring at around 40% of the normalized duration, and the velocity peak on the Z axis is half the size of the peak on the X axis (Figs. 32 A3 vs. A2).

In relation to the Z axis distribution, within short trajectories (Fig. 29B) we can distinguish two modalities of reach start, depending on the position of the paw in that precise moment, i.e. in the stance or swing phase of the last step. Quantitative analysis reveals that 53% of swing trajectories were short trajectories, and 79% are distributed above the value of -18 mm along the Z axis.

Video-recording analysis highlighted that the wrist/paw position at the end of RC tended to occupy the same spatial position as the nose at the end of OR (Figs. 34, A and B). To verify this observation, we plotted the cumulative normalized displacements of the nose marker during OR, and the wrist marker during RC on the X, Y and Z axes separately (Fig. 34 C–E), and then as 3D coordinates (Fig. 34 F). X, Y and 3D plots clearly show a convergence of nose and wrist marker displacements at the end of the OR and RC movements, while the Z plot shows a parallel displacement of the two markers due to the their anatomical position.

5.3- Kinematic variables and successful trials

Finally, we were interested in identifying which of the described start and end point variables could determine correct prehension of the pellet, i.e. a successful trial. To this end, we used a logistic regression statistical model to find kinematic variables with statistically significant regression coefficients for the nose/wrist and digit markers (Fig.36, A and B).

After the final refinement of the nose/wrist marker model, we found five kinematic variables (Fig. 36 C 1–5), specifically: 1) the wrist position on the X axis at RC end (regression coefficient = -0.306, P=2.08e-15); 2) the wrist position on the Y axis at RC end (regression coefficient = 0.353, P=1.4e-11); 3) the nose position on the X axis at RC end (regression coefficient = 0.277, P=3.75e-06); 4) the nose position on the Y axis at RC end (regression coefficient = -0.206, P=9.71e-05); and 5) the nose position on the Z axis at RC end (regression coefficient = -0.189, P=3.14e-05). Final refinement of the digit marker model, on the other hand, yielded four kinematic variables (Fig.36 D 1–4), specifically: 1) the digit position on the X axis at GR start (regression coefficient = -0.581, P=0.003); 2) the digit position on the Y axis at GR start (regression coefficient = -0.734, P=0.001); 3) the digit position on the Z axis at GR start (regression coefficient = 0.457, P=0.031); and 4) the digit position on the Z axis at GR end (regression coefficient = -0.570, P=0.037). The ability of the model to correctly discriminate between successful and unsuccessful trials was assessed by computing the area under the ROC curve (AUC), plotted by computing the True Negative Rate (specificity) and the True Positive Rate (sensitivity) at each threshold of sensitivity and specificity. The AUC value was 0.83 for the final nose/wrist model (Fig. 36 E), and 0.92 for the final digit model (Fig. 36 F).

6. Discussion

6.1- Bulbectomy vs. olfaction in guiding skilled reaching behaviour

In this study, the high-speed video-recording followed by frame-by-frame analysis enabled us to investigate more exhaustively how olfactory cues influence single-pellet skilled reaching.. In order to identify the specific role of olfactory cues, we considered each trial as composed of three behavioural responses: Orient (approach to front wall, slot localisation and nose poke until reach start), Transport (reaching-grasping) and Withdrawal (paw retraction) (Alaverdashvili & Whishaw, 2013). In this study, the trial started when the whiskers contacted the front wall and ended when the paw re-crossed the slot during retraction. This enabled us to study the behavioural events preceding as well as following nose poke.

To verify the use of olfaction in pellet detection, we employed two different experimental conditions: P and no-P trials. We used no-P trials instead of the non-food odour pellet to avoid potential confounding odours (Hermer-Vazquez et al., 2007). Control rats never executed reaching in no-P trials, while after bulbectomy the same rats did so, confirming the use of olfaction rather than vision in pellet detection (Whishaw and Tomie, 1989).

In exploratory behaviour, characterised by a coordination of orofacial motor actions (Ranade et al., 2013; Kurnikova et al., 2017; Severson & O'Connor, 2017), walking occurred with a head-down posture (Alaverdashvili et al., 2008), and only the longer mystacial macrovibrissae of row D and E contacted the box floor (Berg & Kleinfeld, 2003). The frame analysis in control rats showed that Orient could be subdivided into three phases of equal duration: Whisk T–First NT, i.e., the time spent in detecting the front wall; First NT–Poke, i.e., the time spent in the locating slot; and Poke–Reach start, i.e., the time spent in sensorimotor integration until the reach start. The observation that in controls there were no differences between P and no-P trials in the first two quantifiable aspects of Orientation suggests that intact rats do not make use of specific olfactory cue to reach the target. Basically, they learn, after training, where exactly to go and once the slot is poked, they switch into olfactory mode, finally deciding whether to grasp or not the pellet.

After bulbectomy, rats seem to have partially lost the orienting strategy, indeed, they reduced the frequency of approaches to the front wall and, secondly, they approached the front wall and contacted it with a head-down posture, so the first nose contact was localised below the level of the

shelf. A possible explanation is that rat explored the box with the intact whisker/nose sense, causing it to maintain a head-down posture until its nose arrived at the wall. Bulbectomy had profound and enduring effects on the total orient duration; indeed, this remained longer than the pre-surgical value throughout the two weeks of recording. Surprisingly, when considering each orient phase, the Whisker T–First NT phase duration did not change after bulbectomy, suggesting that the delay between macrovibrissae collision and the nose touching the wall did not depend on olfaction. Conversely, First NT–Poke duration greatly increased in all rats throughout all recording sessions, concurrent with a significant increase in the number of nose touches in each trial before poking. Bulbectomized rats used microvibrissae/snout tactile sense to search for the slot with the nose repetitively hitting the wall. These altered orient aspects were seen in all rats, and persisted over the entire recording period. Then, bulbectomy, but not necessarily olfaction, affects the searching strategies by impairing the motor behaviour whereas olfaction determines the choice to reach/grasp the target. 14 days after bulbectomy, it appears a partial recovery in the First NT-Poke phase, suggesting that rats have only partially re-gained some sort of spatial information.

First NT–Poke duration and the number of nose touches in single trials also increased in rats deprived of vibrissae/nose tactile sense following infraorbital nerve severing (Parmiani et al., 2018). This indicates that the presence of olfactory as well as vibrissal systems are necessary for fast and efficient detection of the slot.

Finally, we calculated the Poke–Reach start duration in order to obtain a measurement of the sensorimotor integration time that elapses between the insertion of the nose into the slot and the start of reach. We did not find any differences in this value between experimental groups of rats. A possible explanation is that sniffing to detect the pellet on the shelf is carried out in parallel with the tactile exploration of the slot, which makes the animal aware of the nose position. Therefore, the olfactory cue subtraction may not affect the duration of the tactile integration that leads to reach start. Indeed, in bulbectomised rat, sniffing was absent and the nose was raised almost immediately after poking, so the interval between nose insertion and nose raise was shorter than in controls, as shown by Whishaw and Tomie (1989). However, we observed that there was no fixed relationship between nose elevation and reach start, since in some trials nose elevation preceded reaching and in others it followed it. The nose-in–nose-elevation interval did not match the Poke-Reach start interval, and represents only a variable part of it.

In a previous paper we suggested that microvibrissae/nose-mediated sensory information is the trigger for reaching movement, since after bilateral infraorbital nerve severing, reaching does not automatically follow nose poking, and the sequence of trial is interrupted (Parmiani et al., 2018).

The observation that bulbectomised rats execute the full sequence of movements in P as well as in no-P trials from the first recording session suggests that olfactory cues are not involved in triggering reaching movement.

In summary, the present study suggests, in line with previous results (Whishaw and Tomie 1989) that olfaction is not used to guide reaching once the movement begins. Indeed, bulbectomy results in no changes to the reaching-grasping-retracting components of skilled reaching; neither the number nor the temporal sequence of the task differed with respect to the same rat before bulbectomy. Finally, the observation that success rates are maintained in bulbectomised rats confirms that the success of reaching-grasping is not dependent upon olfaction.

To postulate a hypothesis about the role of olfactory cues in reaching, we can start from the following observations: i) control animals always perform reaching in P trials but never in no-P trials; ii) bulbectomised animals always perform reaching, in both P and no-P trials; and iii) bulbectomy does not alter any reaching-related parameter. Taken together, these results suggest three possible conclusions about the function of olfactory cue: i) it has an inhibitory role on reaching start when the pellet is not present; ii) this inhibitory role is suppressed when the pellet is present; and iii) the inhibitory role is persistently lost after bulbectomy.

6.2- Whisker sense in skilled reaching behaviour

This experiment was designed to investigate whether and how rats use their whisker sense in skilled motor behaviour. Indeed, previous studies have found a significant role of whisker sense in many types of motor behaviour (Anjum et al, 2006; Hartmann, 2011; Grant et al., 2012), but its role in skilled reaching has never previously been explored. However, present data our data confirmed previous data shows that whisker sense is in fact an important tool in skilled reaching task execution.

Skilled reaching is a composite behaviour (Alaverdashvili et al., 2008) and, in order to better identify the specific roles of whisker sense in this pattern, we consider each trial as composed of four successive behavioural phases. The first, phase A, which consists of the rat walking from the back of the box towards the front wall, was interpreted as a measure of the rat's ability to orientate itself in the box towards the food. It is already known that whisker sense plays a role in environmental navigation (Brecht et al., 1997; Erlich et al., 2011; Mitchinson and Prescott, 2013), and we therefore speculated that it could drive active exploration in the box under our experimental conditions. Consistent with this hypothesis, the bilaterally ION-severed rats performed a smaller number of approaches to the front wall, the subtraction of whisker sense apparently reducing their

ability to explore. Phase A was followed by Phase N, which consists of localisation of the slot position and nose insertion through it to locate the food. In this phase, the rat switches from using its whiskers to explore the floor surface during the approach (Arkley et al., 2014) to using them to explore the front wall in order to determine the position of the slot; in this case, the whiskers are primarily utilised for depth perception (Ahissar and Knutsen, 2011) with the aim of locating the slot and inserting its nose. In accordance with this hypothesis, bilaterally ION-severed rats show a transient but significant reduction in phase N frequency, with trial sequence interruption after approaching the front wall. This suggests that subtraction of whisker sense also reduces the ability of the rat to explore the front wall and prevents slot recognition. Despite the loss of whisker sense, however, the rat should be able to locate the pellet using its sense of smell, since olfaction is used to locate food and direct reaching (Whishaw and Tomie, 1989; Hermer-Vasquez et al., 2007; Parmiani et al., 2019, submitted). Unlike the data from the above two experiments in which olfaction is suppressed and whisker sense preserved, we observed that when the bilaterally ION-severed rat succeeds in placing its nose in the slot, the reaching-grasping movement does not automatically follow. This observation strongly suggests that whisker sense triggers skilled reaching in rats. Specifically, having observed that macrovibrissae trimming does not alter the behavioural sequence recorded in controls, it follows therefore that microvibrissae-mediated sensory information may be the trigger for the reaching movement. Furthermore, our observation (data not presented) that unilateral ION severing does not alter the sequence of movements recorded in controls indicates that the sensorimotor whisker system contains dense reciprocal connections that enable sensory information from one whisker pad to trigger reaching in the preferred forelimb, regardless of whether it is contra- or ipsilateral to the lesion.

Before bilateral ION severing, all rats explored the front wall of the box exclusively with their whiskers, while forelimbs were involved in postural adjustments (Alaverdashvili et al., 2008). From the sixth day after lesion, however, the rat in some trials explores the front wall with repetitive forelimb movements for a few seconds without inserting its nose into the slot or reaching to grasp the pellet. We hypothesise that this phase could be the expression of a sensorimotor strategy utilised to collect sensory information from active paw sense to compensate for the absence of active whisker sense.

Nevertheless, on the same or subsequent day, the reaching-grasping-retract movement reappeared in all rats. In rodents the reach-to-grasp movement is not visually guided, and is pre-planned and semi-ballistic (Sacrey and Whishaw, 2012; Karl et al., 2013). In light of this, skilled reaching should not be altered by suppression of the whisker sense.

A major aspect of our findings is that post-lesion behavioural deficits occur immediately after injury, and are consistent in all bilaterally ION-severed rats. Interestingly, however, bilaterally ION-severed rats present different recovery times of reaching-grasping and retracting movements. Although we cannot provide a direct explanation of these different recovery rates, we did note that rats with slower recovery spent more time achieving stable performance in the skilled reaching task before ION severing (almost 6–7 vs. 4–5 weeks).

At this point the significant question arises as to whether functional recovery is a peripheral or central phenomenon. Our data strongly support the latter hypothesis, since whisker pad sense was proven to be blocked throughout the recording period (see Methods), and all rats presented a severe and persistent alteration in spontaneous grasping, with no recovery. While the rat normally grasps the pellet with its mouth, after bilateral ION severing it is rarely able to grasp with the mouth, but instead grasps with the paw when the paw comes into contact with the pellet 'by accident'.

Another question regards the real causal role of whisker sense in skilled reaching behaviour. That is whether, in accordance with current debate, whisker sense provides permissive or instructive information in skilled reaching behaviour control (Otchy et al., 2015; Stuttgen and Schwarz, 2017). Briefly, Otchy et al., 2015 defined a brain area "permissive" for a function if it does not provide essential information for any task-relevant computation, and "instructive" for a function if it contributes essential information that is not otherwise available. Thus, when monitoring the time course of effects of chronic lesions, the circuit involved is considered permissive if the effects, beginning immediately after surgery, disappear days later, and is instead considered instructive if the effects persist for a prolonged period of time. Our results, based on a behavioural study, show that bilateral ION severing effects are reversible, suggesting that whisker sense may be permissive for skilled reaching, i.e. that it is a learned, rather than spontaneous behaviour.

The last question arising from our behavioural data regards how and where the recovery mechanisms take place. It is known that rats' olfactory, whisker sense and proprioceptive input interact with one another to guide skilled reaching behaviour (Whishaw and Tomie, 1989; Kleinfeld et al., 2014), and that projections from various sensory cortical areas, including somatosensory, visual, auditory and entorhinal cortices, converge on the posterior parietal cortex (Reep et al., 1994; Lee et al., 2011), which plays a causal role in guiding sensorimotor responses (Save et al., 2005; Raposo et al., 2014; Licata et al., et al., 2017). In conclusion, therefore, we suggest that permanent whisker sense removal may have far-reaching effects in all connected central sensorimotor structures normally used by rat in this behaviour, and that compensation could be mediated by olfactory information from the entorhinal cortex converging on the posterior parietal area.

6.3- Skilled Reaching Kinematics discussion

This study provided the a new experimental set-up for 3D recording of skilled-reaching kinematics; it represents a step forward with respect to the conventional descriptions made from frame-by frame or cineradiographic analysis (Whishaw and Pellis, 1990; Alaverdashvili et al., 2008). In addition, the logistic regression analysis we performed provided new perspectives in defining predictors related to the outcome of skilled-reaching tasks.

The method provides insight into the motor organization of skilled movement in the rat, highlighting the orienting-to-food behaviour, the relationship between wrist movement and nose movement. Using three high-speed infrared digital cameras to track the entire expected range motion of marker movements in a large capture volume, we obtained a 3D recording of full skilled reaching kinematics in a rat moving freely in the reaching box, which was previously unavailable. 3D kinematics were analysed by Qualisys Track Manager software and MATLAB, a set-up designed to be reliable, high-performance and easy to use, which measures the distance between two constantly visible markers rotating in the capture volume. Using this set-up, tracking can be done in real-time, with minimal latency, or in post-processing. Qualisys trajectory editing made it easy to identify, edit and process trajectories and detect artefacts. This approach undoubtedly represents an improvement with respect to high-speed single camera recording (Wong et al., 2015; Ellens et al., 2016; Nica et al., 2018; Parmiani et al., 2018), but Qualysis, as all passive optical systems, is limited by its inability to measure motion when markers move within 2 mm of each other, as well as a high set-up cost. Although the new approach involving machine-learning algorithms such as DeepLabCut presents higher resolution and greater degrees of freedom at a single digit level than our method, it requires time-consuming digitization of joint segments for markerless videorecordings (Mathis et al., 2018; Bova et al., 2019). Our method, on the other hand, required significantly reduced time to label data, and obviates the need for off-line manual marking of videos. Furthermore, it provides an efficient means of capturing volumes containing the entire range of marker movements in the rat.

Indeed, the set-up allowed us to simultaneously record the movements of the wrist and nose markers. By off-line reconstruction and analysis of these marker trajectories, we identified kinematic criteria for defining the beginning and the end of each movement which proved to classify the movement components effectively in all the animals studied.

6.3.a- Orienting movement

The orienting movement comprises the coordination of different body parts, including the eyes, ears, head, and trunk. Unlike higher vertebrates, the rat uses the head as the primary prehensile organ, so in OR head movements this plays a major role. In fact, such functional repertoires may have generated different neck muscle architecture and their functional control (Isa and Sasaki, 2002). In previous papers, the OR movement was considered to consist of walking from the back to the front of the box, where the rat poked and sniffed to detect the presence of the pellet on the shelf (Whishaw and Pellis, 1990; Gharbawie and Whishaw, 2006; Alaverdashvili and al., 2008).In our experiments, OR was considered to comprise the head movement after the macrovibrissae contact the front wall, followed by slot localization and the nose poke through it (Parmiani et al., 2018). Walking to front wall, the rats approached it from the right or the left with respect to the midline, and the subsequent OR start points were symmetrically distributed along the Y axis. Indeed, when starting OR, the nose could be below or above the target/pellet, and behaviourally speaking the OR movement could consist of elevating, lowering or linear advancement of the head toward the front wall. Comparing kinematics values for OR vs. RC movements, OR was characterized by a slightly shorter trajectory length but longer duration, while maximum and mean speeds were lower than RC values. Both behavioural and kinematic analyses highlighted that OR movement was composed of three successive steps: HA (head advance), SL (slot localization) and PK (poke). Triggered by macrovibrissae collision with front wall, HA was rapid, wide head displacement until the snout contacted the front wall. Then, SL, guided by repetitive snout/microvibrissae tactile exploration of the front wall, was characterized by slow, small head displacements around the slot. Finally, PK was a slow, small movement as the nose approached the pellet along the X axis. These data suggested that all of these three steps involved in OR could be feedback–guided, and that olfactory, somatosensory and proprioceptive input could be integrated in specific ways in the spatio-temporal development of each step (Whishaw and Tomie, 1989; Parmiani et al., 2018).

6.3.b- Reaching movement

Our kinematic analysis showed that RC movements were characterized by smooth trajectory displacement and bell-shape velocity profiles. Compared to the OR movement, RC showed similar

trajectory length, but with half the duration and double the speed. This suggested that RC was less controlled by sensory feedback than OR, and presented a ballistic nature (Jeannerod, 1988; Whishaw and Karl, 2014). These findings seem to support the idea that rodents, monkeys and humans share a number of kinematic features with regard to RC movements (Christel and Billard, 2002; Sacrey et al., 2009; Whishaw and Karl, 2014). In primates, the reach-to-grasp movement demonstrates consistency with regard to the effect of object size and object distance (Jeannerod, 1984; Jakobson and Goodale, 1991; Sartori et al., 2013a). In our set-up, the object/target size and position were fixed, and the reaching began at various distances from the target, allowing us to evaluate trajectories of different amplitude. Distance effects were significant for trajectory length, shape and duration, as well as the amplitude and number of velocity peaks, and the percentage of time to peak velocity. These kinematics parameters did not support the principle of "isochrony", according to which the movement velocity, depending on the amount of distance to cover, produces a constant duration of movement (Viviani and Mcollum 1983). However, in the rat, skilled reaching is a conditioned behaviour, constrained in a box, and is therefore not comparable to the primate's reaching behaviour in a naturalistic setting, where isochrony is the rule (Sartori et al., 2013b).

Our kinematic results highlight two different modalities of starting the reach, namely in the stance or swing phase of the last step. In rodents and primates, behavioural and video-recording analyses have revealed similarities between forelimb stepping and reaching movements, which supported the theory of a common origin (Karl and Whishaw 2013). Semi-independent control of a single forelimb allowed the stepping movement to be adapted for a reaching movement (Bracha et al., 1990; Beloozerova and Sirot, 1993). This theory was corroborated by our results, which showing that RC can start either as an independent movement, during the stance phase of the last step, or it can originate within the last step itself, during the swing phase. The rat performed both stepping and RC movements in the absence of visual and on-line sensory cues (Metz and Whishaw, 2000; Wilkson and Sherk, 2005), but the whiskers, and/or tactile and olfactory information from the nose could be used to determine whether RC starts in stance or swing of the last step.

Interestingly, our findings showed that the wrist/paw position at the end of the RC movement tended to occupy the same spatial position as the nose at the end of the OR, and this relationship was a fixed spatial link in the present context. We therefore propose that the nose works as pointing system for wrist/paw positioning. Moreover, when considering the OR and RC end point distributions in all trials vs. successful trials, we noted that the OR distribution did not substantially change, while the RC distribution lacked points more distant from the target. This suggested that

unsuccessful reaching was explained not by the OR end-point positions, but rather by the RC end-point positions.

6.4- Spatial positions and outcome

Logistic regression analysis highlighted variables that contributed to determine a successful trial, and for each variable we tried to put forward a hypothesis to explain how it affected the outcome. For instance, the finding that the outcome was positively related to the nose position on the X, Y and Z axes at the end of RC suggests that head and forelimb displacements were also spatially coordinated within a pointing system in which the head was carried upward to allow the paw to cross through the slot. Furthermore, the negative relationship between the X axis RC end point and outcome was in line with the finding that error trials corresponded to the more distant end position from the target. Likewise, taking into account the fact that all rats were right handed, the positive Y axis RC end point/outcome relationship was in line with the observation that the final part of RC was a pronation that moved the palm over the pellet by abduction of the elbow and consequently displaced the marker laterally.

Overall, our results agreed with the idea, suggested for humans by Thaler and Todd (2009), that in the rat the sensorimotor system flexibly controls the nose/paw final position, as well as displacement kinematics.

7. References

Ahl, A.S. (1982) Evidence of use of vibrissae in swimming in Sigmo don fulviventer. *Animal Behaviour*, **30**, 1203–1206.

Alaverdashvili, M., Leblond, H., Rossignol, S., & Whishaw, I.Q. (2008) Cineradiographic (video X-ray) analysis of skilled reaching in a single pellet reaching task provides insight into relative contribution of body, head, oral, and forelimb movement in rats. *Behav. Brain Res.*, **192**, 232–247.

Alaverdashvili, M. & Whishaw, I.Q. (2013) A behavioral method for identifying recovery and compensation: hand use in a preclinical stroke model using the single pellet reaching task. *Neurosci Biobehav Rev*, **37**, 950–967.

Alloway, K.D., Lou, L., Nwabueze-Ogbo, F., & Chakrabarti, S. (2006) Topography of cortical projections to the dorsolateral neostriatum in rats: multiple overlapping sensorimotor pathways. *J. Comp. Neurol.*, **499**, 33–48.

Alloway, K.D., Smith, J.B., & Beauchemin, K.J. (2010) Quantitative analysis of the bilateral brainstem projections from the whisker and forepaw regions in rat primary motor cortex. *J. Comp. Neurol.*, **518**, 4546–4566.

Alloway, K.D., Smith, J.B., Beauchemin, K.J., & Olson, M.L. (2009) Bilateral projections from rat MI whisker cortex to the neostriatum, thalamus, and claustrum: forebrain circuits for modulating whisking behavior. *J. Comp. Neurol.*, **515**, 548–564.

Anjum, F., Turni, H., Mulder, P.G.H., van der Burg, J., & Brecht, M. (2006) Tactile guidance of prey capture in Etruscan shrews. *Proc. Natl. Acad. Sci. U.S.A.*, **103**, 16544–16549.

Arkley, K., Grant, R.A., Mitchinson, B., & Prescott, T.J. (2014) Strategy change in vibrissal active sensing during rat locomotion. *Curr. Biol.*, **24**, 1507–1512.

Arleo, A. & Rondi-Reig, L. (2007) Multimodal sensory integration and concurrent navigation strategies for spatial cognition in real and artificial organisms. *J. Integr. Neurosci.*, **6**, 327–366.

Aronoff, R., Matyas, F., Mateo, C., Ciron, C., Schneider, B., & Petersen, C.C.H. (2010) Long-range connectivity of mouse primary somatosensory barrel cortex. *Eur. J. Neurosci.*, **31**, 2221–2233.

Azim, E., Jiang, J., Alstermark, B., & Jessell, T.M. (2014) Skilled reaching relies on a V2a propriospinal internal copy circuit. *Nature*, **508**, 357–363.

Balbinot, G., Schuch, C.P., Jeffers, M.S., McDonald, M.W., Livingston-Thomas, J.M., & Corbett, D. (2018) Post-stroke kinematic analysis in rats reveals similar reaching abnormalities as humans. *Sci Rep*, **8**, 8738.

Beloozerova, I.N. & Sirota, M.G. (1993) The role of the motor cortex in the control of vigour of locomotor movements in the cat. *J. Physiol. (Lond.)*, **461**, 27–46.

Berg, R.W. & Kleinfeld, D. (2003) Rhythmic whisking by rat: retraction as well as protraction of the vibrissae is under active muscular control. *J. Neurophysiol.*, **89**, 104–117.

Berthoz, A. & Viaud-Delmon, I. (1999) Multisensory integration in spatial orientation. *Curr. Opin. Neurobiol.*, **9**, 708–712.

Bonnevie, T., Dunn, B., Fyhn, M., Hafting, T., Derdikman, D., Kubie, J.L., Roudi, Y., Moser, E.I., & Moser, M.-B. (2013) Grid cells require excitatory drive from the hippocampus. *Nat. Neurosci.*, **16**, 309–317.

Bova, A., Kernodle, K., Mulligan, K., & Leventhal, D. (2019) Automated Rat Single-Pellet Reaching with 3-Dimensional Reconstruction of Paw and Digit Trajectories. *J Vis Exp*,.

Brácha, V., Zhuravin, I.A., & Bures, J. (1990) The reaching reaction in the rat: a part of the digging pattern? *Behav. Brain Res.*, **36**, 53–64.

Brecht, M., Preilowski, B., & Merzenich, M.M. (1997) Functional architecture of the mystacial vibrissae. *Behav. Brain Res.*, **84**, 81–97.

Carvell, G.E. & Simons, D.J. (1990) Biometric analyses of vibrissal tactile discrimination in the rat. *J. Neurosci.*, **10**, 2638–2648.

Carvell, G.E. & Simons, D.J. (1996) Abnormal tactile experience early in life disrupts active touch. *J. Neurosci.*, **16**, 2750–2757.

Chakrabarti, S., Zhang, M., & Alloway, K.D. (2008) MI neuronal responses to peripheral whisker stimulation: relationship to neuronal activity in si barrels and septa. *J. Neurophysiol.*, **100**, 50–63.

Christel, M.I. & Billard, A. (2002) Comparison between macaques' and humans' kinematics of prehension: the role of morphological differences and control mechanisms. *Behav. Brain Res.*, **131**, 169–184.

Cicirata, F., Angaut, P., Cioni, M., Serapide, M.F., & Papale, A. (1986) Functional organization of thalamic projections to the motor cortex. An anatomical and electrophysiological study in the rat. *Neuroscience*, **19**, 81–99.

Deschenes, M. & Urbain, N. (2009) Vibrissal afferents from trigeminus to cortices. *Scholarpedia*, **4**, 7454.

Desmurget, M., Prablanc, C., Jordan, M., & Jeannerod, M. (1999) Are Reaching Movements Planned to be Straight and Invariant in the Extrinsic Space? Kinematic Comparison Between Compliant and Unconstrained Motions. *QUART J EXP PSYCH A-HUM EXP*, P. 52.

Diamond, M.E. & Arabzadeh, E. (2013) Whisker sensory system - from receptor to decision. *Prog. Neurobiol.*, **103**, 28–40.

Ellens, D.J., Gaidica, M., Toader, A., Peng, S., Shue, S., John, T., Bova, A., & Leventhal, D.K. (2016) An automated rat single pellet reaching system with high-speed video capture. *J. Neurosci. Methods*, **271**, 119–127.

Erlich, J.C., Bialek, M., & Brody, C.D. (2011) A cortical substrate for memory-guided orienting in the rat. *Neuron*, **72**, 330–343.

Farkas, T., Kis, Z., Toldi, J., & Wolff, J.R. (1999) Activation of the primary motor cortex by somatosensory stimulation in adult rats is mediated mainly by associational connections from the somatosensory cortex. *Neuroscience*, **90**, 353–361.

Filimon, F. (2010) Human cortical control of hand movements: parietofrontal networks for reaching, grasping, and pointing. *Neuroscientist*, **16**, 388–407.

Franchi, G. (2001) Persistence of vibrissal motor representation following vibrissal pad deafferentation in adult rats. *Exp Brain Res*, **137**, 180–189.

Gharbawie, O.A. & Whishaw, I.Q. (2006) Parallel stages of learning and recovery of skilled reaching after motor cortex stroke: "oppositions" organize normal and compensatory movements. *Behav. Brain Res.*, **175**, 249–262.

Grant, R.A., Sperber, A.L., & Prescott, T.J. (2012) The role of orienting in vibrissal touch sensing. *Front Behav Neurosci*, **6**, 39.

Gregoire, S.E. & Smith, D.E. (1975) Mouse-killing in the rat: effects of sensory deficits on attack behaviour and stereotyped biting. *Anim Behav*, **23**, 186–191.

Gustafson, J.W. & Felbain-Keramidas, S.L. (1977) Behavioral and neural approaches to the function of the mystacial vibrissae. *Psychol Bull*, **84**, 477–488.

Hartmann, M.J.Z. (2011) A night in the life of a rat: vibrissal mechanics and tactile exploration. *Ann. N. Y. Acad. Sci.*, **1225**, 110–118.

Hatsopoulos, N.G. & Suminski, A.J. (2011) Sensing with the motor cortex. *Neuron*, **72**, 477–487.

Hatsopoulos, N.G., Xu, Q., & Amit, Y. (2007) Encoding of movement fragments in the motor cortex. *J. Neurosci.*, **27**, 5105–5114.

Hermer-Vazquez, L., Hermer-Vazquez, R., & Chapin, J.K. (2007) The reach-to-grasp-food task for rats: a rare case of modularity in animal behavior? *Behav. Brain Res.*, **177**, 322–328.

Hermer-Vazquez, R., Hermer-Vazquez, L., Srinivasan, S., & Chapin, J.K. (2007) Beta- and gamma-frequency coupling between olfactory and motor brain regions prior to skilled, olfactory-driven reaching. *Exp Brain Res*, **180**, 217–235.

Hok, V., Poucet, B., Duvelle, É., Save, É., & Sargolini, F. (2016) Spatial cognition in mice and rats: similarities and differences in brain and behavior. *Wiley Interdiscip Rev Cogn Sci*, **7**, 406–421.

Hooks, B.M. (2016) Sensorimotor Convergence in Circuitry of the Motor Cortex. *Neuroscientist*,.

Hooks, B.M., Mao, T., Gutnisky, D.A., Yamawaki, N., Svoboda, K., & Shepherd, G.M.G. (2013) Organization of cortical and thalamic input to pyramidal neurons in mouse motor cortex. *J. Neurosci.*, **33**, 748–760.

Huntley, G.W. (1997) Correlation between patterns of horizontal connectivity and the extend of short-term representational plasticity in rat motor cortex. *Cereb. Cortex*, **7**, 143–156.

Huston, S.J. & Jayaraman, V. (2011) Studying sensorimotor integration in insects. *Curr. Opin. Neurobiol.*, **21**, 527–534.

Isa, T. & Sasaki, S. (2002) Brainstem control of head movements during orienting; organization of the premotor circuits. *Prog. Neurobiol.*, **66**, 205–241.

Iwaniuk, A.N. & Whishaw, I.Q. (2000) On the origin of skilled forelimb movements. *Trends Neurosci.*, **23**, 372–376.

Jacobs, L.F. (2012) From chemotaxis to the cognitive map: the function of olfaction. *Proc. Natl. Acad. Sci. U.S.A.*, **109 Suppl 1**, 10693–10700.

Jakobson, L.S. & Goodale, M.A. (1991) Factors affecting higher-order movement planning: a kinematic analysis of human prehension. *Exp Brain Res*, **86**, 199–208.

Jeannerod, M. (1984) The timing of natural prehension movements. *J Mot Behav*, **16**, 235–254.
Jeannerod, M. (1990) *The Neural and Behavioural Organization of Goal-Directed Movements*. Clarendon Press ;;Oxford University Press, Oxford [England] ;New York.
Jones, L.M., Depireux, D.A., Simons, D.J., & Keller, A. (2004) Robust temporal coding in the trigeminal system. *Science*, **304**, 1986–1989.
Karl, J.M., Schneider, L.R., & Whishaw, I.Q. (2013) Nonvisual learning of intrinsic object properties in a reaching task dissociates grasp from reach. *Exp Brain Res*, **225**, 465–477.
Karl, J.M. & Whishaw, I.Q. (2013) Different evolutionary origins for the reach and the grasp: an explanation for dual visuomotor channels in primate parietofrontal cortex. *Front Neurol*, **4**, 208.
Kawai, R., Markman, T., Poddar, R., Ko, R., Fantana, A.L., Dhawale, A.K., Kampff, A.R., & Ölveczky, B.P. (2015) Motor cortex is required for learning but not for executing a motor skill. *Neuron*, **86**, 800–812.
Klein, A., Sacrey, L.-A.R., Whishaw, I.Q., & Dunnett, S.B. (2012) The use of rodent skilled reaching as a translational model for investigating brain damage and disease. *Neurosci Biobehav Rev*, **36**, 1030–1042.
Kleinfeld, D. & Deschênes, M. (2011) Neuronal basis for object location in the vibrissa scanning sensorimotor system. *Neuron*, **72**, 455–468.
Kleinfeld, D., Deschênes, M., Wang, F., & Moore, J.D. (2014) More than a rhythm of life: breathing as a binder of orofacial sensation. *Nat. Neurosci.*, **17**, 647–651.
Kurnikova, A., Moore, J.D., Liao, S.-M., Deschênes, M., & Kleinfeld, D. (2017) Coordination of Orofacial Motor Actions into Exploratory Behavior by Rat. *Curr. Biol.*, **27**, 688–696.
Larson, M.A. & Stein, B.E. (1984) The use of tactile and olfactory cues in neonatal orientation and localization of the nipple. *Dev Psychobiol*, **17**, 423–436.
Lee, T., Alloway, K.D., & Kim, U. (2011) Interconnected cortical networks between primary somatosensory cortex septal columns and posterior parietal cortex in rat. *J. Comp. Neurol.*, **519**, 405–419.
Licata, A.M., Kaufman, M.T., Raposo, D., Ryan, M.B., Sheppard, J.P., & Churchland, A.K. (2017) Posterior Parietal Cortex Guides Visual Decisions in Rats. *J. Neurosci.*, **37**, 4954–4966.
Macfarlane, N.B.W. & Graziano, M.S.A. (2009) Diversity of grip in Macaca mulatta. *Exp Brain Res*, **197**, 255–268.
Matelli, M. & Luppino, G. (2001) Parietofrontal circuits for action and space perception in the macaque monkey. *Neuroimage*, **14**, S27-32.

Mathis, A., Mamidanna, P., Cury, K.M., Abe, T., Murthy, V.N., Mathis, M.W., & Bethge, M. (2018) DeepLabCut: markerless pose estimation of user-defined body parts with deep learning. *Nat. Neurosci.*, **21**, 1281–1289.

Matyas, F., Sreenivasan, V., Marbach, F., Wacongne, C., Barsy, B., Mateo, C., Aronoff, R., & Petersen, C.C.H. (2010) Motor control by sensory cortex. *Science*, **330**, 1240–1243.

Metz, G.A. & Whishaw, I.Q. (2000) Skilled reaching an action pattern: stability in rat (Rattus norvegicus) grasping movements as a function of changing food pellet size. *Behav. Brain Res.*, **116**, 111–122.

Meyer, M.E. & Meyer, M.E. (1992) The effects of bilateral and unilateral vibrissotomy on behavior within aquatic and terrestrial environments. *Physiol. Behav.*, **51**, 877–880.

Miyashita, E., Keller, A., & Asanuma, H. (1994) Input-output organization of the rat vibrissal motor cortex. *Exp Brain Res*, **99**, 223–232.

Moon, S.-K., Alaverdashvili, M., Cross, A.R., & Whishaw, I.Q. (2009) Both compensation and recovery of skilled reaching following small photothrombotic stroke to motor cortex in the rat. *Exp. Neurol.*, **218**, 145–153.

Nadel, L. (1991) The hippocampus and space revisited. *Hippocampus*, **1**, 221–229.

Naito, E., Matsumoto, R., Hagura, N., Oouchida, Y., Tomimoto, H., & Hanakawa, T. (2011) Importance of precentral motor regions in human kinesthesia: a single case study. *Neurocase*, **17**, 133–147.

Nica, I., Deprez, M., Nuttin, B., & Aerts, J.-M. (2017) Automated Assessment of Endpoint and Kinematic Features of Skilled Reaching in Rats. *Front Behav Neurosci*, **11**, 255.

Nii, Y., Uematsu, S., Lesser, R.P., & Gordon, B. (1996) Does the central sulcus divide motor and sensory functions? Cortical mapping of human hand areas as revealed by electrical stimulation through subdural grid electrodes. *Neurology*, **46**, 360–367.

Omrani, M., Kaufman, M.T., Hatsopoulos, N.G., & Cheney, P.D. (2017) Perspectives on classical controversies about the motor cortex. *J. Neurophysiol.*, jn.00795.2016.

Omrani, M., Murnaghan, C.D., Pruszynski, J.A., & Scott, S.H. (2016) Distributed task-specific processing of somatosensory feedback for voluntary motor control. *Elife*, **5**.

Otchy, T.M., Wolff, S.B.E., Rhee, J.Y., Pehlevan, C., Kawai, R., Kempf, A., Gobes, S.M.H., & Ölveczky, B.P. (2015) Acute off-target effects of neural circuit manipulations. *Nature*, **528**, 358–363.

Parmiani, P., Lucchetti, C., Bonifazzi, C., & Franchi, G. (2019) A kinematic study of skilled reaching movement in rat. *J. Neurosci. Methods*, **328**, 108404.

Parmiani, P., Lucchetti, C., & Franchi, G. (2018) Whisker and Nose Tactile Sense Guide Rat Behavior in a Skilled Reaching Task. *Front Behav Neurosci*, **12**, 24.

Paxinos, G. (2004) The Rat Nervous System. *Forebrain and Midbrain*, **I**, 335–352.

Prescott, T.J., Ahissar, E., & Izhikevich, E. (2016) *Scholarpedia of Touch*, Scholarpedia. Atlantis Press.

Prescott, T.J., Mitchinson, B., & Grant, R.A. (2011) Vibrissal behavior and function. *Scholarpedia*, **6**, 6642.

Ranade, S., Hangya, B., & Kepecs, A. (2013) Multiple modes of phase locking between sniffing and whisking during active exploration. *J. Neurosci.*, **33**, 8250–8256.

Raposo, D., Kaufman, M.T., & Churchland, A.K. (2014) A category-free neural population supports evolving demands during decision-making. *Nat. Neurosci.*, **17**, 1784–1792.

Rathelot, J.-A. & Strick, P.L. (2006) Muscle representation in the macaque motor cortex: an anatomical perspective. *Proc. Natl. Acad. Sci. U.S.A.*, **103**, 8257–8262.

Ravassard, P., Kees, A., Willers, B., Ho, D., Aharoni, D.A., Cushman, J., Aghajan, Z.M., & Mehta, M.R. (2013) Multisensory control of hippocampal spatiotemporal selectivity. *Science*, **340**, 1342–1346.

Reep, R.L., Chandler, H.C., King, V., & Corwin, J.V. (1994) Rat posterior parietal cortex: topography of corticocortical and thalamic connections. *Exp Brain Res*, **100**, 67–84.

Sacrey, L.-A.R., Alaverdashvili, M., & Whishaw, I.Q. (2009) Similar hand shaping in reaching-for-food (skilled reaching) in rats and humans provides evidence of homology in release, collection, and manipulation movements. *Behav. Brain Res.*, **204**, 153–161.

Sacrey, L.-A.R. & Whishaw, I.Q. (2012) Subsystems of sensory attention for skilled reaching: vision for transport and pre-shaping and somatosensation for grasping, withdrawal and release. *Behav. Brain Res.*, **231**, 356–365.

Sartori, L., Camperio Ciani, A., Bulgheroni, M., & Castiello, U. (2013) Reaching and grasping behavior in Macaca fascicularis: a kinematic study. *Exp Brain Res*, **224**, 119–124.

Sartori, L., Camperio-Ciani, A., Bulgheroni, M., & Castiello, U. (2013) Reach-to-grasp movements in Macaca fascicularis monkeys: the Isochrony Principle at work. *Front Psychol*, **4**, 114.

Save, E., Paz-Villagran, V., Alexinsky, T., & Poucet, B. (2005) Functional interaction between the associative parietal cortex and hippocampal place cell firing in the rat. *Eur. J. Neurosci.*, **21**, 522–530.

Schwarz, C. & Möck, M. (2001) Spatial arrangement of cerebro-pontine terminals. *J. Comp. Neurol.*, **435**, 418–432.

Sereno, M.I. & Huang, R.-S. (2014) Multisensory maps in parietal cortex. *Curr. Opin. Neurobiol.*, **24**, 39–46.

Severson, K.S. & O'Connor, D.H. (2017) Active Sensing: The Rat's Nose Dances in Step with Whiskers, Head, and Breath. *Curr. Biol.*, **27**, R183–R185.

Sreenivasan, V., Karmakar, K., Rijli, F.M., & Petersen, C.C.H. (2015) Parallel pathways from motor and somatosensory cortex for controlling whisker movements in mice. *Eur. J. Neurosci.*, **41**, 354–367.

Stoddart, D.M. (1980) The olfactory system of vertebrates. In Stoddart, D.M. (ed), *The Ecology of Vertebrate Olfaction*. Springer Netherlands, Dordrecht, pp. 1–33.

Stüttgen, M.C. & Schwarz, C. (2017) Barrel cortex: What is it good for? *Neuroscience*,.

Szwed, M., Bagdasarian, K., & Ahissar, E. (2003) Encoding of vibrissal active touch. *Neuron*, **40**, 621–630.

Szwed, M., Bagdasarian, K., Blumenfeld, B., Barak, O., Derdikman, D., & Ahissar, E. (2006) Responses of trigeminal ganglion neurons to the radial distance of contact during active vibrissal touch. *J. Neurophysiol.*, **95**, 791–802.

Thaler, L. & Todd, J.T. (2009) The control parameters used by the CNS to guide the hand depend on the visuo-motor task: evidence from visually guided pointing. *Neuroscience*, **159**, 578–598.

Viaro, R., Bonazzi, L., Maggiolini, E., & Franchi, G. (2017) Cerebellar Modulation of Cortically Evoked Complex Movements in Rats. *Cereb. Cortex*, **27**, 3525–3541.

Vincent, S.Burnham. (1912) *The Function of the Vibrissae in the Behavior of the White Rat*. H. Holt & Co., Cambridge Mass.

Viviani, P. & McCollum, G. (1983) The relation between linear extent and velocity in drawing movements. *Neuroscience*, **10**, 211–218.

Völgyi, B., Farkas, T., & Toldi, J. (1993) Compensation of a sensory deficit inflicted upon newborn and adult animals. A behavioural study. *Neuroreport*, **4**, 827–829.

Wallace, S.A. & Weeks, D.L. (1988) Temporal constraints in the control of prehensile movement. *J Mot Behav*, **20**, 81–105.

Welker, W.I. (1964) Analysis of Sniffing of the Albino Rat 1). *Behaviour*, **22**, 223–244.

Whishaw, I.Q. (1996) An endpoint, descriptive, and kinematic comparison of skilled reaching in mice (Mus musculus) with rats (Rattus norvegicus). *Behav. Brain Res.*, **78**, 101–111.

Whishaw, I.Q., Dringenberg, H.C., & Pellis, S.M. (1992) Spontaneous forelimb grasping in free feeding by rats: motor cortex aids limb and digit positioning. *Behav. Brain Res.*, **48**, 113–125.

Whishaw, I.Q., Faraji, J., Kuntz, J.R., Mirza Agha, B., Metz, G.A.S., & Mohajerani, M.H. (2017) The syntactic organization of pasta-eating and the structure of reach movements in the head-fixed mouse. *Sci Rep*, **7**, 10987.

Whishaw, I.Q. & Karl, J.M. (2014) The contribution of the reach and the grasp to shaping brain and behaviour. *Can J Exp Psychol*, **68**, 223–235.

Whishaw, I.Q., Pellis, S.M., & Gorny, B.P. (1992) Skilled reaching in rats and humans: evidence for parallel development or homology. *Behav. Brain Res.*, **47**, 59–70.

Whishaw, I.Q. & Tomie, J.A. (1988) Food wrenching and dodging: a neuroethological test of cortical and dopaminergic contributions to sensorimotor behavior in the rat. *Behav. Neurosci.*, **102**, 110–123.

Whishaw, I.Q. & Tomie, J.A. (1989) Olfaction directs skilled forelimb reaching in the rat. *Behav. Brain Res.*, **32**, 11–21.

Whishaw, I.Q., Travis, S.G., Koppe, S.W., Sacrey, L.-A., Gholamrezaei, G., & Gorny, B. (2010) Hand shaping in the rat: conserved release and collection vs. flexible manipulation in overground walking, ladder rung walking, cylinder exploration, and skilled reaching. *Behav. Brain Res.*, **206**, 21–31.

Whishaw, I.Q., Whishaw, P., & Gorny, B. (2008) The structure of skilled forelimb reaching in the rat: a movement rating scale. *J Vis Exp*,.

Wilkinson, E.J. & Sherk, H.A. (2005) The use of visual information for planning accurate steps in a cluttered environment. *Behav. Brain Res.*, **164**, 270–274.

Wiltschko, R. & Wiltschko, W. (2017) Considerations on the role of olfactory input in avian navigation. *J. Exp. Biol.*, **220**, 4347–4350.

Wong, C.C., Ramanathan, D.S., Gulati, T., Won, S.J., & Ganguly, K. (2015) An automated behavioral box to assess forelimb function in rats. *J. Neurosci. Methods*, **246**, 30–37.

Fig.1

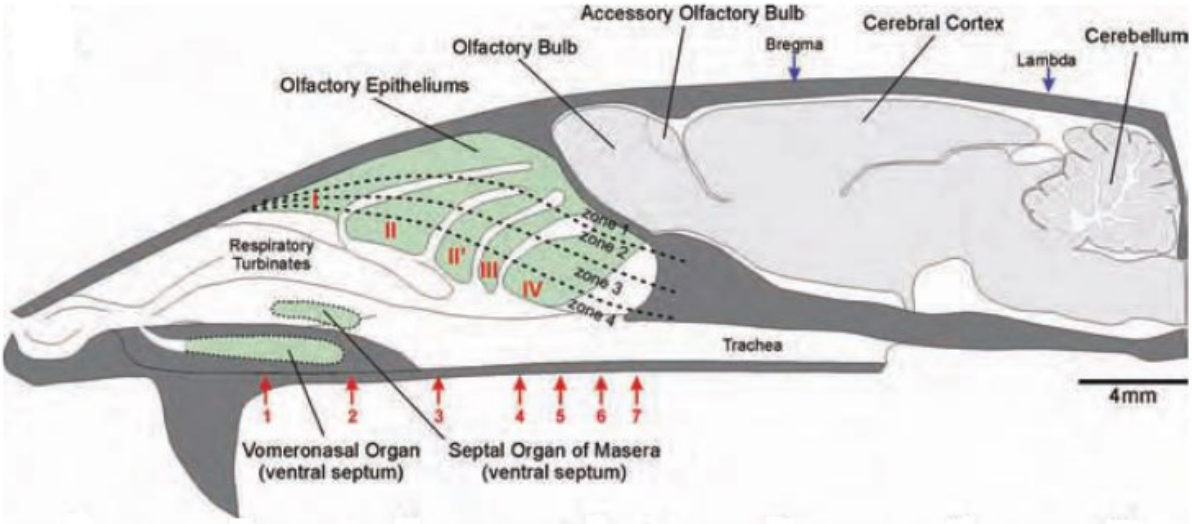

Fig. 1. Scale diagram of the rat nasal cavity and brain shown in a lateral view. Edited from Paxinos, G. (2004).

Fig.2

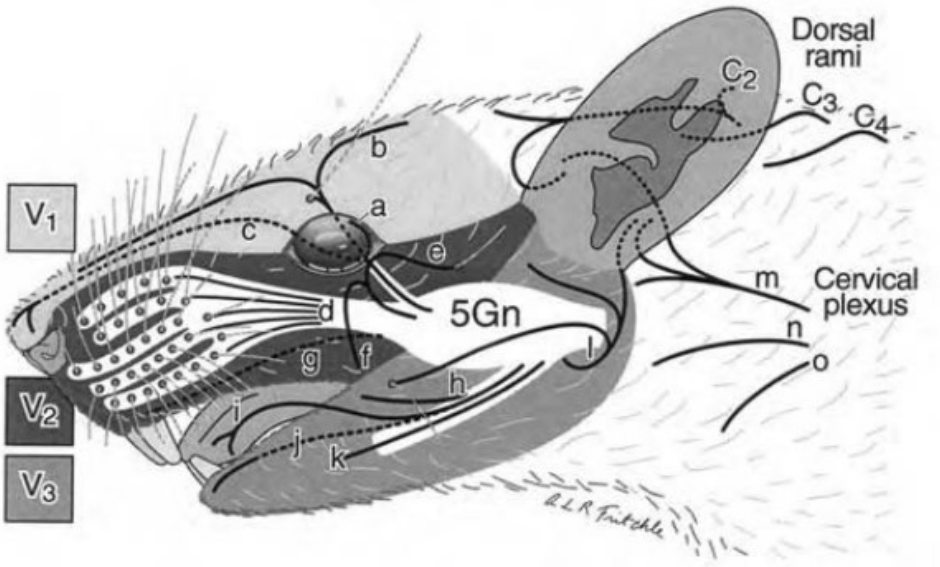

Fig. 2. Sensory trigeminal innervation of the rat head. The trigeminal ganglion (5Gn) is shown with its three divisions supplying the ophthalmic (V1),maxillary (V2) and mandibular (V3) regions. The main nerves innervating cutaneuous or mucosal surfaces are indicated diagrammatically. Edited from Paxinos, G. (2004).

Fig.3

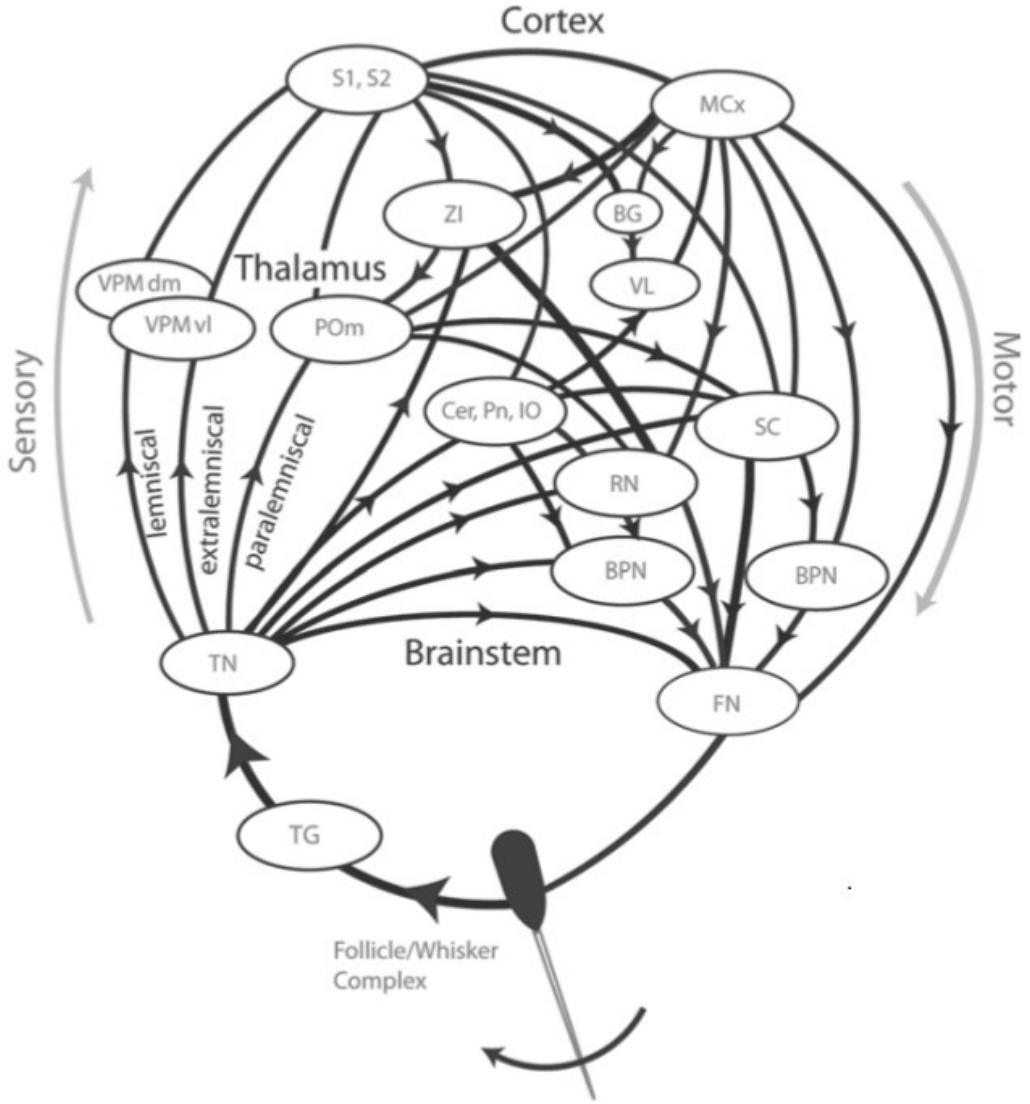

Fig.3. Closed loop structure of the whisker system. BG basal ganglia, BPN brainstem premotor nuclei, Cer cerebellum,FN facial nucleus, IO inferior olive, MCx motor cortex, Pn pontine nucleus, POm Posteromedial thalamic nuclei, Rn red nucleus, S1 primary somatosensory cortex, S2 secondary somatosensory cortex, SC superior colliculus, TG trigeminal ganglion, Tn trigeminal nucleus, VL ventrolateral thalamic nucleus, VPMdm dorsomedial Ventroposteromedial thalamic nuclei, VPMvl ventrolateral Ventroposteromedial thalamic nuclei, ZI zona incerta. Edited from Prescott TJ. (2016).

Fig.4

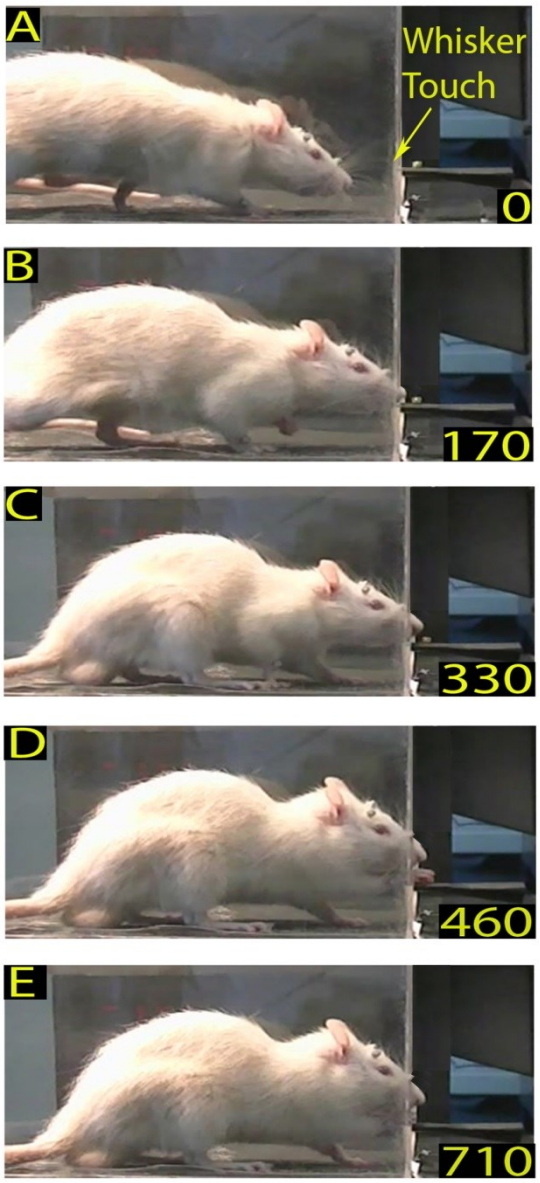

Fig. 4. Example of skilled reaching in P trial in control rat: video-recording from Rat 2. Each frame represents a salient step in the trial sequence. The top frame corresponds to the start of trial and shows the first whisker contact with the front wall during approach before the rat raised its head (A). The bottom frame corresponds to the end of trial and shows the rat paw re-crossing the slot after pellet grasping (E). The intermediate frames show the rat inserting its nose in the slot (B), and the reach start and grasping movements (C-D), respectively. In each frame, the number at the bottom right is the timing (in ms). Markers are present (see Methods).

Fig.5

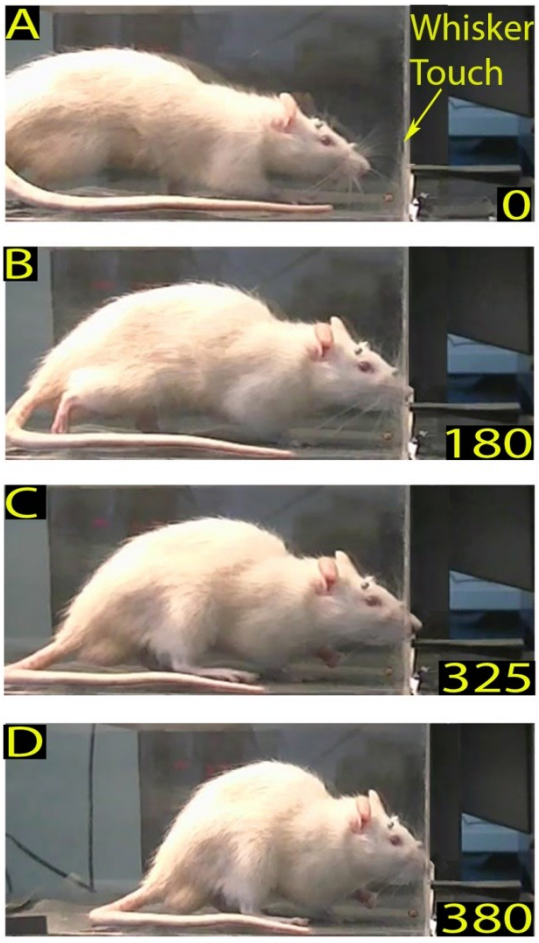

Fig. 5. Example of skilled reaching in no-P trial in control rat: video-recording from Rat 2. Each frame as in Fig. 1. Note that the trial interrupts after poke (D). Markers are present (see Methods).

Fig.6

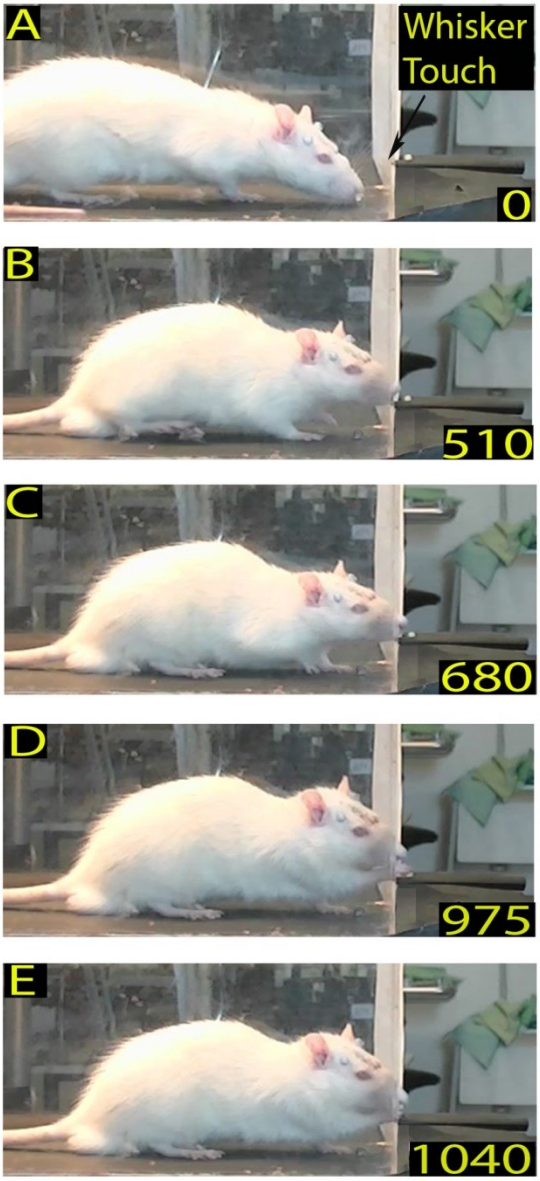

Fig. 6. Example of skilled reaching in P trial 3–5 days after bulbectomy: video-recording from Rat 2. Each frame as in Fig. 1. Note that the rat carries out the full task sequence with a significant increase in Whisker touch–Poke with respect to control (see frame B: Fig. 3 vs. Fig. 1). Markers are present (see Methods).

Fig.7

Fig. 7. Example of skilled reaching in no-P trial 3–5 days after bulbectomy: video-recording from Rat 2. Each frame as in Fig. 1. Note that the trial sequence and timing are similar to those in Figure 3. Markers are present (see Methods).

Fig.8

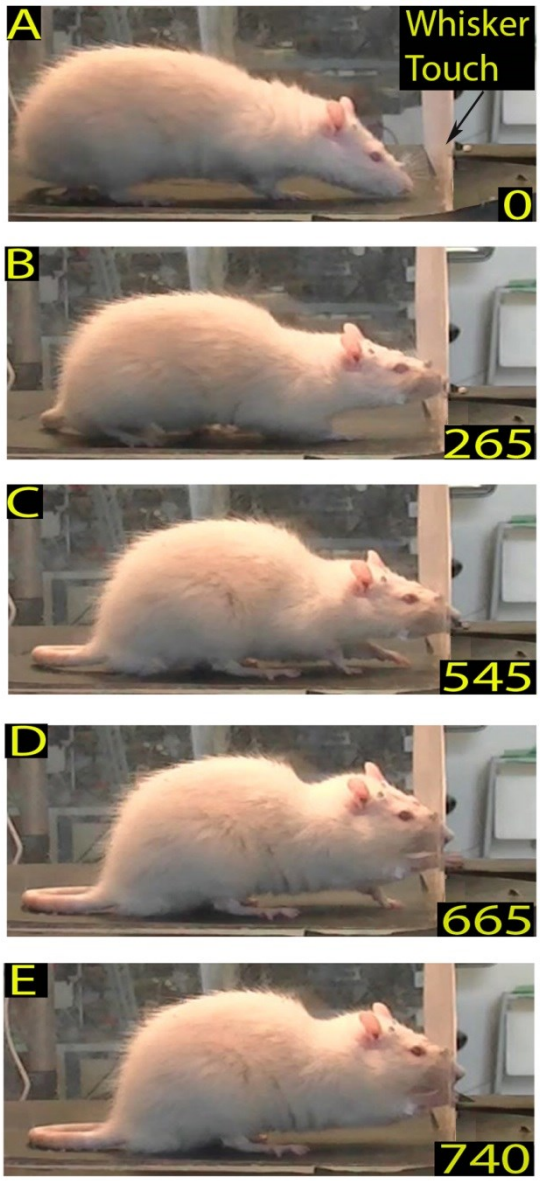

Fig. 8. Example of skilled reaching in P trial 12–14 days after bulbectomy: video-recording from Rat 2. Each frame as in Fig. 1. Note that the rat carries out the full task sequence still with a significant increase in Whisker touch–Poke with respect to control (see frame B in Fig. 1). Markers are present (see Methods).

Fig.9

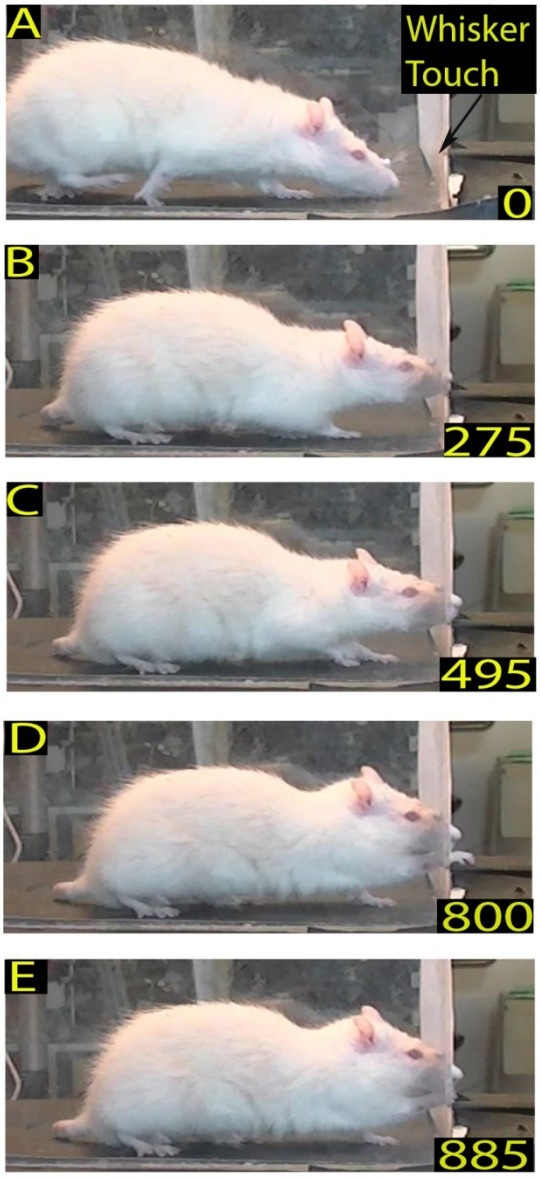

Fig. 9. Example of skilled reaching in no-P trial 12–14 days after bulbectomy: video-recording from Rat 2. Each frame as in Fig. 1. Note that the trial sequence and timing are similar to those in Figure 5. Markers are present (see Methods).

Fig.10

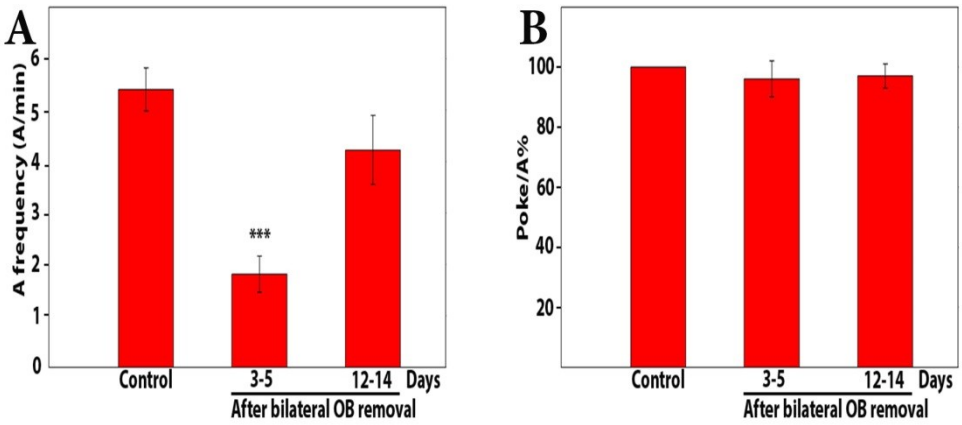

Fig. 10. A: Frequency of approach to the front wall. The histogram presents data on 5 rats collected under control conditions and at 3–5 and 12–14 days after bulbectomy. Each bar shows the mean and standard error of approaches expressed as a frequency (A/min). Note that the frequency is significantly reduced with respect to control at 3–5 days (*** P= 0.001, post-hoc Dunn's test) but not at 12–14 days (P= 0.127, post-hoc Dunn's test). B: Nose poke percentage expressed as a ratio with respect to the approach (PK/A%). Note that in controls as well as at 3–5 and 12–14 days after bulbectomy, all approaches to the front wall are followed by insertion of the nose into the slot (100%). Each bar shows the mean and standard error.

Fig.11

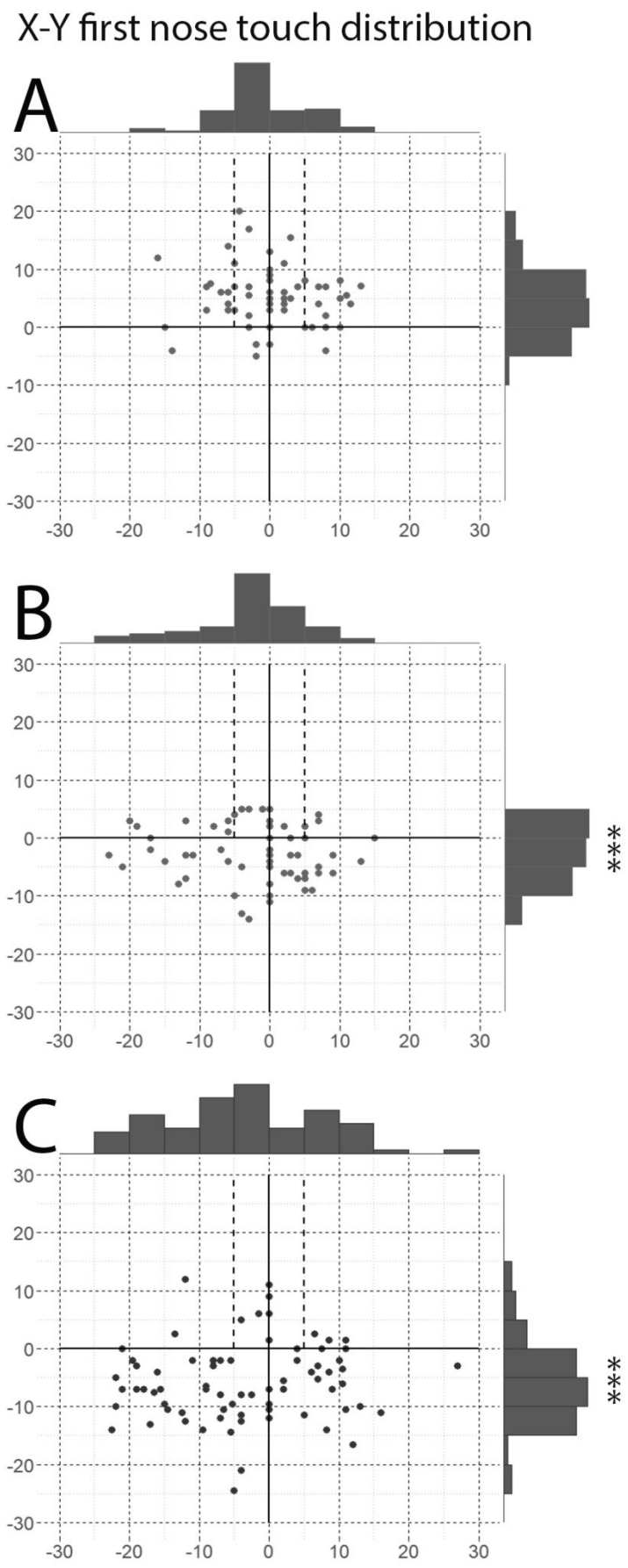

Fig. 11. A-C: XY first nose touch position distribution. In this distribution, each point corresponds to the first nose contact with the front wall for each single trial. Data derive from 20 trials of 3 rats collected under control conditions (A) and at 3–5 (B) and 12–14 days (C) after bulbectomy. X axis: corresponds to mediolateral dimension of the front wall positioned at the shelf level; Y axis: corresponds to the vertical dimension of the front wall positioned on the midline; 00: corresponds to the pellet on the shelf. Broken lines correspond to the vertical borders of the slot. Along X and Y axes, distribution frequency histograms are reported (bin width: 0.5 mm). Note that, after bulbectomy the first nose touches are distributed below the shelf.

Fig.12

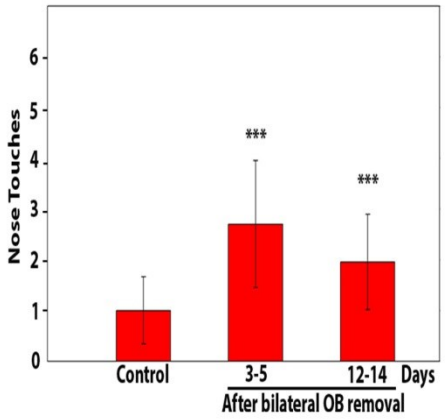

Fig. 12. Number of nose touches preceding nose poking.

Note the significant increase in the number of nose touches/trial at 3–5 and 12–14 days after bulbectomy (p=0.000, Kruskal-Wallis test). Each bar shows the mean and standard error.

Fig.13

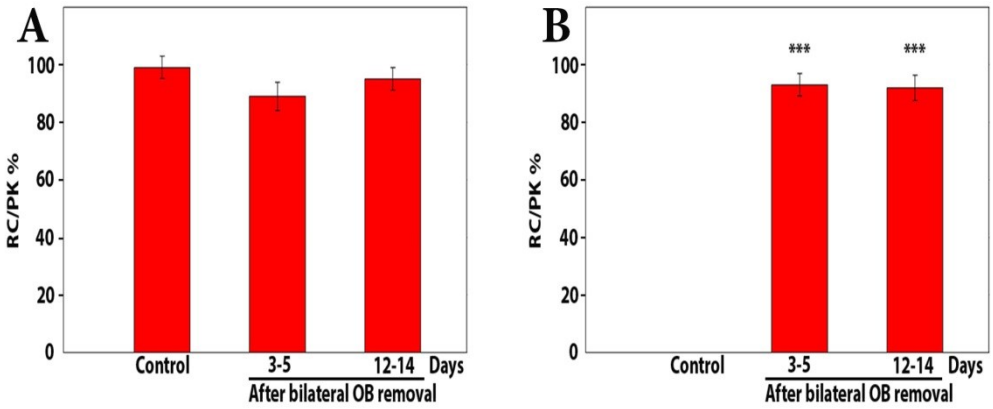

Fig. 13. Reaching-grasping percentage expressed as a ratio with respect to Poke (RC/PK%) in controls, and 3–5 and 12–14 days after bulbectomy, in P and no-P trials (A and B respectively). Note that in P trials, in controls as well as at 3–5 and 12–14 days after bulbectomy, all insertions of the nose into the slot are followed by reaching. Conversely, in no-P trials, the insertion of the nose into the slot is not followed by reaching in controls; by contrast, all insertions of the nose into the slot are followed by reaching after bulbectomy (*** P= 0.001, post-hoc Dunn's test).

Fig.14

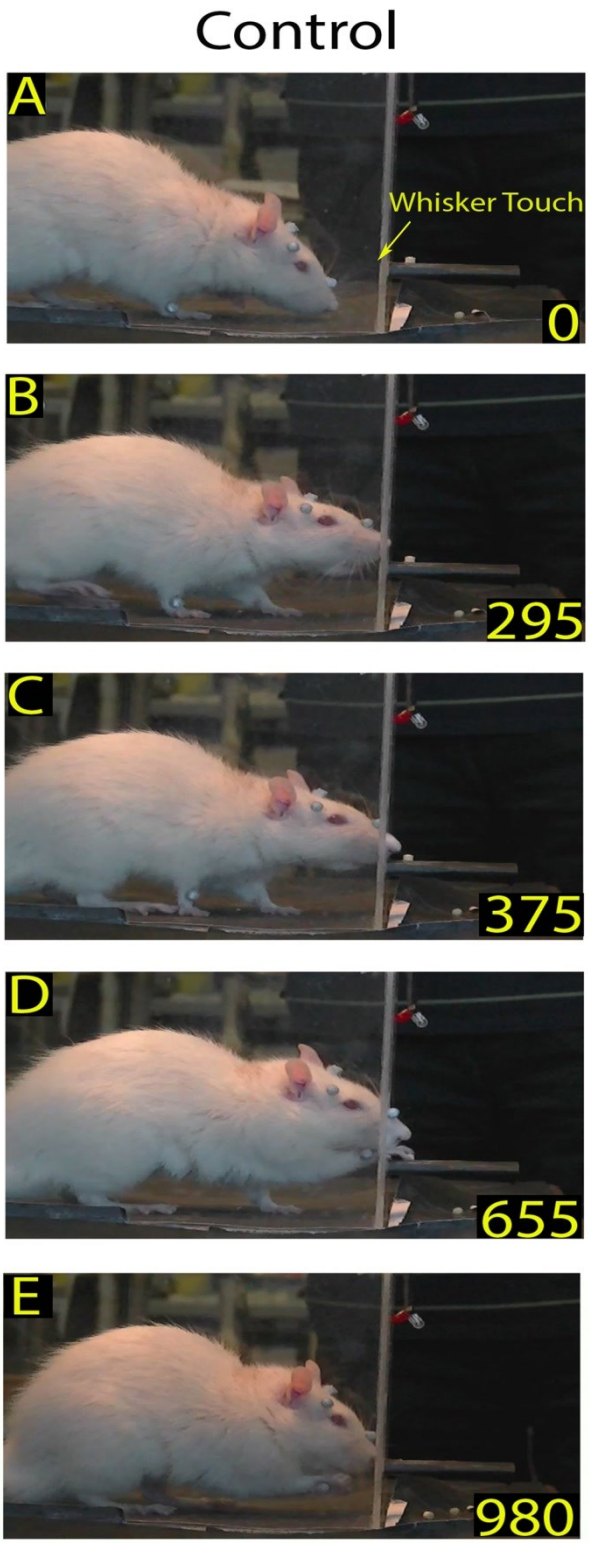

Fig.14. Example of a skilled reaching trial in Control rat: videorecording from Rat 2. Each frame represents a highlight of a phase in the trial sequence. The top frame shows the rat approaching the frontal wall before rising its head (end of phase A); the bottom frame shows the rat putting the pellet into the mouth (end of phase Rt). The intermediate frames show the rat with the nose into the slot (Phase N) and during reaching-grasping movement (phase R/G). In each frame, the letter in the top left refers to the phase and the number in the bottom right is the timing (in ms.). Markers are present (see methods).

Fig.15

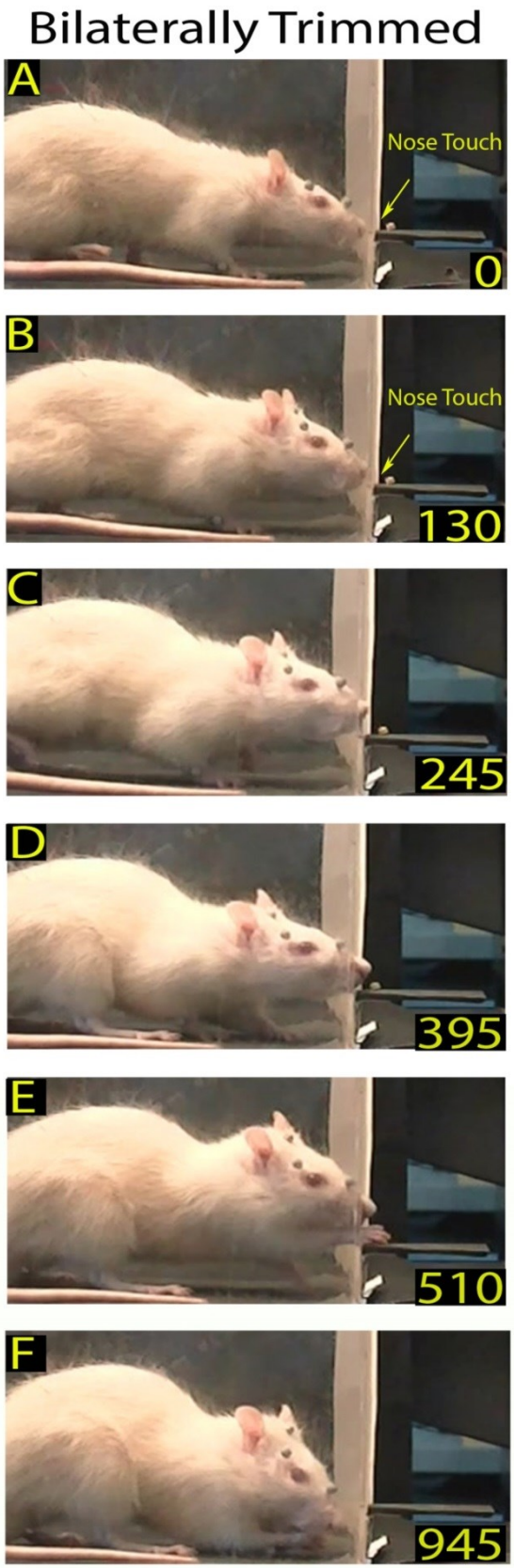

Fig. 15. Example of a skilled reaching trial in bilaterally trimmed rat. Phases and trial timing as in Fig 14. Markers are present (see methods).

Fig.16

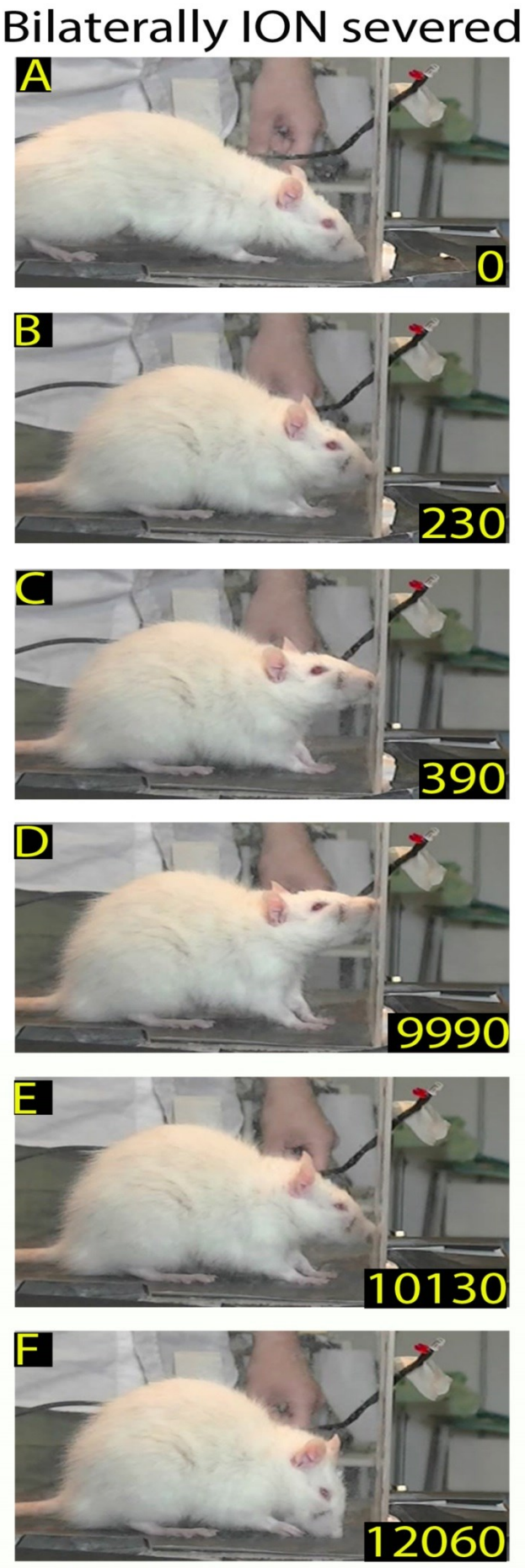

Fig. 16. Example of rat behavior after bilaterally ION severing: videorecording from Rat 2 four days after surgery. The rat approaches the frontal wall (phase A), does not insert the nose into the slot and then, after a long standing there (phase noN), it moves away. Note that the rat stays long in front of the wall and the sequence is interrupted.

Fig.17

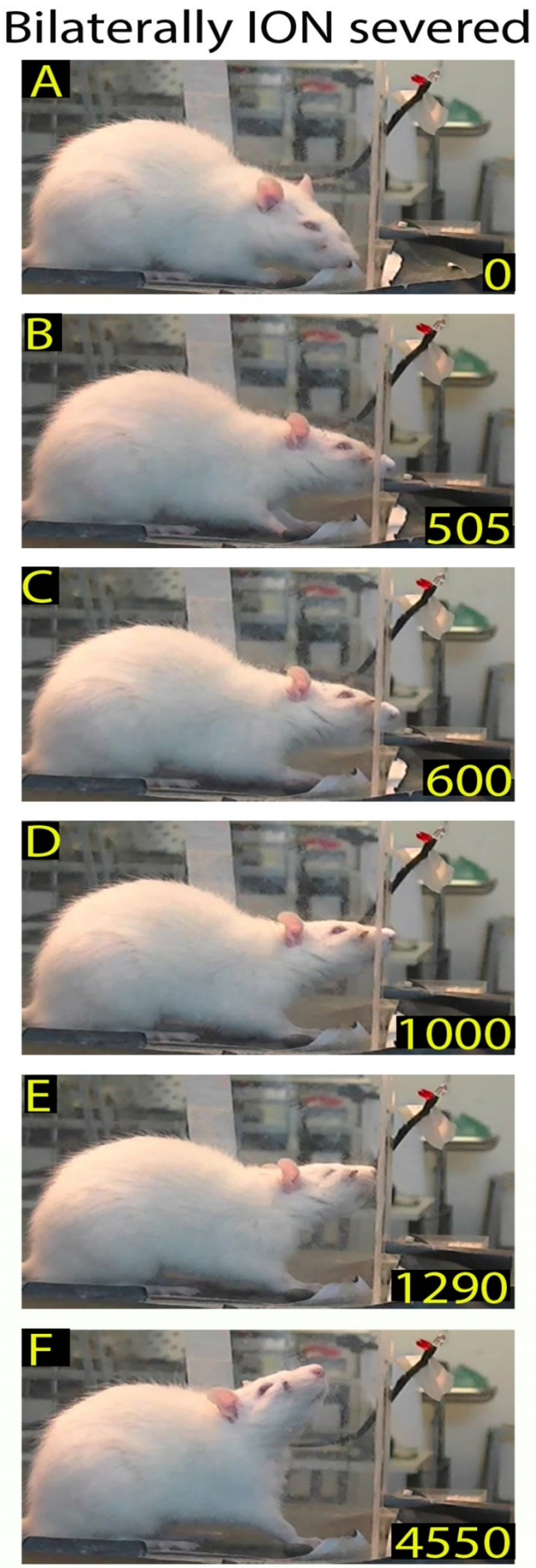

Fig. 17. Example of rat behavior after bilaterally ION severing: videorecording from Rat 2 ten days after surgery. The rat approaches the frontal wall (phase A), inserts the nose into the slot and then, after a long standing there (phase N), it moves away. Note that although the prolonged insertion of the nose into the slot, the rat does not execute the reaching-grasping and retract movement.

Fig.18

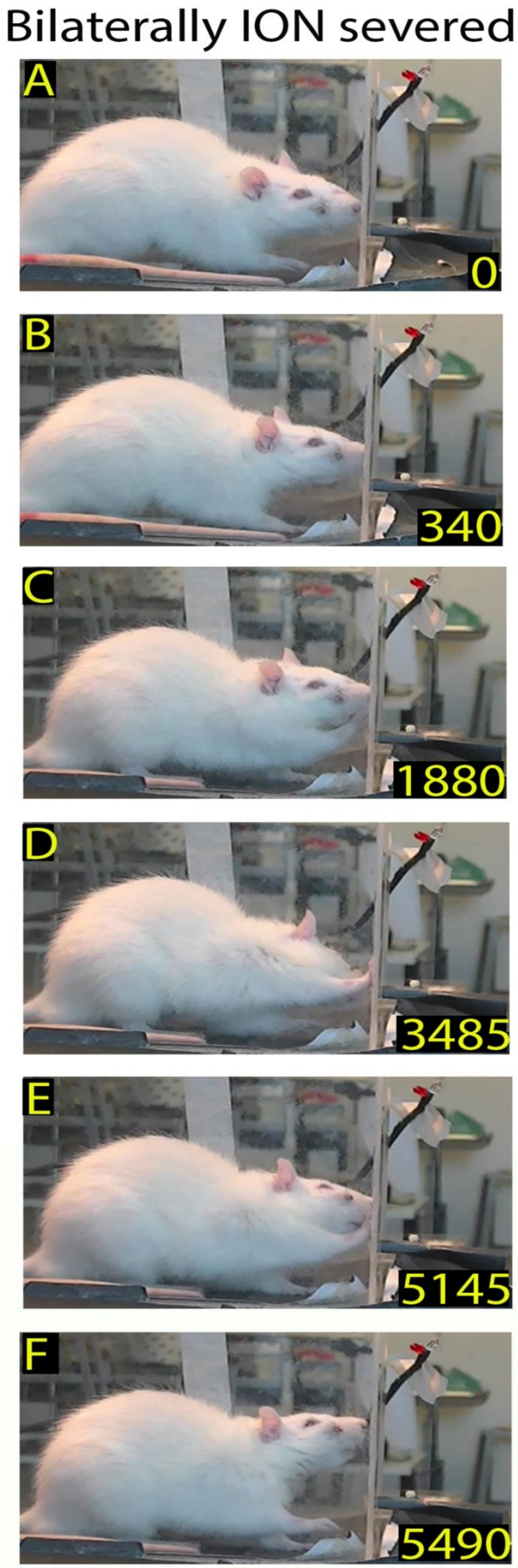

Fig. 18. Example of rat behavior after bilaterally ION severing: videorecording from Rat 2 twelve days after surgery. The rat approaches the frontal wall (phase A), and explores it with repetitive forelimb movements (Phase P) before moving away. Note that although the prolonged exploration of the frontal wall, the rat does not insert the nose into the slot, nor executes the reaching-grasping and retract movement.

Fig.19

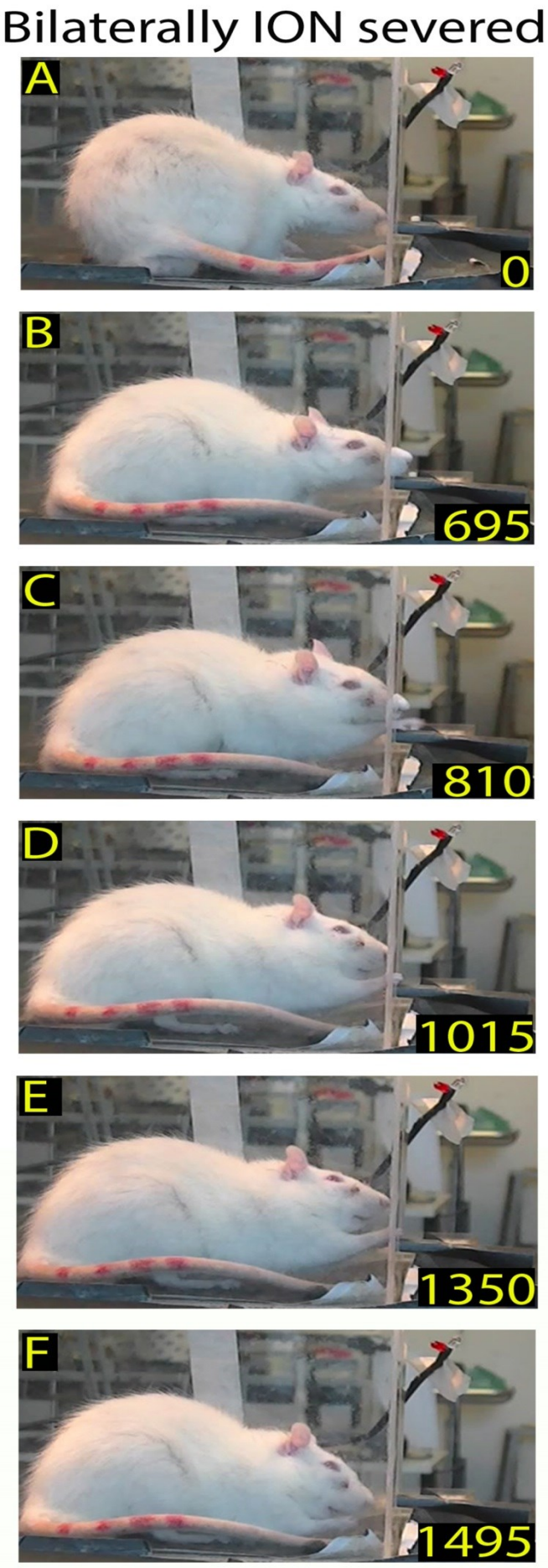

Fig. 19. Example of a reaching-grasping and retract movements recovery in bilaterally ION severed rat: videorecording from Rat 2 twelve days after surgery. The rat approaches the frontal wall (phase A), inserts the nose into the slot (phase N) and slowly executes the sequence of reaching-grasping and retract movement (R/G and Rt phases). Note that this is one of the first complete trials performed by the rat after the lesion and that it is slowed in all the phases in comparison to the trial in Fig.14.

Fig.20

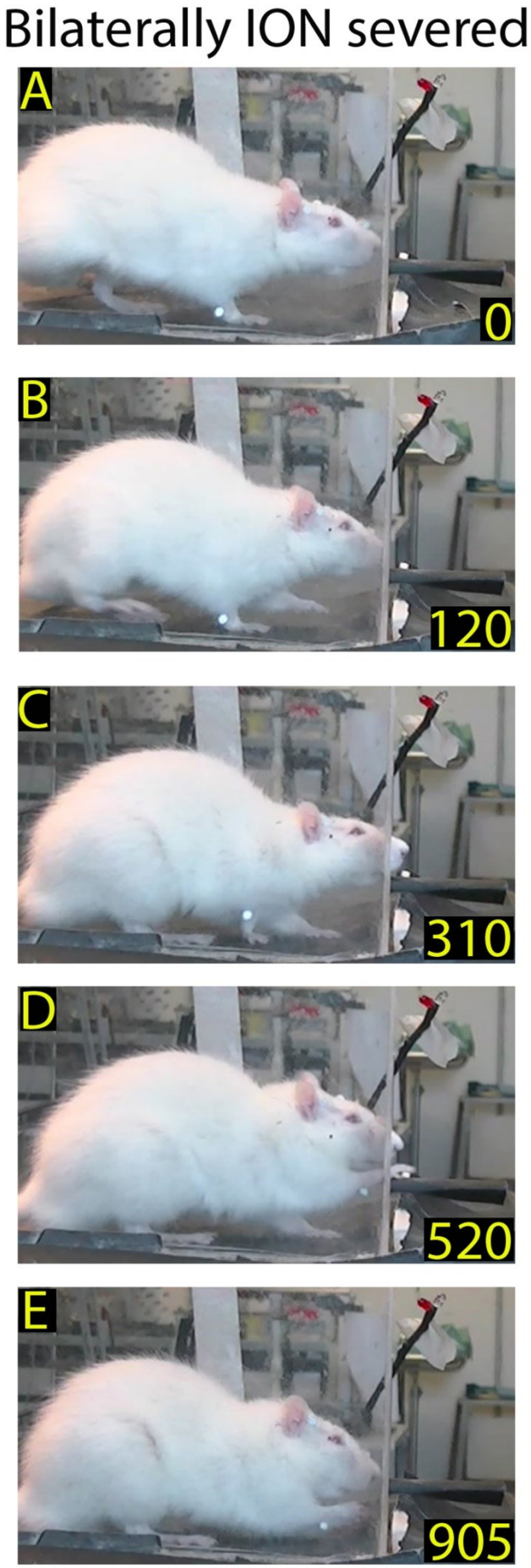

Fig. 20. Example of a reaching-grasping and retract movements recovery in bilaterally ION severed rat: videorecording from Rat 2 seventeen days after surgery. Note that phases sequence and trial timing are similar to those shown in Figure 14.

Fig.21

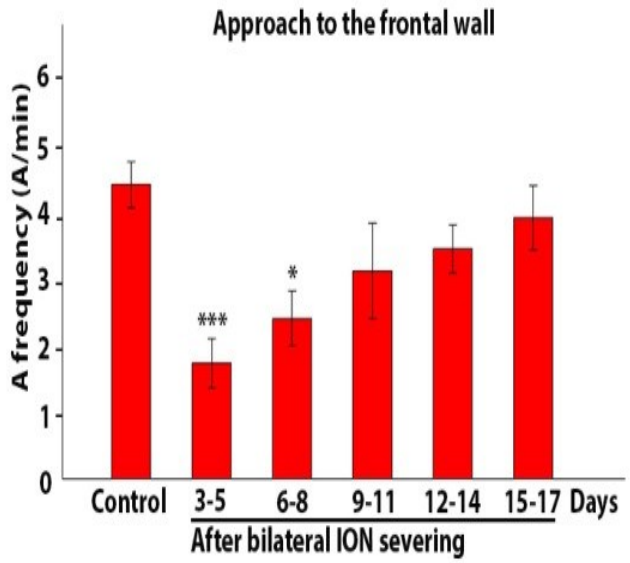

Fig. 21. Approaching to the frontal wall frequency (phase A). The histogram presents data collected in 5 rats in control and at different time intervals after bilateral ION severing. Each bar shows the mean and standard error of approaches expressed as a frequency (A/min). Note that the frequency is significantly reduced at 3-5 and 6-8 days respect to control. *** *P*= 0.0001; * *P*= 0.014, post hoc Bonferroni test.

Fig.22

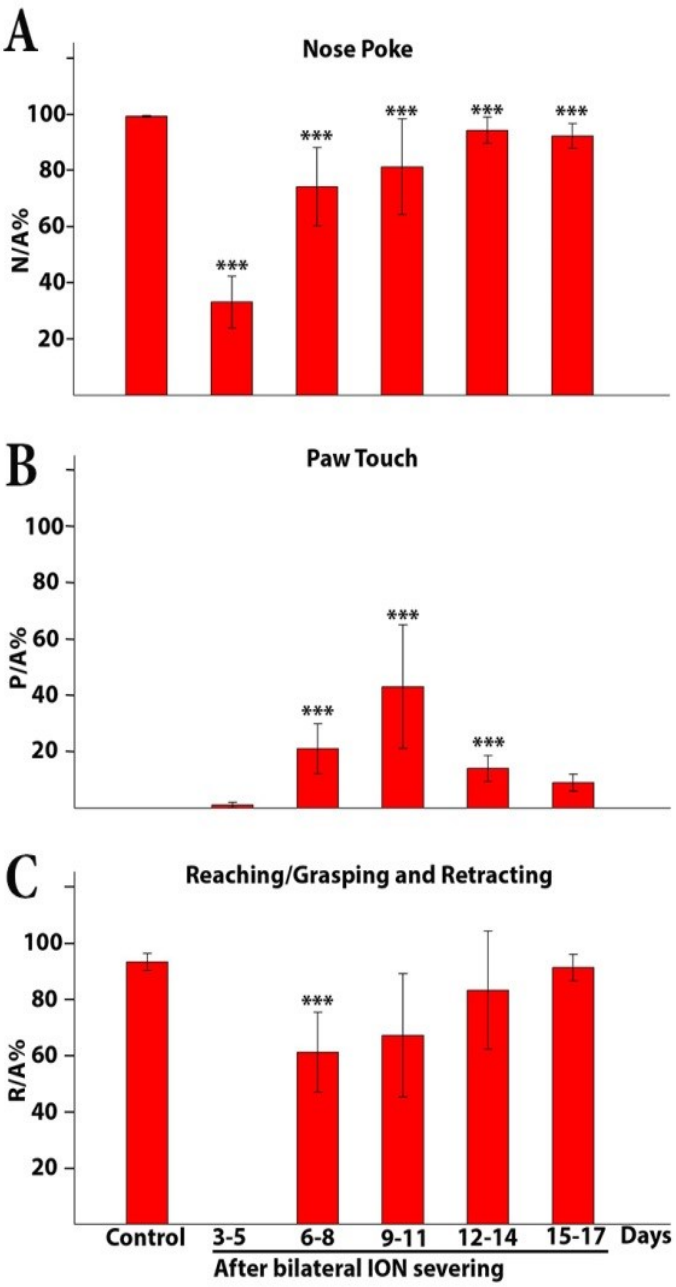

Fig. 22. **A-C**. Phases frequency expressed as a percentage ratio with respect to the approaches. The histograms present data collected in 5 rats in control and at different time intervals after bilateral ION severing. Each bar shows the mean and standard error.

Fig.23

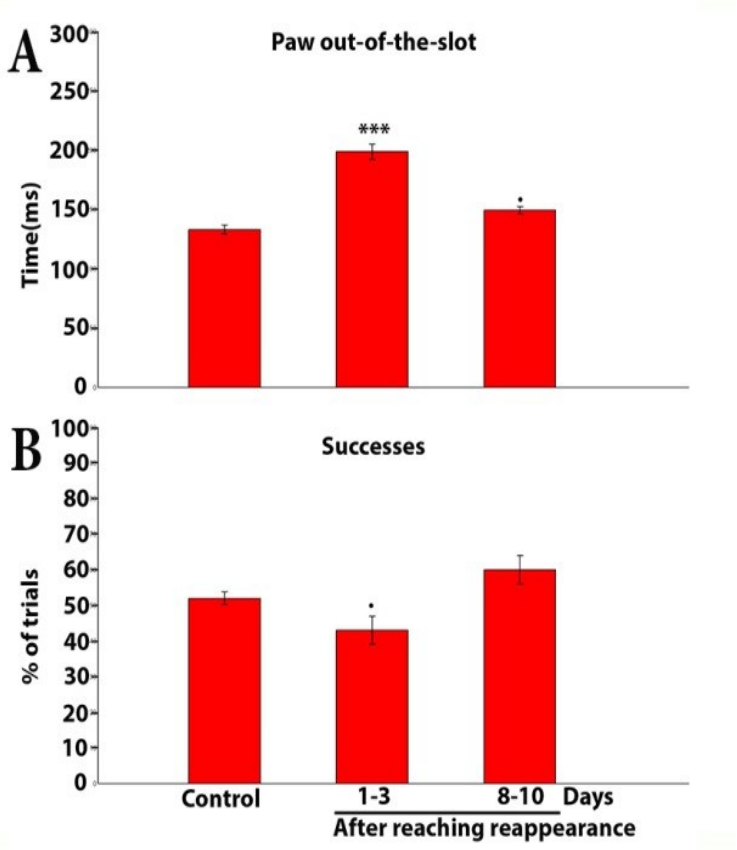

Fig.23 A: Cumulative histogram showing the average time spent by the paw beyond the slot during reaching-grasping-retract movement. Each bar shows the mean and standard error in ms. Note that the frequency is significantly reduced at 3-5 and 6-8 days respect to control. *** P= 0.0001; * P= 0.014, post hoc Bonferroni test. **B**: Cumulative histogram of the success frequency in control and after reaching reappearance in ION severed rat. Note that success frequency is slightly reduced only in 1-3 days after reaching reappearance (P= 0.095).

Fig.24

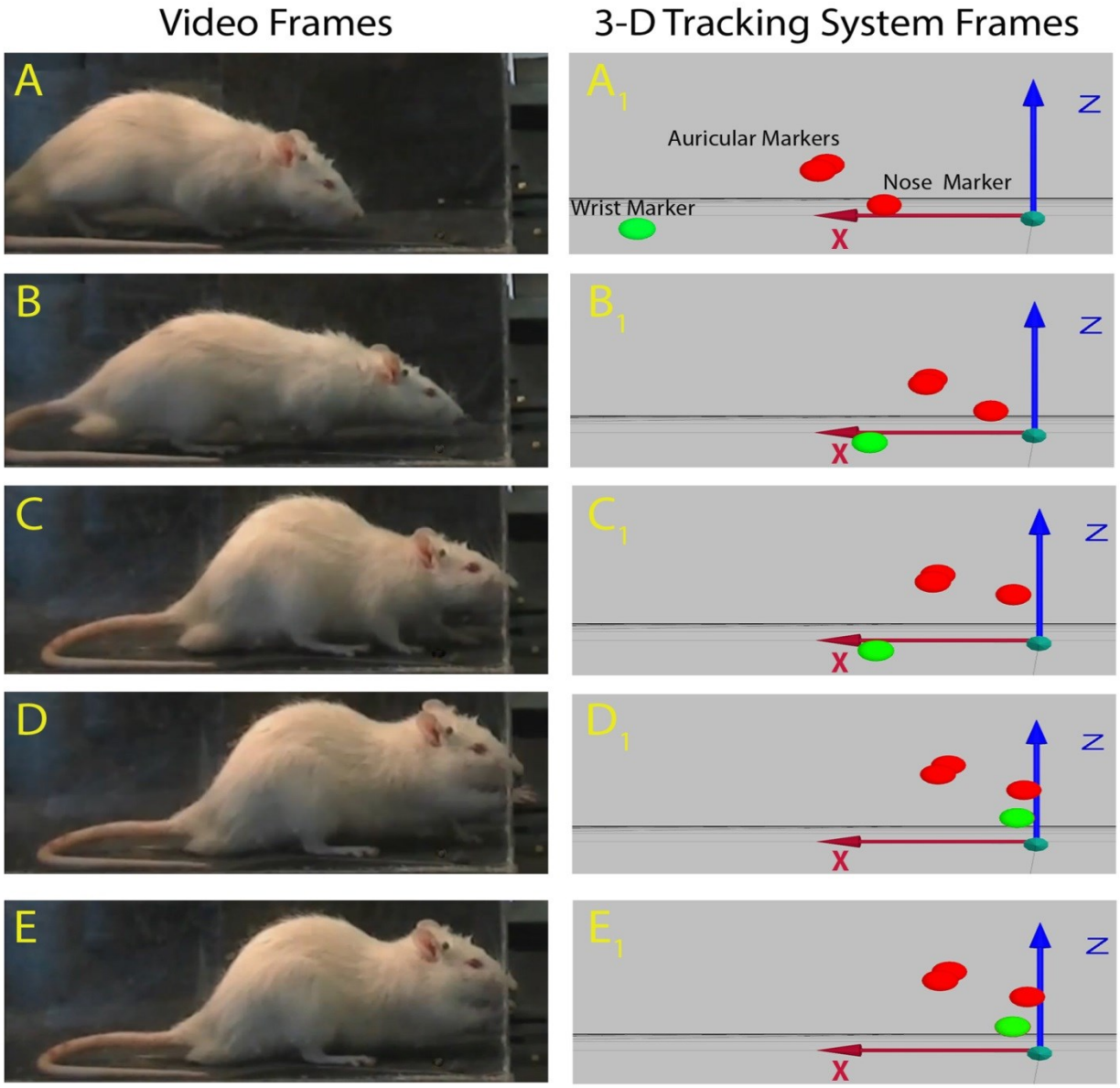

Fig. 24. Example of a skilled reaching trial. Left: video-camera recording: each frame represents a salient step of the trial sequence. A- approaching by walk to the front wall of the box; B- orienting, when the head starts to elevate from the floor toward the slot; C- reaching, i.e. advancing forelimb through the slot toward the pellet; D- grasping the pellet on the sheet; E-retracting the grasped food. Right: Qualysis System recording: the frames are the same as in the left. Only markers positions are visible.

Fig.25

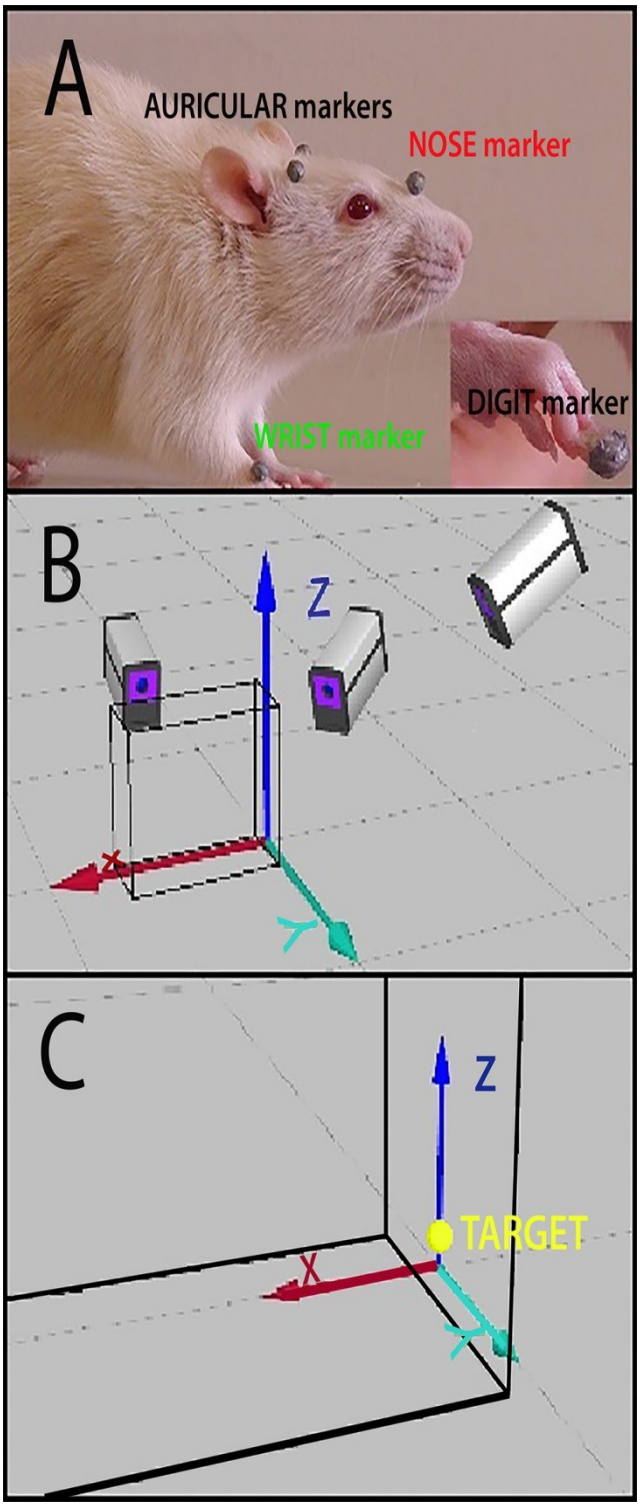

Fig. 25. Qualisys System setup. A: markers positioning on the rat's body. B: Qualisys cameras positioning respect to the reaching box. C: 3D-coordinates system origin (0,0,0) and axes orientation (X,Y,Z), as obtained by Qualisys calibration. Target in yellow: pellet position..

Fig.26

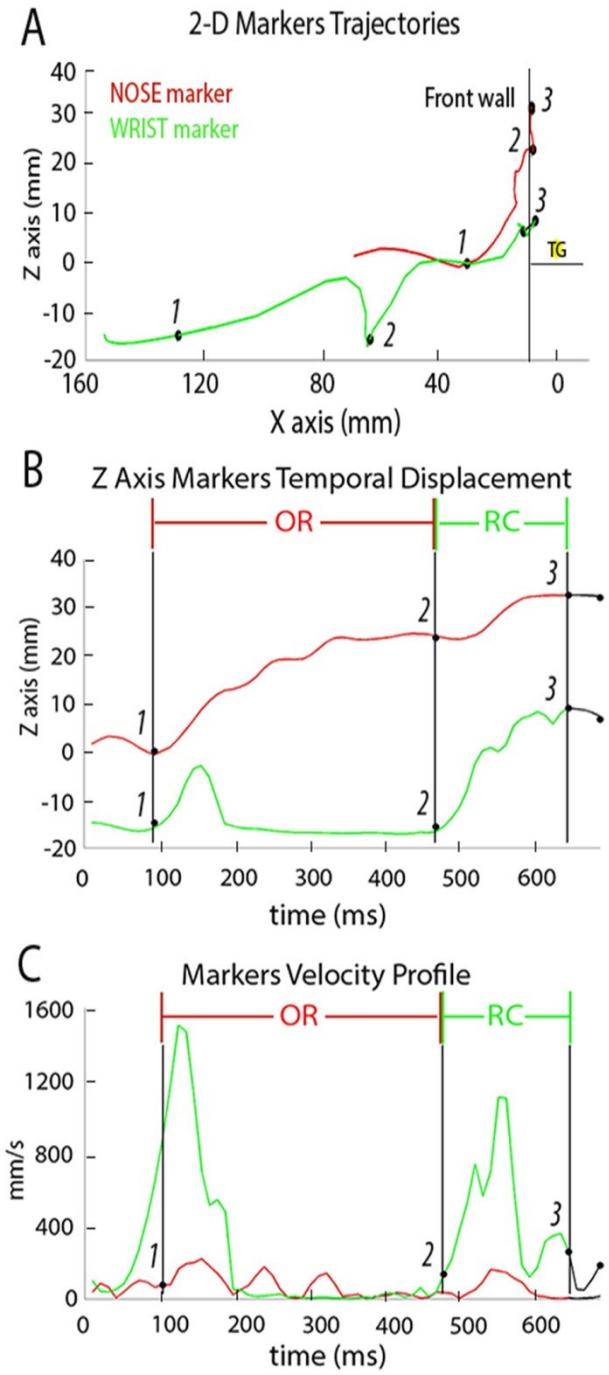

Fig. 26. An example of orienting (OR) and reaching (RC) movements in the same trial as recorded by Qualisys and splitted off-line. A: 2D (X-Z) markers trajectories. X axis: 0 corresponded to target position, Y axis: 0 corresponded to Qualisys axes origin. Nose marker in red, wrist marker in green, target/pellet (TG) in yellow. Numbers: 1, orienting start point; 2, orienting end point/reaching start point; and 3) reaching end point. The vertical line represents the front wall of the box. B: Z axis temporal markers displacements. The vertical lines represent the start or the end of movements. Colours, numbers and Y axis 0 as in A. The displacements of the two markers are temporally aligned so that we can see at the same time the displacement of both markers during orienting and reaching. C: markers velocity profiles in X-Y-Z axes. Colours, numbers and vertical lines as in B.

Fig.27

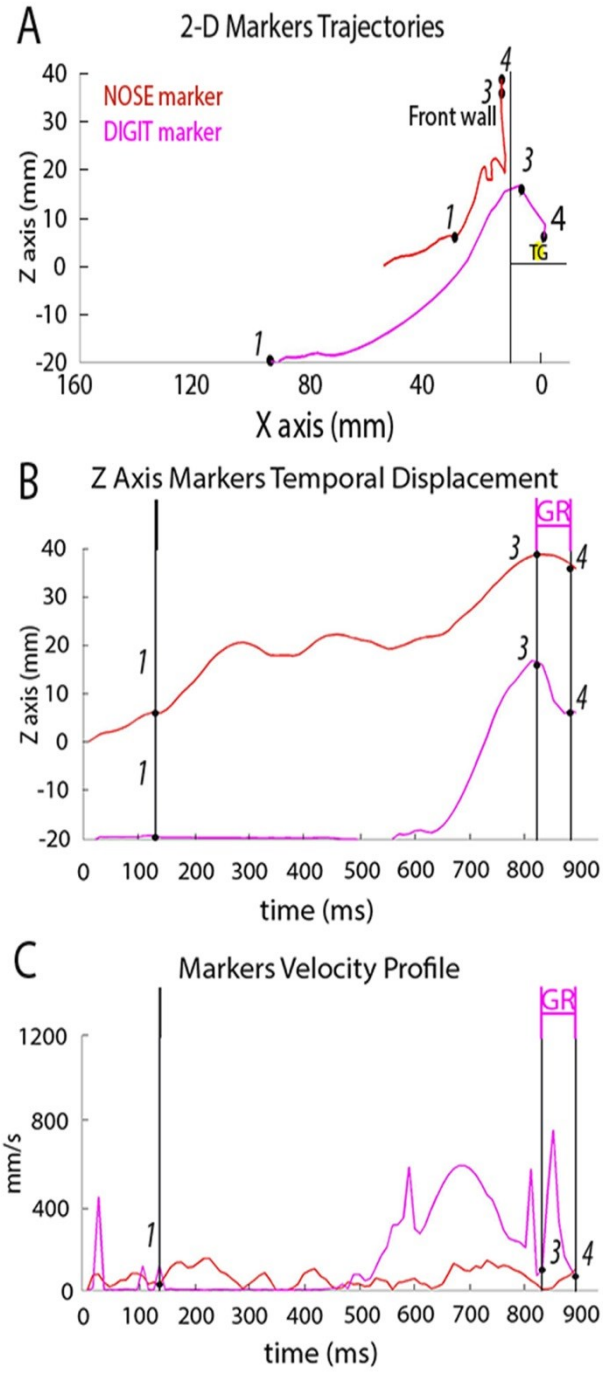

Fig. 27. An example of orienting reaching and grasping movements in the same trial as recorded by Qualisys and splitted off-line. Note that reaching has been recorded by digit marker and not by wrist marker as in Fig.26 and it will not be further taken into account in subsequent data processing. A: 2D (X-Z) markers trajectories. Nose marker in red, digit marker in pink, target/pellet (TG) in yellow. Numbers reported in the figure: 5-starting point of grasping, 6-ending point of grasping, other numbers, vertical lines and X Y coordinates as in Fig.26. B: Z axis temporal markers displacements. Colours, numbers and Y axis 0 as in A. Here the displacements of the two markers are temporally aligned so that we can see at the same time the displacement of both markers during orienting (OR), reaching (RC) and grasping (GR). C: markers velocity profiles in X-Y-Z axes. Colours, numbers and vertical line as in B.

Fig.28

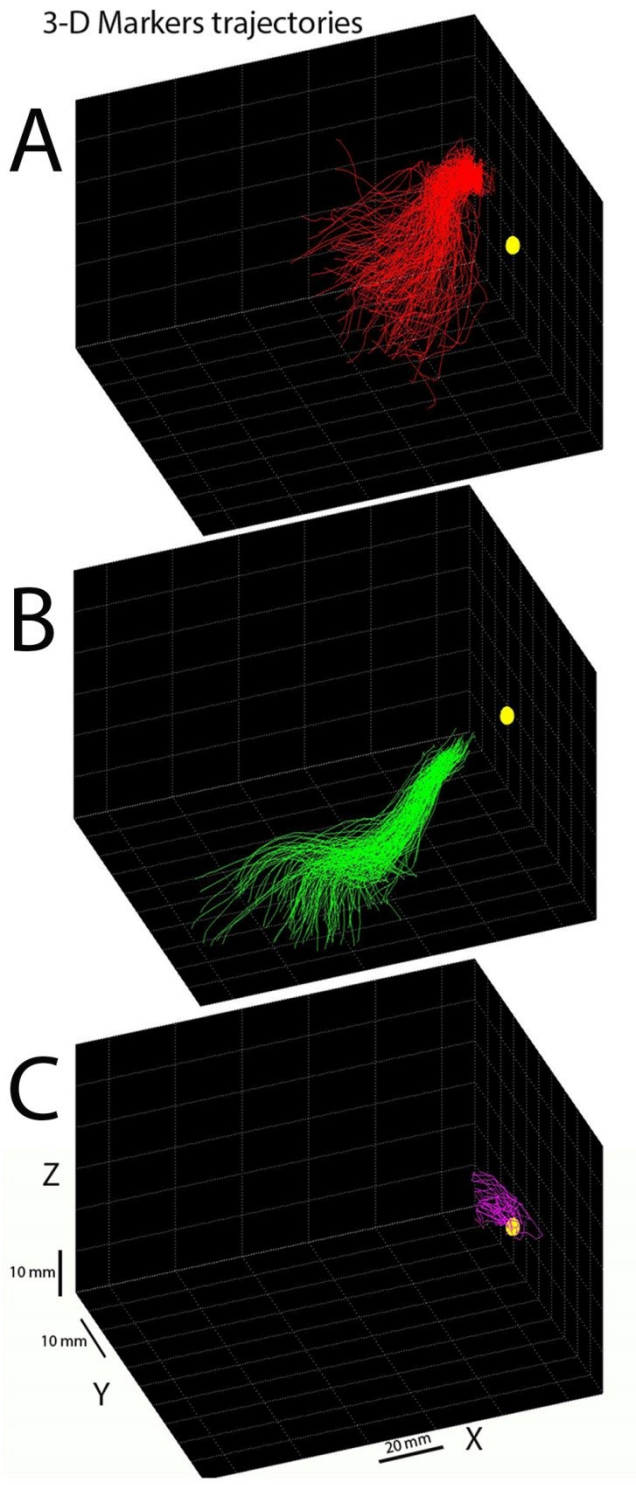

Fig. 28. 3D trajectories reconstruction in rat 3. 3D-coordinates system origin (0,0,0) corresponded to the center of target (yellow sphere). A: Orienting (red, n=78); B: Reaching (green, n=78); C: Grasping (pink, n=33). We can appreciate the variability of trajectories and of the movement starting points.

Fig.29

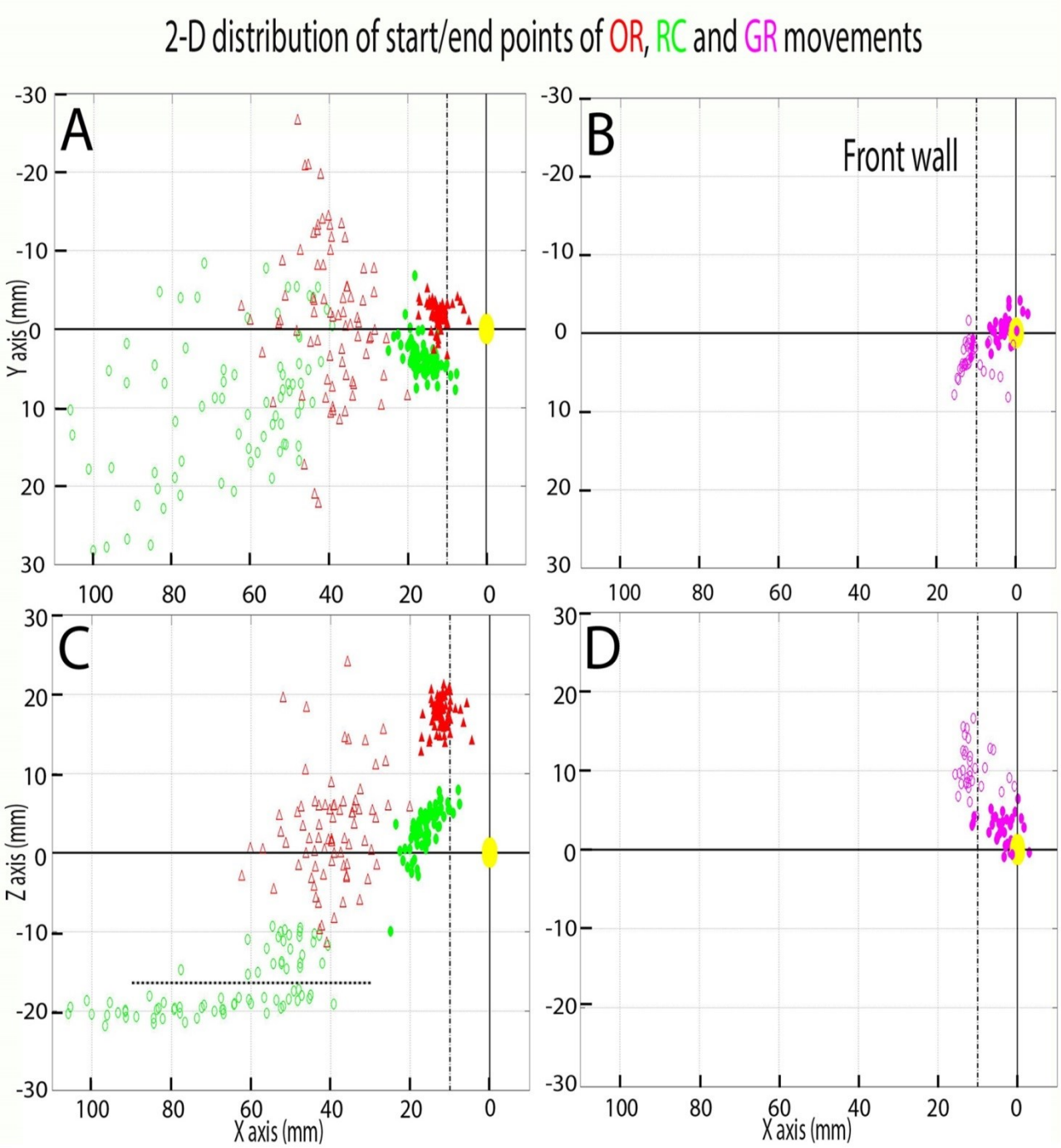

Fig. 29. 2D distribution of trajectories starting and ending points in the same rat as in fig. 28. A: XY distribution of starting/ending points of Orienting (red triangles) and Reaching (green circles). Empty symbols: starting points; filled symbols: ending points. 0,0: origin of axes at target position (yellow circle). This is a top view of distribution of starting/ending points inside the box. The broken line represent the position of the front wall of the box. B: XY distribution of starting/ending points of Grasping (pink circles), top view; other specifications as in A. C: XZ distribution of starting/ending points of Orienting and Reaching. This is a side view of distribution of starting/ending points inside the box. Other specifications as in A. D: XZ distribution of starting/ending points of Grasping, side view; other specifications as in A, B.

Fig.30

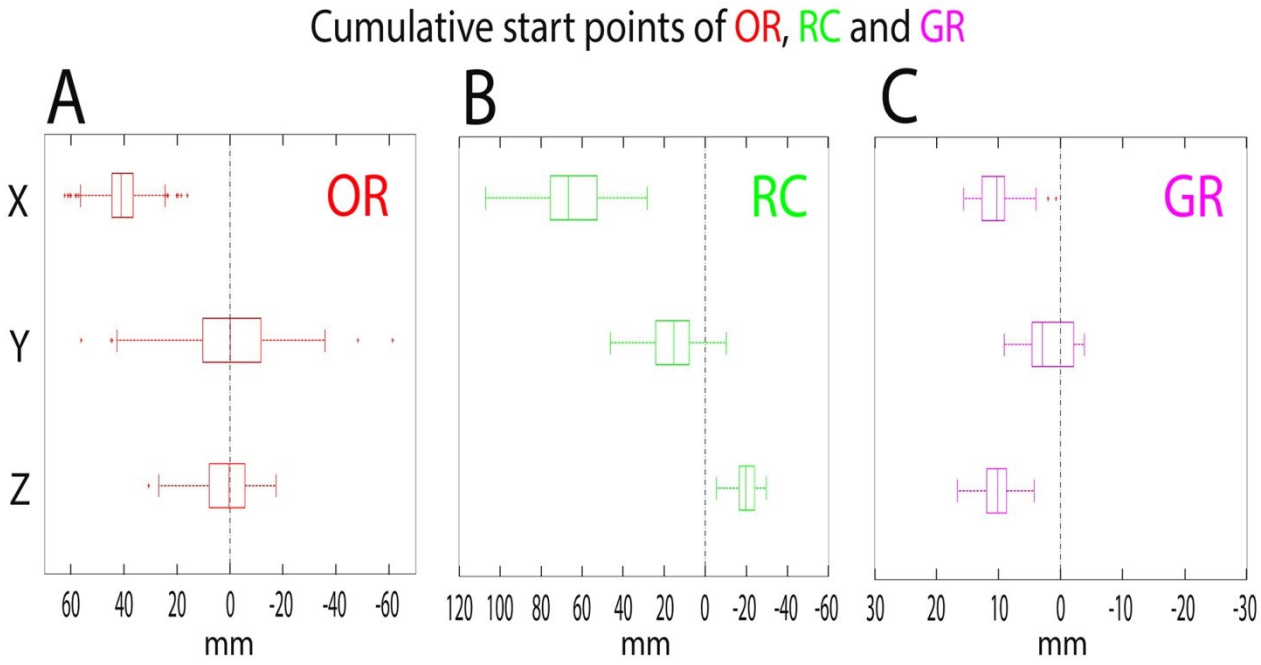

Fig. 30. Box plots of starting and ending points values for Orienting, Reaching and Grasping in all rats. Zero and vertical broken line correspond to target. X axis: positive values mean positions in front of the target; Y axis: positive values mean positions on the right side of the target. Z axis: positive values mean positions above the target. In Orienting the major dispersion of values is on the Y axis; in Reaching the major dispersion of values is on the X axis, and all Y values are positive since all animals were right-handed; in Grasping, Y values are distributed around 0.

Fig.31

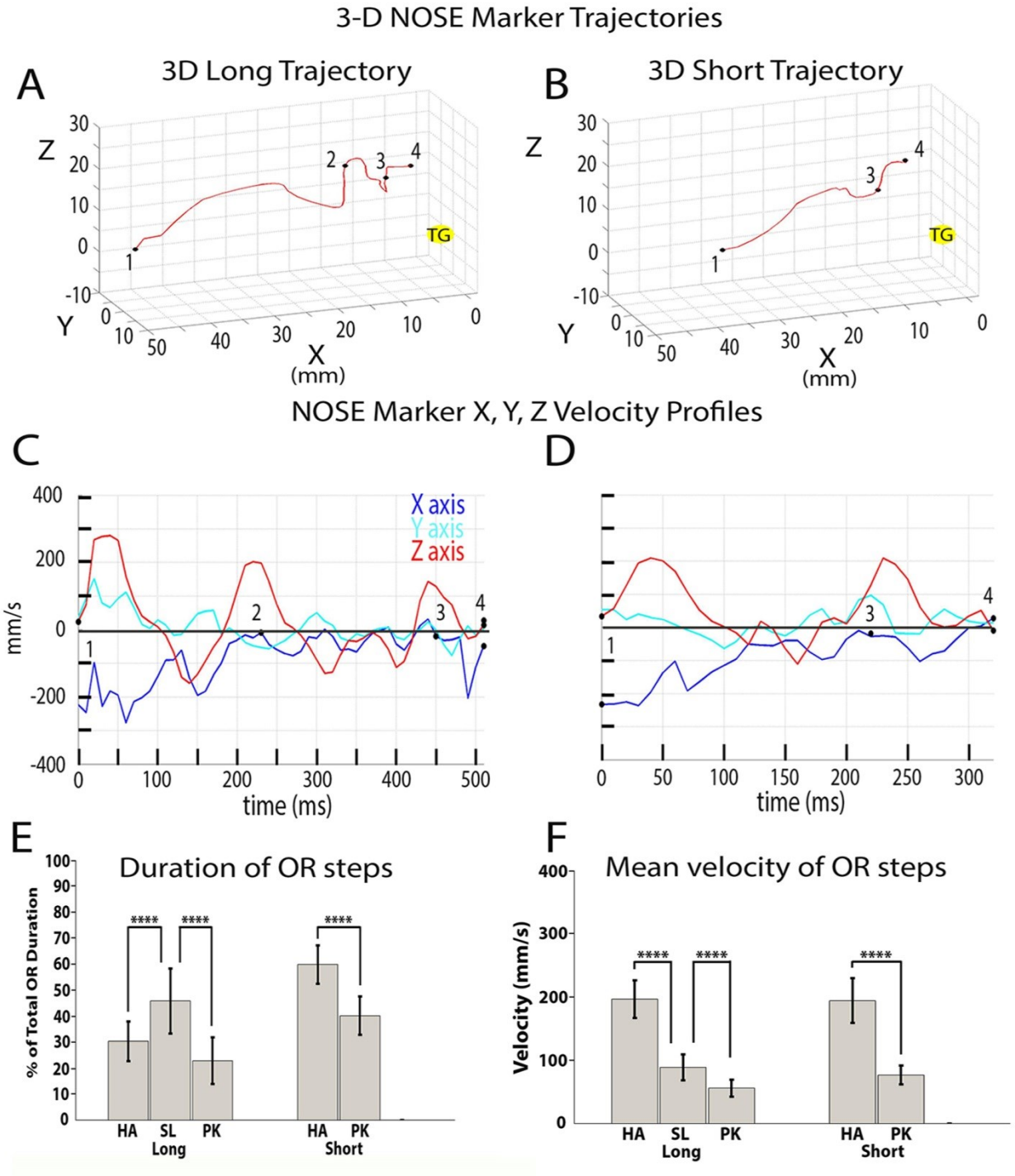

Fig. 31. Orienting: long and short trajectories. Example of a long (A) and a short (B) orienting trajectory in XZ axes. Starting (1) and ending (2) of movement as in Fig. 26 and 27. C and D: long and short normalized trajectories averaging in XZ axes of all rats. E, F, G and H: long and short normalized velocity profile averaging respectively in X (E-F) and Z (G-H) axes of all rats. In X axes the movement duration in percentage. Shadows represent SD. Note the difference in E vs. F velocity profiles and the similarity in G and H velocity profiles.

Fig.32

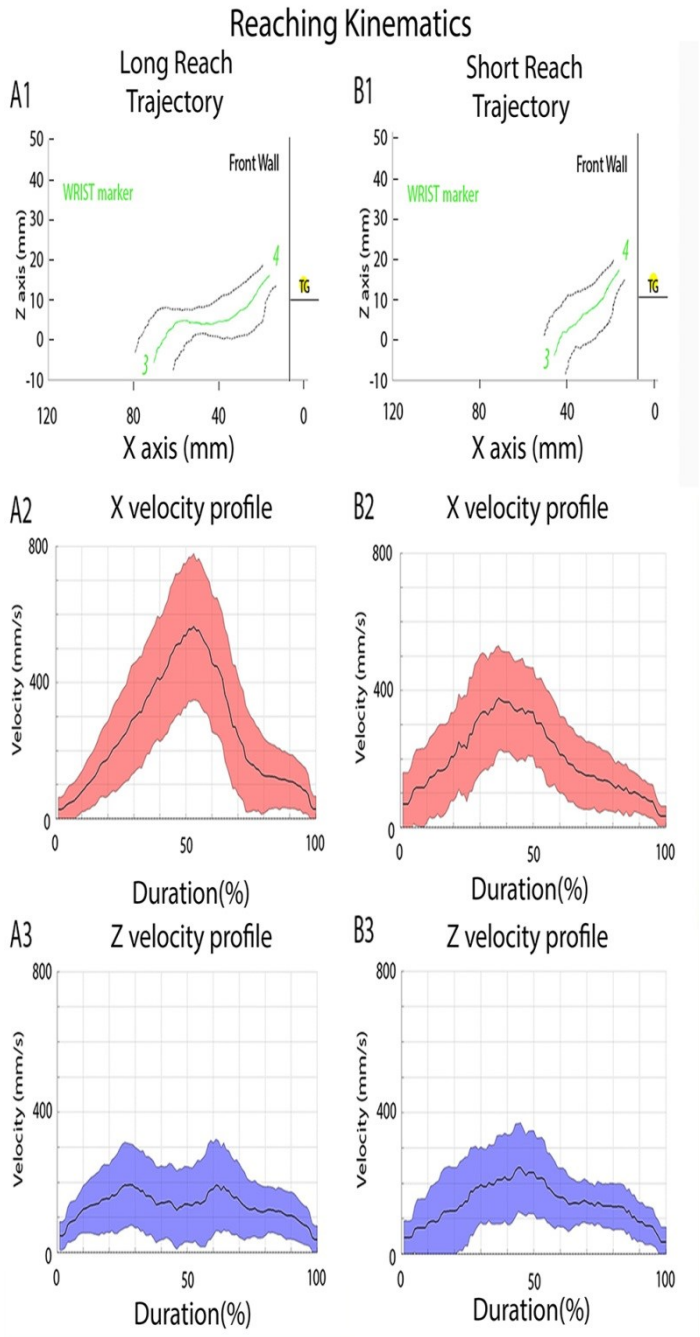

Fig. 32. Reaching kinematics: long and short trajectories. Reaching cumulative averaging of long (A) and short (B) trajectories expressed as median ± MAD. Lines and axes 0 as in Fig. 26A. C) and D) normalized velocity profile on horizontal (X) axis. E) and F) normalized velocity profile on vertical (Z) axis. Note the different trajectory shapes and velocity profiles, depending on the distance of start points from target.

Fig.33

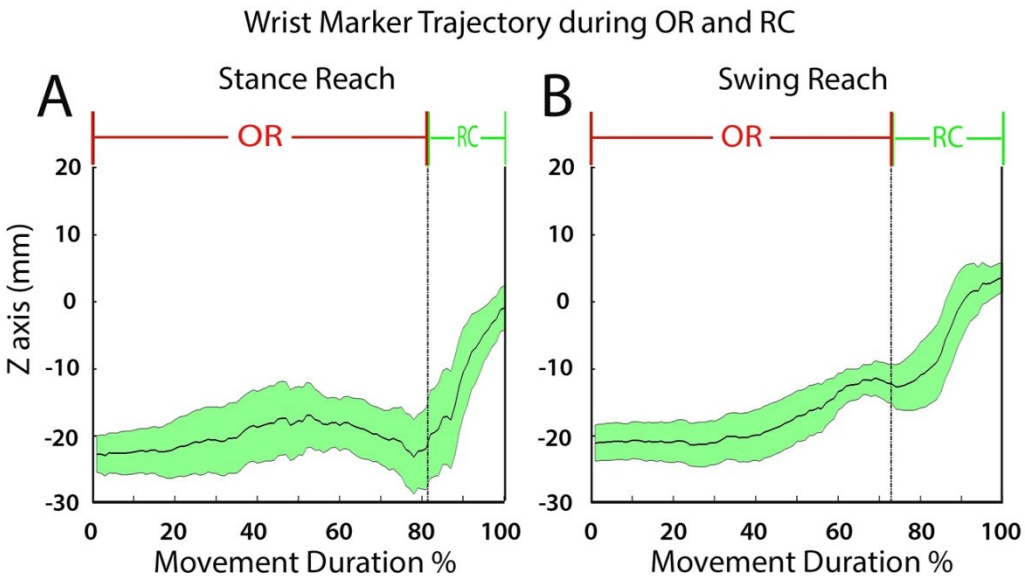

Fig. 33. Wrist marker trajectory during orienting (OR) and reaching (RC) movements. Averaging of normalized trajectories when reaching begins in stance (A, n=337) and swing (B, n=79) phases of the last step. Values are expressed as median ± MAD. Vertical broken line: orienting end/reaching start. Vertical unbroken line: reaching end. Horizontal (X) axis 0: orienting start; vertical (Z) axis 0: target position.

Fig.34

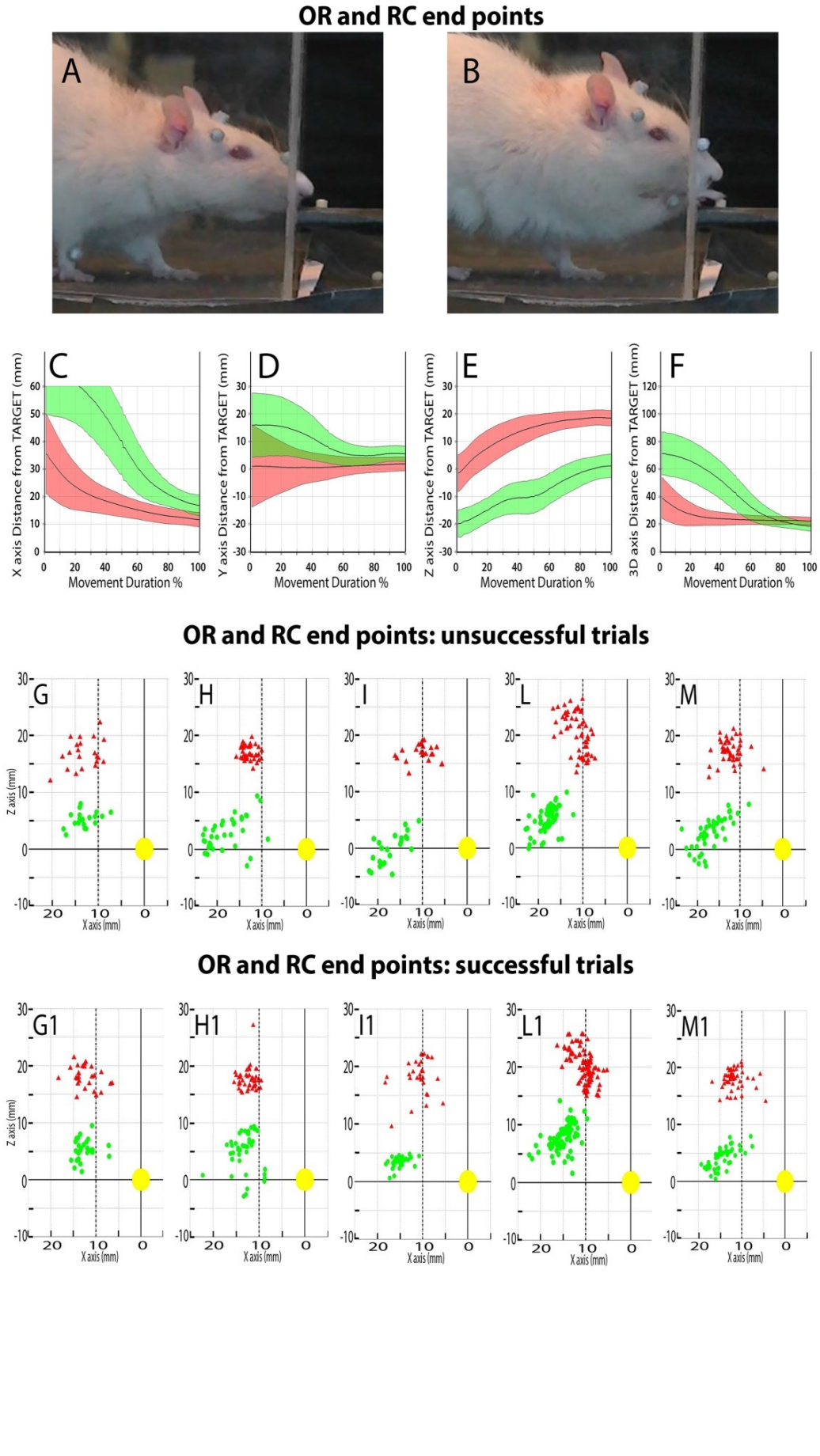
OR and RC end points
A
B
C
D
E
F
X axis Distance from TARGET (mm)
Y axis Distance from TARGET (mm)
Z axis Distance from TARGET (mm)
3D axis Distance from TARGET (mm)
Movement Duration %
OR and RC end points: unsuccessful trials
G
H
I
L
M
Z axis (mm)
X axis (mm)
OR and RC end points: successful trials
G1
H1
I1
L1
M1

Fig. 34. . Orienting (OR) and reaching (RC) end point positions. Video frame at the end of orienting (A) and at the end of reaching (B). C–F): cumulative normalized displacements of nose marker during orienting, and wrist marker during reaching in horizontal (C), depth (D) and vertical (E) axes and then in 3D coordinates (F). Note the convergence of markers at the end of movements in C, D and F, and the parallel marker displacement in E. G–M: orienting and reaching end point distributions for unsuccessful trials in each animal. G1–M1: orienting and reaching end point distributions for successful trials in each animal. Note that wrist/paw positions in successful trials tended to be closer to the target.

Fig.35

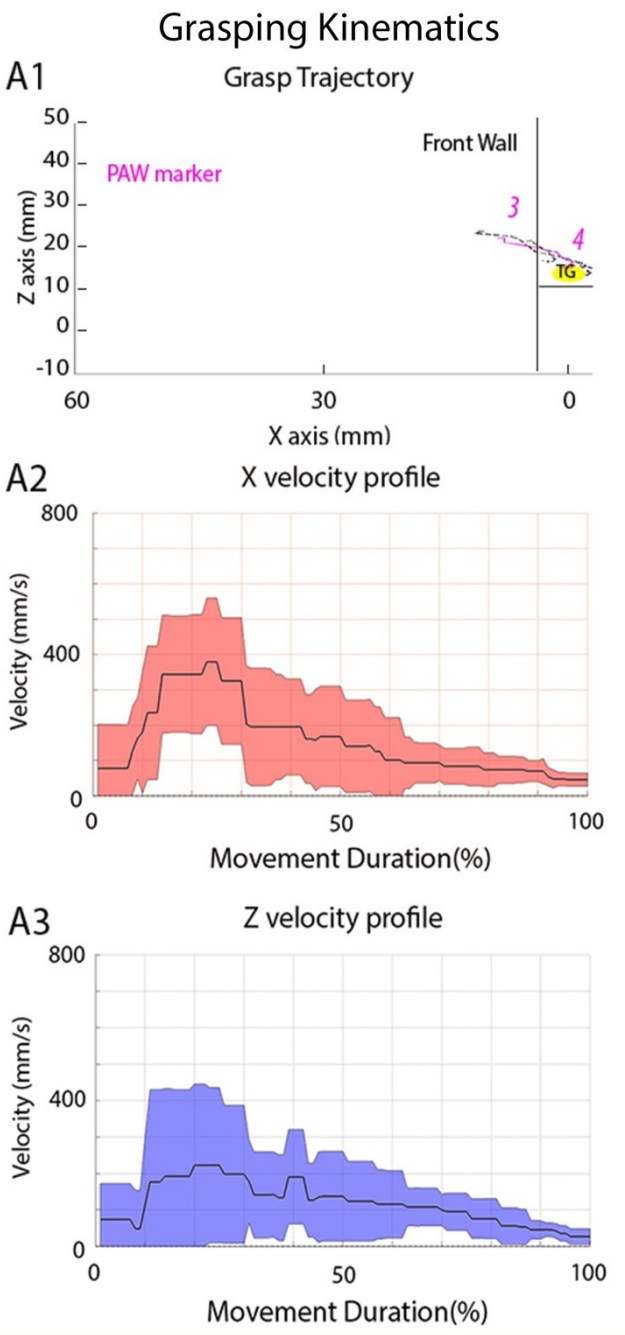

Fig. 35. . Grasping kinematics. Cumulative averaging of GR trajectories (A) expressed as median ± MAD. Lines and axes 0 as in Fig. 26A. B: normalized velocity profile on X axis. C: normalized velocity profile on Z axis. Note that velocity peak falls between the first and second quarter of the normalized movement duration.

Fig.36

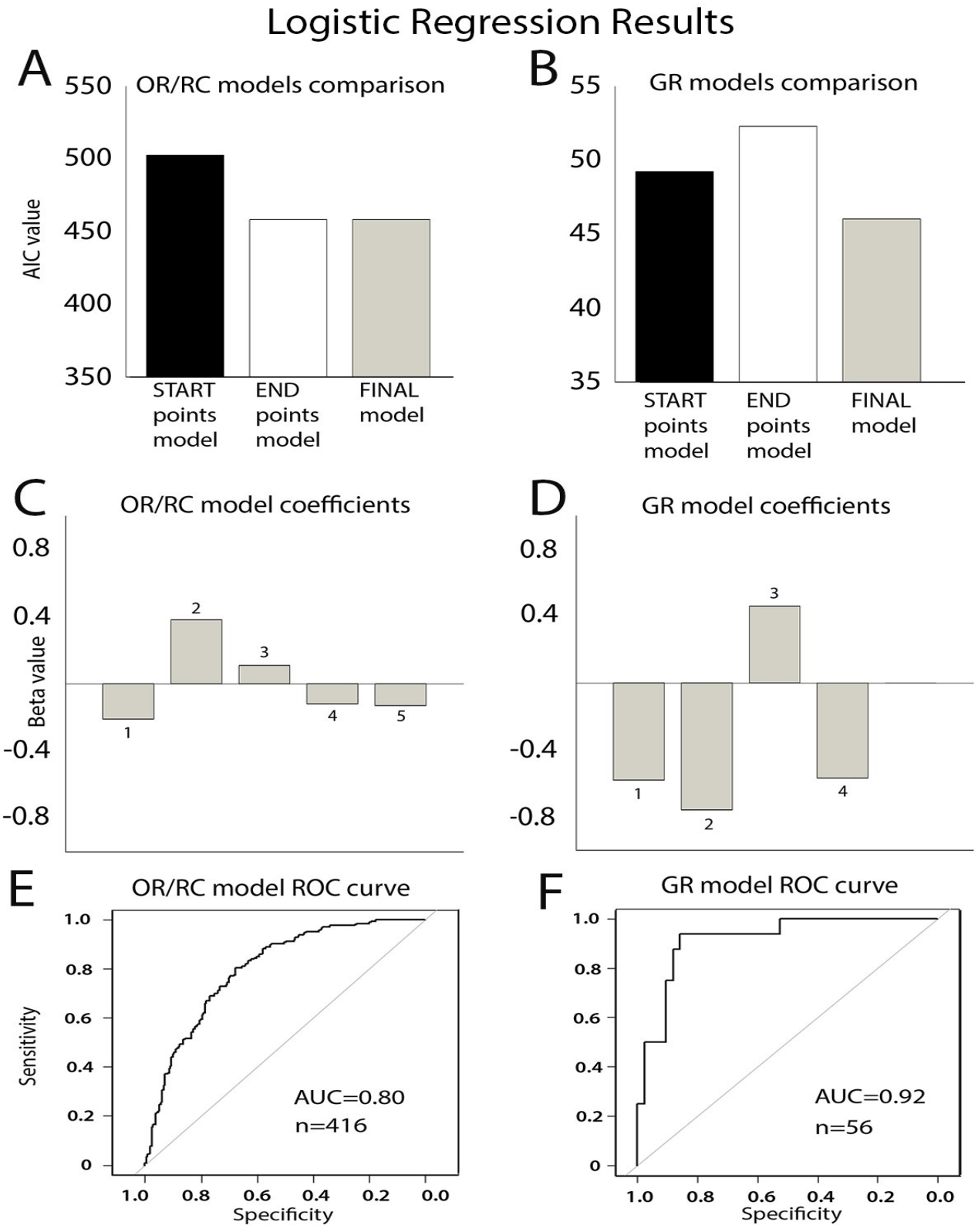
Logistic Regression Results
A
OR/RC models comparison
AIC value
550
500
450
400
350
START points model
END points model
FINAL model
B
GR models comparison
55
50
45
40
35
START points model
END points model
FINAL model
C
OR/RC model coefficients
Beta value
0.8
0.4
-0.4
-0.8
1
2
3
4
5
D
GR model coefficients
0.8
0.4
-0.4
-0.8
1
2
3
4
E
OR/RC model ROC curve
Sensitivity
1.0
0.8
0.6
0.4
0.2
0
AUC=0.80
n=416
1.0 0.8 0.6 0.4 0.2 0.0
Specificity
F
GR model ROC curve
1.0
0.8
0.6
0.4
0.2
0
AUC=0.92
n=56
1.0 0.8 0.6 0.4 0.2 0.0
Specificity

Fig. 36. . Logistic Regression. Nose/wrist marker (A) and digit marker (B) models. The Final Model in A and B displayed the lowest AIC value. Final nose/wrist marker model predictors coefficient value (C): 1, wrist position on the X axis at RC end (P=2.08e-15); 2, wrist position on the Y axis value at RC end (P=1.4e-11); 3, nose position on the X axis at RC end (P=3.75e-06); 4, nose position on the Y axis value at RC end (P=9.71e-05); and 5, nose position on the Z axis at RC end (P=3.14e-05). Final digit marker model predictors coefficient value (C): 1, digit position on the X axis value at GR start (P=0.003); 2, digit position on the Y axis at GR start (P=0.001); 3, digit position on the Z axis value at GR start (P=0.031); and 4, digit position on the Z axis at GR end (P=0.037). ROC curve and AUC value for OR/RC Final Model (E) and GR Final Model (F). X axis: True Positive Rate (sensitivity); Y axis: True Negative Rate (specificity).

Tab.1

The table summarises the behavioural parameters in single rats and the group value.

	R1		R2		R3		R4		R5		GROUP	
Trial	**P**	**No P**	**P**	**No P**	**P**	**No P**	**P**	**No P**	**P**	**No P**	**P**	**No P**
Whisk T - First NT	**121.56** 6.40	**122.69** 21.93	**82.50** 8.11	**184.00** 51.59	**123.50** 10.09	**137.86** 25.81	**170.83** 11.48	**71.36** 6.03	**142.95** 10.97	**140.36** 16.63	**132.10** 5.31	**130.89** 12.17
First NT - Poke	**126.25** 11.26	**142.31** 19.08	**135.00** 21.51	**172.00** 27.12	**146.25** 16.61	**171.53** 19.87	**104.72** 10.26	**143.64** 12.95	**214.32** 18.16	**190.71** 22.18	**149.60** 8.25	**164.75** 9.27
Poke - Start Reach	**208.04** 18.01		**161.40** 16.76		**121.20** 9.84		**178.48** 18.36		**85.63** 6.39		**150.08** 7.50	
Transport duration	**142.83** 10.07		**100.80** 8.46		**95.40** 6.90		**123.04** 14.47		**80.63** 3.59		**107.96** 4.52	
Paw out of the slot	**521.30** 73.43		**359.00** 60.02		**223.20** 26.69		**127.61** 16.93		**199.58** 25.29		**285.58** 25.29	

Estimated parameters: *Whisker T–First NT*: time lapse between first front wall whisker touch and first nose touch. *First NT–Poke*: time lapse between first front wall nose touch and nose poke. *Poke–Reach start*: time lapse between poke and start of Transport. *Transport Duration*: time lapse between paw lifting and paw crossing the slot. *Paw beyond slot*: time spent by the paw beyond the slot. The sum of the firsts three variables defines the Orient duration; the sum of all variables defines the trial duration. In each box, the top number is the mean value, and the bottom number is the standard error. For each animal, P trial: n=25, no-P trial: n=15. Note that in no-P trials the last three boxes are empty since very few complete trials were observed, and only in R1 (n=3) and R2 (n=1).

Tab.2

Behavioural parameter values in rats 3–5 days after bulbectomy in P and no-P trials.

	R1		R2		R3		R4		R5		GROUP	
Trial	**P**	**No P**	**P**	**No P**	**P**	**No P**	**P**	**No P**	**P**	**No P**	**P**	**No P**
Whisk T - First NT	**182** 16.56	**231.67** 43.90	**175.65** 15.71	**197.65** 21.94	**207.00** 25.40	**192.06** 25.41	**110** 18.33	**197.33** 29.14	**175.16** 18.14	**144.64** 24.93	**169.86** 9.10	**193.40** 13.27
First NT - Poke	**298.50** 24.45	**316.67** 25.24	**226.74** 25.44	**339.71** 56.96	**355.40** 25.01	**391.77** 19.87	**254.80** 34.17	**533.33** 81.11	**425.64** 70.59	**415.36** 80.50	**314.75** 19.54	**397.44** 27.35
Poke - Start Reach	**170.71** 24.71	**166.79** 36.87	**198.96** 21.46	**268.67** 36.26	**129.23** 12.88	**102.65** 18.57	**185** 16.74	**232.67** 33.41	**91.20** 10.30	**121.79** 21.80	**146.60** 7.82	**177.40** 15.00
Transport duration	**151.90** 14.79	**144.64** 15.81	**140.63** 10.32	**175.33** 12.05	**96.35** 10.55	**77.35** 5.91	**156.80** 16.48	**220.33** 44.10	**97.00** 4.97	**104.64** 12.11	**127.40** 5.79	**143.20** 11.39
Paw out of the slot	**686.43** 94.55	**695.67** 103.77	**262.08** 60.20	**181.00** 16.47	**336.15** 37.04	**304.71** 26.25	**145.40** 28.05	**314.00** 96.92	**174.80** 29.49	**181.07** 47.50	**309.50** 28.54	**336.51** 36.39

Parameters and numbers of trials as in Table 1. Note that in no-P trials there are no empty boxes and that the *First NT–Poke* value is significantly increased in all animals as compared to controls (P=0.000, Kruskal-Wallis test).

Tab.3 Behavioural parameter values in rats 12–14 days after bulbectomy in P and no-P trials.

	R1		R2		R3		R4		R5		GROUP	
Trial	**P**	**No P**	**P**	**No P**	**P**	**No P**	**P**	**No P**	**P**	**No P**	**P**	**No P**
Whisk T - First NT	**190.83** 13.97	**169.33** 16.42	**150.33** 21.37	**133.00** 15.00	**117.00** 18.81	**166.67** 22.09	**51.67** 6.25	**100.36** 6.98	**117.61** 10.65	**94.67** 10.71	**123.47** 7.79	**133.24** 7.61
First NT - Poke	**351.67** 40.84	**305.33** 22.29	**221.00** 20.44	**240.67** 67.41	**239.60** 20.93	**243.67** 16.26	**137.92** 11.32	**158.57** 16.75	**222.82** 16.87	**252.67** 19.77	**235.86** 12.94	**241.28** 16.14
Poke - Start Reach	**196.25** 26.85	**264.29** 22.29	**167.60** 17.08	**203.89** 18.22	**59.60** 6.32	**45.00** 8.59	**136.00** 12.39	**128.21** 14.04	**105.63** 13.48	**167.67** 34.01	**132.72** 8.44	**161.97** 15.68
Transport duration	**195.83** 17.95	**186.43** 22.45	**133.00** 9.27	**150.56** 17.59	**71.00** 2.18	**75.67** 6.15	**104.80** 5.93	**167.86** 41.58	**95.42** 7.78	**94.33** 4.11	**119.59** 5.83	**134.47** 10.65
Paw out of the slot	**635.21** 89.48	**629.33** 98.32	**305.20** 51.00	**168.33** 39.45	**361.60** 37.88	**302.33** 54.32	**92.80** 14.94	**247.86** 85.31	**245.67** 46.65	**226.67** 50.46	**326.27** 28.31	**310.06** 34.67

Parameters and numbers of trials as in Table 1. Note that in no-P trials there are no empty boxes, and that the *First NT–Poke* value is significantly increased in all animals as compared to controls (P=0.000, Kruskal-Wallis test).

Tab. 4 Behavioural parameters in control vs. trimmed rats

	CONTROL				TRIMMED			
	R1	R3	R4	GROUP	R1	R3	R4	GROUP
Whisker-T Poke	285.75 *±17.00*	257.00 *±14.68*	191.05 *±11.77*	244.6 *±9.78*				
Nose-T Poke					196.25 *±15.01*	284.50 *±34.55*	104.10 *±12.14*	194.95 *±16.13*
N-Nose T	0.40 *±0.15*	0.85 *±0.08*	0.30 *±0.11*	0.52 *±0.07*	2.60 *±0.17*	2.85 *±0.31*	1.90 *±0.18*	2.45 *±0.14*
Poke-Start-Rch	93.10 *±8.72*	180.24 *±19.45*	173.57 *±17.03*	148.97 *±10.12*	124.29 *±13.63*	171.67 *±16.59*	177.48 *±16.12*	157.81 *±9.31*
Rch Dur	108.75 *±12.16*	163.00 *±14.06*	113.50 *±8.84*	128.42 *±7.46*	106.25 *±9.99*	130.75 *±8.08*	105.50 *±6.53*	114.17 *±4.96*
Attempts	0.70 *±0.11*	0.05 *±0.05*	0.00 *±0.00*	0.25 *±0.06*	0.20 *±0.09*	0.05 *±0.05*	0.00 *±0.00*	0.08 *±0.04*

Table 4.. The table summarizes the behavioural parameters before and after trimming. Estimated parameters: *Whisker-T Poke*: time lapse between first front wall whisker touch and nose poke. *Nose-T Poke*: time lapse between first front wall nose touch and nose poke. *N. Nose T*: number of nose touches preceding nose poking. *Poke Reach-Start*: time lapse between poke and start of reaching. *Reach Duration*: time lapse between paw lifting and paw crossing the slot. *N. Attempts*: a forelimb extension toward the slot without crossing it. In each box the top number is the mean value and the bottom number is the standard error, for n=20. Note the significant increase in the number of nose touches after trimming (p=0.000, Kruskal-Wallis test) while poke-start reach and reach duration do not change significantly (control vs trimmed: p= 0.47 and 0.32, respectively, Kruskal-Wallis test).

Table 5. Behavioural parameters in control vs. ION severed rats

	CONTROL						ION 1-3D						ION 8-10D					
	R1	R2	R3	R4	R5	GROUP	R1	R2	R3	R4	R5	GROUP	R1	R2	R3	R4	R5	GROUP
Whisker-T Poke	170.75 9.08	178.75 11.64	243.75 17.77	141.25 7.13	197.75 15.7	186.45 6.60												
Nose-T Poke							641.25 104.44	752.5 138.81	675 159.86	752.75 108.41	781.25 112.87	720.55 55.75	413.00 79.34	602.75 107.66	386.25 82.42	248.50 59.76	257.50 50.92	381.6 36.76
N-Nose T	0.60 0.11	0.30 0.11	0.80 0.20	0.10 0.07	0.10 0.07	0.38 0.06	4.35 0.51	4.4 0.58	3.7 0.44	3.75 0.40	4 0.44	4.04 0.21	2.80 0.50	2.75 0.38	2.00 0.50	1.85 0.33	2.40 0.28	2.36 0.18
Poke-End Reach	258.10 6.19	391.14 18.29	393.00 14.05	307.75 6.13	325 10.3	330.08 10.76	795.00 127.44	767.62 56.03	771.82 103.67	400.50 56.66	713.03 56.33	519.47 46.54	557.73 58.07	298.81 13.20	300.65 41.05	338.41 17.42	325.00 30.76	342.63 15.93
Attempts	0.05 0.05	0.10 0.07	0.10 0.07	0 0	0 0	0.05 0.02	1.40 0.52	0.50 0.15	1.95 0.30	1.30 0.26	2.15 0.33	1.46 0.16	1.20 0.19	0.00 0	0.40 0.20	0.10 0.07	0.10 0.07	0.43 0.09

Tab.5. The table summarizes the behavioural parameters before and after ION severing at 1-3 and 8-10 days. Estimated parameters: *Poke End Reach*: time lapse between Poke and paw crossing the slot. Other parameters as in Table 4. In each box the top number is the mean value and the bottom number is the standard error, for n=20. Note that at 1-3 days all behavioural parameters are significantly increased in comparison to controls (p=0.000, Kruskal-Wallis test) while at 8-10 days only the poke-end reach values overlap values in controls (p=0.000, Kruskal-Wallis test).

Tab. 6 Reaching/grasping frequency in relation to approach

		Control	3-5D	6-8D	9-11D	12-14D	15-17D
R1		0.82	0	0	0.35	0.34	0.63
R2		0.93	0	0	0	0.76	0.99
R3		0.99	0	0.75	1	1	0.99
R4		0.99	0	0.98	1	1	1
R5		1	0	0.88	1	1	0.99
Average		0.95	0	0.52	0.67	0.82	0.92
Std error		0.03	0	0.22	0.21	0.13	0.07

Table 6. Ratio between reaching/grasping and approach expressed as a percentage for each animal in controls and at different time intervals after ION severing. Note that in rats R3, R4 and R5 the movement reappears 6–8 days after the lesion, while in R1 and R2 the movement reappears later.

Tab. 7 Reaching/grasping frequency in relation to poke

		Control	3-5D	6-8D	9-11D	12-14D	15-17D
R1		0.88	0	0	0.5	0.52	0.90
R2		0.93	0	0	0	0.8	0.99
R3		1	0	0.8	1	1	1
R4		1	0	1	1	1	1
R5		1	0	0.82	1	1	0.99
Average		0.96	0	0.45	0.70	0.86	0.98
Std error		0.02	0	0.24	0.22	0.09	0.02

Table 7. Ratio between reaching/grasping and poke expressed as a percentage for each animal in controls and at different time intervals after ION severing. This ratio gives an indication of the triggering power of nose insertion into the slot for the subsequent reaching/grasping movement. Note that all control rats present a ratio of almost 1:1. At 3–5 days, poke does not trigger reaching/grasping; in R3, R4 and R5, poke triggers reaching/grasping after 6-8 days, and in R1 and R2 this triggering function reappears later.

Tab.8 Kinematic parameters values for the Orienting, Reaching and grasping movements (median and inter quartile range)

	Orienting						**Reaching**						**Grasping**					
	R1 n=47	**R3** n=86	**R6** n=77	**R5** n=150	**R4** n=56	**GROUP** n=416	**R1** n=47	**R3** n=86	**R6** n=77	**R5** n=150	**R4** n=56	**GROUP** n=416	**R1** n=16	**R3** n=9	**R6** n=33	**R5**	**R4**	**GROUP** n=58
Trajectory Length (mm)	**52.47** 22.29	**51.49** 11.27	**56.26** 19.02	**74.81** *19.18*	**71.17** *25.65*	**63.26** 25.18	**78.30** 26.05	**71.66** 15.28	**68.07** 28.78	**73.91** *24.38*	**62.65** *27.62*	**70.84** 24.33	**15.49** 3.01	**22.86** 4.93	**19.82** 6.90	**/**	**/**	**19.27** 8.41
Duration (ms)	**280** 145	**530** 150	**400** 120	**590** *200*	**520** *210*	**495** 225	**170** 50	**220** 60	**170** 70	**170** *70*	**230** *115*	**185** 75	**50** 30	**80** 30	**60** 30	**/**	**/**	**60** 20
Max speed (mm/s)	**426.83** 170.20	**289.35** 85.28	**430.86** 144.71	**361.73** *140.16*	**340.51** *134.12*	**359.58** 160.61	**976.18** 257.17	**750.18** 177.64	**779.16** 276.89	**979.28** *353.14*	**530.83** *172.43*	**815.49** 347.96	**568.59** 140.22	**545.67** 319.90	**745.58** 228.22	**/**	**/**	**656.73** 301.17
Mean speed (mm/s)	**162.93** 55.68	**88.37** 17.36	**128.19** 32.08	**117.12** *22.76*	**125.70** *44.40*	**118.56** 43.14	**435.31** 94.96	**304.78** 55.64	**346.23** 86.16	**378.28** *98.61*	**240.29** *87.50*	**340.39** 113.16	**243.16** 116.13	**264.98** 110.30	**314.71** 90.55	**/**	**/**	**280.51** 103.27

Table 8. The table summarizes kinematic parameters values for orienting, reaching and grasping movements in each animal and in the group. Each movement is identified by four kinematic variables: - movement trajectory length (in mm); - movement duration (in msec); - mean velocity (in mm/s); and - peak velocity (in mm/s). In each box the top number is the median value and the bottom number is the interquartile range. s: number of sessions; n: number of trials. All kinematic parameters show a relatively high inter- and intra-subject variability, as demonstrated by the IQR.